

LOAN COPY: RETURN TO  
AFWL TECHNICAL LIBRARY  
KIRTLAND AFB, N.M.

NASA  
TP  
1562  
c.1

## NASA Technical Paper 1562



# Elastic Constants for Superplastically Formed/Diffusion-Bonded Corrugated Sandwich Core

William L. Ko

MAY 1980

**NASA**



NASA Technical Paper 1562

# Elastic Constants for Superplastically Formed/Diffusion-Bonded Corrugated Sandwich Core

William L. Ko  
*Dryden Flight Research Center*  
*Edwards, California*



National Aeronautics  
and Space Administration

**Scientific and Technical  
Information Office**

1980

# ELASTIC CONSTANTS FOR SUPERPLASTICALLY FORMED/DIFFUSION-BONDED CORRUGATED SANDWICH CORE

William L. Ko  
Dryden Flight Research Center

## INTRODUCTION

Since the first successful application of the sandwich structure in the British all-wood-constructed Mosquito fighter-bomber aircraft during World War II, the use of sandwich structural technology (mainly metallic) has become widespread in aerospace design (for example, for wings, wall panels, webs of beams, tails, and so forth).

The typical sandwich structure consists of two relatively thin high strength face sheets separated by and bonded to a relatively thick, low density, low strength core. Thus, the sandwich structure is characterized by light weight and high flexural stiffness.

The most extensively used sandwich structure in aerospace technology is the honeycomb core sandwich structure, which is usually made of aluminum face sheets and an aluminum or titanium honeycomb core. In this structure, the honeycomb cell generatrix is perpendicular to the face sheet and, therefore, the bonding between the honeycomb core and the face sheet can be achieved only by line contact. This is the major drawback of this type of sandwich structure, because the line-contact bonding between the honeycomb cross section and the face sheet can easily lose its bonding integrity as a result of corrosion.

In recent years, an entirely new process known as superplastic forming with concurrent diffusion bonding (SPF/DB) has emerged (ref. 1). This process involves the fabrication of sandwich structures by using superplastic materials, such as the titanium alloys. The SPF/DB process capitalizes on two natural characteristics of titanium alloys. The first is superplasticity, which is the ability of a material to undergo large plastic deformations (up to 1000 percent strain) at high temperatures without localized thinning (or necking). Second, the alloys have the capacity for

solid state diffusion bonding, which is the joining of the superplastic alloys under pressure at elevated temperatures without melting or the use of bonding agents.

Utilizing the above two characteristics, an SPF/DB sandwich structure can be fabricated by diffusion bonding at least three superplastic alloy sheets at selected areas and then superplastically expanding apart the face sheets by pressure inside the containment (or die cavity) to give the desired configuration. This new process eliminates the use of bonding agents, and allows surface-contact bonding instead of line-contact bonding as in the case of honeycomb sandwich structures. Through this new technique, a number of new shapes and symmetries for the sandwich core become possible. These include corrugated cores, truss cores (the limit case of corrugated core), dimpled cores, and sine-wave cores (where the axis of corrugation is sinusoidal in shape), which are described in reference 1; and egg-carton-like cores, which have projections that are shaped like hollow truncated cones, hollow truncated squares, or hexagonal pyramids and are arranged in square or hexagonal arrays (refs. 2 and 3).

The corrugated, the truss, and the sine-wave cores have relatively high out-of-plane bending stiffness in the direction of the corrugation axis, but they have very low out-of-plane bending stiffness in the direction transverse to the corrugation axis. The egg-carton-like cores have relatively low flexural stiffness in any in-plane direction. However, if these cores are joined with face sheets, the overall stiffness of the sandwich structure is greatly enhanced.

In most of the SPF/DB sandwich structures, the sandwich cores are relatively flexible in the thickness direction, and there is usually a sharp angle at the juncture of the face sheet and core. Thus, if the swelling modes of vibration (that is, the oscillation of the two face sheets in opposite directions) should occur under aerospace service conditions (for example, engine noise, high frequency flutter, and so forth), these vibration modes could create situations favorable to the formation of fatigue cracks at the face sheet/core junction sites, resulting in possible damage to the face sheet/core bond.

In order to study this problem, the assumption that the sandwich core is rigid in the thickness direction (which is the conventional approach to the analysis of sandwich plates) must be abandoned, and the sandwich core must be treated as it is or as an equivalent homogeneous elastic solid. For the latter case, the effective elastic constants for the sandwich core are needed.

The purpose of this paper is to present formulae and graphs for evaluating the effective elastic constants for the SPF/DB corrugated sandwich core. The paper also discusses the relative structural advantages and disadvantages of this sandwich core as compared with the conventional honeycomb sandwich core.

## SYMBOLS

$B$	nondimensional parameter associated with displacement ( $\delta$ )
$b$	one-half of horizontal projected length of circular arcs and straight diagonal segments of corrugation leg
$D$	bending stiffness per unit width
$d$	one-half of the length of straight diagonal segment of corrugation leg
$E$	modulus of elasticity
$F$	vertical load in sandwich thickness direction, per unit width in $x$ -direction, concentrated at end points of corrugation leg
$f$	length of corrugation flat segment
$G$	shear modulus
$H$	horizontal load (in $y$ -direction), per unit width in $x$ -direction, concentrated at end points of corrugation leg
$h_c$	corrugated core thickness (vertical distance between upper and lower corrugation flat segment centerlines)
$\ell$	length of one corrugation leg
$M$	bending moment
$p$	one-half of corrugation pitch (or half wave length of corrugation)
$R$	radius of circular arc segments of corrugation leg
$s$	distance measured along corrugation centerline
$t$	thickness
$x, y, z$	Cartesian coordinates
$\gamma$	effective shear strain of corrugated core in $yz$ -plane
$\delta$	displacement
$\epsilon$	strain
$\theta$	corrugation angle (angle between centerline of straight diagonal segment and that of corrugation flat segment)

$\nu$	Poisson ratio
$\rho$	density
$\sigma$	stress
$\tau$	$= \frac{F}{h_c} = \frac{H}{p}$ , averaged shear stress in corrugated core in yz-plane
$\psi$	angle between tangent to corrugation leg centerline and a horizontal line

## GEOMETRY OF SANDWICH PLATE

Figure 1 shows an SPF/DB corrugated core sandwich plate. This structure is formed by diffusion bonding three superplastic alloy sheets (two face sheets and one core sheet) in selected areas (ref. 2) and then superplastically expanding the multiple sheet pack inside a die cavity by using gas pressure. This structure is slightly different from the conventional corrugated core sandwich structure because the corrugation leg does not have uniform thickness. Because of superplastic expansion, the diagonal segment of the corrugation leg is always thinner than the flat segment (crest or trough) of the corrugation leg, which has a thickness that is nearly the preexpansion thickness. Thus, the results given by reference 4, which are for the corrugation leg of uniform thickness, cannot be used to evaluate the present structure without considerable modification.

This report analyzes only a symmetric corrugation (that is, a corrugation symmetric with respect to the middle surface of the sandwich plate). The element of the corrugation referred to as the corrugation leg is assumed to be made up of circular arc and straight diagonal segments of thickness  $t_c$  and of flat segments of thickness  $t_f$  (the preexpansion thickness of the core sheet).

## ELASTIC CONSTANTS FOR SUPERPLASTICALLY FORMED/DIFFUSION-BONDED CORRUGATED SANDWICH CORE

The elastic constants evaluated in the following discussion are the effective (or averaged) elastic constants for a homogeneous sandwich core equivalent to the actual sandwich core. This idealization can be adequate when the sandwich plate width (normal to the corrugation axis) is many times the corrugation pitch. The analysis assumes that deformation is infinitesimal and that there is no local buckling of the sandwich structure.

Evaluation of Effective Modulus of Elasticity  $E_x$   
and Effective Shear Moduli  $G_{xy}$  and  $G_{zx}$

The modulus of elasticity in the  $x$ -direction,  $E_x$ , and the shear moduli in the  $xy$ - and  $zx$ -planes,  $G_{xy}$  and  $G_{zx}$ , respectively, may be obtained by modifying the results given in reference 4 by applying the rule of mixture to account for the nonuniform thickness of the corrugation leg. These elastic constants can be expressed in the forms

$$E_x = E_c \frac{1}{p h_c} [f t_f + (\ell - f) t_c] = E_c \frac{t_f}{h_c} \quad (1)$$

$$G_{xy} = G_c \frac{p}{\ell^2 h_c} [f t_f + (\ell - f) t_c] = G_c \frac{p^2 t_f}{\ell^2 h_c} \quad (2)$$

$$G_{zx} = G_c \frac{h_c}{\ell^2 p} [f t_f + (\ell - f) t_c] = G_c \frac{h_c t_f}{\ell^2} \quad (3)$$

where the last terms in the equations are for constant volume superplastic deformations (neglecting small elastic deformations) for which the condition  $f t_f + (\ell - f) t_c = p t_f$  holds and

$E_c$	modulus of elasticity of the corrugated core material
$G_c$	shear modulus of the corrugated core material
$p$	one-half of corrugation pitch (or one-half of a wave length of corrugation)
$h_c$	corrugated core thickness (vertical distance between centerlines of the upper and lower corrugation flat segments)
$\ell$	length of one corrugation leg
$f$	length of corrugation flat segment

For constant volume superplastic deformations, the superplastic incompressibility condition used in equations (1), (2), and (3) may be used to relate the two corrugation leg thicknesses  $t_c$  and  $t_f$  in the forms

$$\frac{t_c}{t_f} = \frac{p - f}{\ell - f} = \frac{b}{d + R\theta} \quad (4)$$

or

$$\frac{t_c}{t_f} = \frac{\cos \theta + 2 \frac{R}{h_c} (1 - \cos \theta)}{1 + 2 \frac{R}{h_c} [\theta \sin \theta - (1 - \cos \theta)]} \quad (5)$$

where

- $b$  one-half of the horizontal projected length of the circular arc and straight diagonal segments of the corrugation leg
- $d$  one-half of the length of the straight diagonal segment of the corrugation leg
- $R$  radius of circular arc segment of the corrugation leg
- $\theta$  corrugation angle (angle between the centerline of the straight diagonal segment and the centerline of the corrugation flat segment)

#### Evaluation of Modulus of Elasticity $E_y$

Figure 2 shows a free body diagram of a corrugation leg subjected to a horizontal loading,  $H$  (per unit width in the  $x$ -direction). Neglecting the Timoshenko beam shear deformation of the corrugation leg because of its thinness, the total horizontal displacement of point 0 with respect to point 0',  $\delta_y^H$ , may be expressed as the summation of bending and stretching effects. Thus, one can write

$$\delta_y^H = \underbrace{\int_0^l \frac{M(-1)z'}{E_c I_i} ds}_{\text{(Bending)}} + \underbrace{\int_0^l \frac{H \cos \psi}{E_c t_i} \cos \psi ds}_{\text{(Stretching)}} \quad (6)$$

where the integrals are taken from point 0 to point 0' (that is, one corrugation leg) and

- $s$  distance measured along the corrugation leg centerline
- $\psi$  angle between tangent to the corrugation leg centerline and a horizontal line
- $M = H \left( \frac{h_c}{2} - z' \right)$ , bending moment at a cross section of the corrugation leg



$z'$  vertical distance from point 0

$I_i = \frac{1}{12} t_i^3$ , moment of inertia of a corrugation leg cross section that is normal to  $s$  and parallel to the  $x$ -axis. In the region of the corrugation flat segment,  $I_i = I_f$ ; and in the circular arc and straight diagonal segments,  $I_i = I_c$

$t_i$  thickness of a corrugation leg. In the region of the corrugation flat segment,  $t_i = t_f$ ; and in the circular arc and straight diagonal segments,  $t_i = t_c$

The (-1) in the bending term of equation (6) indicates that the displacement of point 0 with respect to point 0' is to the left in figure 2 (ref. 5).

The following relationships between the geometric parameters of the corrugation will be useful in the process of evaluating equation (6) and others to follow:

$$\frac{d}{h_c} = \frac{1}{2 \sin \theta} \left[ 1 - 2 \frac{R}{h_c} (1 - \cos \theta) \right] \quad (7)$$

$$\frac{f}{h_c} = \frac{p}{h_c} - 2 \frac{d}{h_c} \cos \theta - 2 \frac{R}{h_c} \sin \theta \quad (8)$$

$$\frac{b}{h_c} = \frac{1}{2} \left( \frac{p}{h_c} - \frac{f}{h_c} \right) \quad (9)$$

$$\frac{\ell}{h_c} = \frac{f}{h_c} + 2 \frac{d}{h_c} + 2 \frac{R}{h_c} \theta \quad (10)$$

Making use of the equations (7) to (10) in the integration of equation (6), one obtains

$$\delta_y^H = \frac{H h_c^3}{E_c I_c} B_y^H \quad (11)$$

where

$$\begin{aligned}
B_y^H \equiv & \frac{2}{3} \left( \frac{d}{h_c} \right)^3 \sin^2 \theta + \frac{1}{2} \left( \frac{R}{h_c} \theta + \frac{1}{2} \frac{f}{h_c} \frac{I_c}{I_f} \right) \\
& - \left( \frac{R}{h_c} \right)^2 \left[ \left( 2 - 3 \frac{R}{h_c} \right) (\theta - \sin \theta) + \frac{R}{h_c} \sin \theta (1 - \cos \theta) \right] \\
& + \frac{I_c}{h_c^2 t_c} \left[ \frac{f}{h_c} \frac{t_c}{t_f} + 2 \frac{d}{h_c} \cos^2 \theta + \frac{R}{h_c} (\theta + \sin \theta \cos \theta) \right]
\end{aligned} \tag{12}$$

The modulus of elasticity  $E_y$  is then given by

$$E_y = \frac{\sigma_y}{\varepsilon_y} = \frac{\frac{H}{h_c}}{\frac{\delta_y^H}{p}} \tag{13}$$

$$= \frac{E_c}{B_y^H} \frac{I_c p}{h_c^4} \tag{14}$$

where  $\sigma_y$  and  $\varepsilon_y$  are, respectively, the effective stress and the effective strain of the corrugated core in the  $y$ -direction.

#### Evaluation of Poisson Ratio $\nu_{zy}$

As illustrated by figure 2, again, the vertical displacement of point 0 with respect to point 0' under horizontal loading  $H$ ,  $\delta_z^H$ , may be written

$$\delta_z^H = \underbrace{\int_0^l \frac{M(-1)y'}{E_c I_i} ds}_{\text{(Bending)}} - \underbrace{\int_0^l \frac{H \cos \psi}{E_c t_i} \sin \psi ds}_{\text{(Stretching)}} \tag{15}$$

where  $y'$  is the horizontal distance from point 0, and the  $(-1)$  in the bending term indicates that the displacement of point 0 with respect to point 0' is downward (ref. 5).

After integration and making use of relationships (7) to (10), equation (15) becomes

$$\delta_z^H = \frac{H h_c^3}{E_c I_c} B_z^H \quad (16)$$

where

$$\begin{aligned} B_z^H = & \frac{2}{3} \left( \frac{d}{h_c} \right)^3 \sin \theta \cos \theta + \frac{1}{2} \frac{I_c}{I_f} \left[ \frac{1}{4} \left( \frac{p}{h_c} \right)^2 - \left( \frac{b}{h_c} \right)^2 \right] \\ & + \frac{R}{h_c} \left\{ \frac{b}{h_c} \theta - 2 \frac{Rb}{h_c^2} (\theta - \sin \theta) - \frac{R}{h_c} (1 - \cos \theta) \left[ 1 - \frac{R}{h_c} (1 - \cos \theta) \right] \right\} \\ & - \frac{I_c}{h_c^2 t_c} \left( 2 \frac{d}{h_c} \sin \theta \cos \theta + \frac{R}{h_c} \sin^2 \theta \right) \end{aligned} \quad (17)$$

The Poisson ratio  $\nu_{zy}$ , which is associated with loading in the  $y$ -direction only, is then given by

$$\nu_{zy} = - \frac{\epsilon_z}{\epsilon_y} = \frac{\frac{\delta_z^H}{h_c}}{\frac{\delta_y^H}{p}} \quad (18)$$

$$= \frac{p}{h_c} \frac{B_z^H}{B_y^H} \quad (19)$$

where  $\epsilon_z$  is the average strain in the  $z$ -direction of the corrugated core.

### Evaluation of Modulus of Elasticity $E_z$

Figure 3 shows a free body diagram of the corrugation leg subjected to a vertical (sandwich thickness direction) loading,  $F$ , per unit width in the  $x$ -direction. The loading is concentrated at points 0 and 0'. Neglecting the Timoshenko beam shear deformation, as before, the total vertical displacement,  $\delta_z^F$ , of point 0 with respect to

point 0' may be written as the summation of the bending and stretching effects. Thus,

$$\delta_z^F = \underbrace{\int_0^l \frac{M(-1)y'}{E_c I_i} ds}_{\text{(Bending)}} + \underbrace{\int_0^l \frac{F \sin \psi}{E_c t_i} \sin \psi ds}_{\text{(Stretching)}} \quad (20)$$

where the (-1) in the bending term indicates that the movement of point 0 with respect to point 0' is upward (ref. 5). In this case,  $M = F\left(\frac{p}{2} - y'\right)$ . Taking equations (7) to (10) in the integration of equation (20), we then obtain

$$\delta_z^F = \frac{F h_c^3}{E_c I_c} B_z^F \quad (21)$$

where

$$\begin{aligned} B_z^F = & \frac{2}{3} \left( \frac{d}{h_c} \right)^3 \cos^2 \theta + \frac{2}{3} \frac{I_c}{I_f} \left[ \frac{1}{8} \left( \frac{p}{h_c} \right)^3 - \left( \frac{b}{h_c} \right)^3 \right] \\ & + \frac{R}{h_c} \left[ 2 \left( \frac{b}{h_c} \right)^2 \theta - 4 \frac{Rb}{h_c^2} (1 - \cos \theta) + \left( \frac{R}{h_c} \right)^2 (\theta - \sin \theta \cos \theta) \right] \\ & + \frac{I_c}{h_c^2 t_c} \left[ 2 \frac{d}{h_c} \sin^2 \theta + \frac{R}{h_c} (\theta - \sin \theta \cos \theta) \right] \end{aligned} \quad (22)$$

The modulus of elasticity  $E_z$  is then given by

$$E_z = \frac{\sigma_z}{\epsilon_z} = \frac{\frac{F}{p}}{\frac{\delta_z^F}{h_c}} \quad (23)$$

$$= \frac{E_c}{B_z^F} \frac{I_c}{p h_c^2} \quad (24)$$

where  $\sigma_z$  is the effective stress in the corrugated core in the  $z$ -direction.

If the vertical loading  $F$  is distributed over the corrugation flat segment, then  $B_z^F$  in equation (22) will have the form

$$\begin{aligned}
 B_z^F = & \frac{2}{3} \left( \frac{d}{h_c} \right)^3 \cos^2 \theta + \frac{1}{4} \frac{f}{h_c} \frac{I_c}{I_f} \left[ \left( \frac{p}{h_c} \right)^2 - \frac{7}{6} \frac{pf}{h_c^2} + \frac{3}{8} \left( \frac{f}{h_c} \right)^2 \right] \\
 & + \frac{R}{h_c} \left[ 2 \left( \frac{b}{h_c} \right)^2 \theta - 4 \frac{Rb}{h_c^2} (1 - \cos \theta) + \left( \frac{R}{h_c} \right)^2 (\theta - \sin \theta \cos \theta) \right] \\
 & + \frac{I_c}{h_c^2 t_c} \left[ 2 \frac{d}{h_c} \sin^2 \theta + \frac{R}{h_c} (\theta - \sin \theta \cos \theta) \right] \quad (25)
 \end{aligned}$$

It is apparent that the only difference between equations (22) and (25) occurs in the second term on the right side of each equation (underlined). Equation (25) will not be used in the subsequent analyses.

#### Evaluation of Poisson Ratio $\nu_{yz}$

From figure 3, the horizontal displacement,  $\delta_y^F$ , of point 0 with respect to point 0' under the concentrated vertical loading,  $F$ , is given by

$$\delta_y^F = \underbrace{\int_0^{\ell} \frac{M(-1)z'}{E_c I_i} ds}_{\text{(Bending)}} - \underbrace{\int_0^{\ell} \frac{F \sin \psi}{E_c t_i} \cos \psi ds}_{\text{(Stretching)}} \quad (26)$$

where the  $(-1)$  in the integrand of the bending term defines the direction of movement of point 0 with respect to point 0' to be to the right in figure 3 (ref. 5).

After integration of equation (26), with relationships (7) to (10) taken into account, it follows that

$$\delta_y^F = \frac{F h_c^3}{E_c I_c} B_y^F \quad (27)$$

where

$$B_y^F = B_z^H \quad (28)$$

Then the Poisson ratio  $\nu_{yz}$ , which is associated with loading in the  $z$ -direction only, is given by

$$\nu_{yz} = -\frac{\epsilon_y}{\epsilon_z} = \frac{\frac{\delta_y^F}{p}}{\frac{\delta_z^F}{h_c}} \quad (29)$$

$$= \frac{h_c}{p} \frac{B_y^F}{B_z^F} \quad (30)$$

If  $F$  is distributed over the corrugation flat segment, then  $B_y^F$  in equation (28) is modified to

$$\begin{aligned} B_y^F = & \frac{2}{3} \left( \frac{d}{h_c} \right)^3 \sin \theta \cos \theta + \frac{1}{4} \frac{f}{h_c} \frac{I_c}{I_f} \left( \frac{p}{h_c} - \frac{2}{3} \frac{f}{h_c} \right) \\ & + \frac{R}{h_c} \left\{ \frac{b}{h_c} \theta - 2 \frac{Rb}{h_c^2} (\theta - \sin \theta) - \frac{R}{h_c} (1 - \cos \theta) \left[ 1 - \frac{R}{h_c} (1 - \cos \theta) \right] \right\} \\ & - \frac{I_c}{h_c^2 t_c} \left( 2 \frac{d}{h_c} \sin \theta \cos \theta + \frac{R}{h_c} \sin^2 \theta \right) \end{aligned} \quad (31)$$

All terms are identical to those in equation (17) except the second term on the right side (underlined). Again, equation (31) will not be used in the subsequent analyses.

For the concentrated vertical loading,  $F$ , the following relationship holds:

$$\frac{\nu_{yz}}{E_z} = \frac{\nu_{zy}}{E_y} \quad (32)$$

However, the relationship does not apply to a distributed vertical loading.

#### Evaluation of Shear Modulus $G_{yz}$

Figure 4 shows the transverse shear deformation of a corrugated core unit element  $0A0'B$  subjected to shearing stress,  $\tau$ , at the four edges of the unit element. This is equivalent to the application of concentrated vertical and horizontal loads

( $F = \tau h_c$  and  $H = \tau p$ ) at the two ends of the corrugation leg  $00'$ . As a result, point 0 is displaced to position  $0_{FH}$  with the vertical and horizontal displacements  $\delta_z$  and  $\delta_y$ . If force  $F$  is acting alone, point 0 will move to point  $0_F$  with the two displacement components  $\delta_y^F$  and  $\delta_z^F$ . Alternatively, if force  $H$  is acting alone, point 0 will move to position  $0_H$  with displacements  $\delta_y^H$  and  $\delta_z^H$ . Displacements  $\delta_y$  and  $\delta_z$  may be expressed

$$\delta_y = \delta_y^H - \delta_y^F \quad (33)$$

$$\delta_z = \delta_z^F - \delta_z^H \quad (34)$$

and the effective shear strain,  $\gamma$ , can be written

$$\gamma = \frac{\delta_y}{h_c} + \frac{\delta_z}{p} \quad (35)$$

Substituting equations (33) and (34) into equation (35) and using equations (11), (16), (21), and (27), the shear modulus  $G_{yz}$  can then be written in the form

$$G_{yz} = \frac{\tau}{\gamma} = \frac{E_c I_c}{h_c^3 \left( \frac{h_c}{p} B_z^F - 2B_z^H + \frac{p}{h_c} B_y^H \right)} \quad (36)$$

when  $t_f$  equals  $t_c$ , the expressions  $B_z^F$ ,  $B_z^H$ , and  $B_y^H$  in equation (36) reduce respectively to the expressions  $B_3$ ,  $B_4$ , and  $B_6$  in reference 4.

#### Evaluation of Poisson Ratio $\nu_{yx}$

The Poisson ratio  $\nu_{yx}$  is associated with loading in the  $x$ -direction only. The effective strain of the corrugated core in the  $x$ -direction,  $\epsilon_x$ , is given by

$$\epsilon_x = \frac{\sigma_x}{E_x} = \frac{\sigma_{xc}}{E_c} \quad (37)$$

where  $\sigma_x$  is the effective stress in the corrugated core in the  $x$ -direction and  $\sigma_{xc}$  is the stress in the corrugation leg in the  $x$ -direction. The two stresses  $\sigma_x$  and  $\sigma_{xc}$  are related as follows:

$$\sigma_x = \sigma_{xc} \frac{\ell t_c}{p h_c} \left[ 1 - \frac{f}{\ell} \left( 1 - \frac{t_f}{t_c} \right) \right] \quad (38)$$

where equation (1) is used.

The effective strain in the  $y$ -direction of the sandwich core,  $\varepsilon_y$ , due to loading in the  $x$ -direction can be written

$$\varepsilon_y = -\frac{1}{p} \int_0^\ell \varepsilon_s \cos \psi \, ds \quad (39)$$

where  $\varepsilon_s$  is the strain in the  $s$ -direction due to loading in the  $x$ -direction and is given by

$$\varepsilon_s = \nu_c \varepsilon_x \quad (40)$$

where  $\nu_c$  is the Poisson ratio of the sandwich core material.

After the integration of equation (39) with equations (37) and (40) taken into consideration,

$$\varepsilon_y = -\frac{\nu_c \sigma_{xc}}{E_c} \quad (41)$$

From equations (37) and (41),

$$\nu_{yx} = -\frac{\varepsilon_y}{\varepsilon_x} = \nu_c \quad (42)$$

#### Evaluation of Poisson Ratio $\nu_{xy}$

The Poisson ratio  $\nu_{xy}$  is associated with loading in the  $y$ -direction only. Using equation (11), the effective strain in the corrugated core in the  $y$ -direction,  $\varepsilon_y$ , is given by

$$\varepsilon_y = \frac{\delta_y^H}{p} = \frac{H h_c^3 B^H}{p E_c I_c} \quad (43)$$



The strain in the  $s$ -direction,  $\epsilon_s^H$ , due to loading  $H$  is given by

$$\epsilon_s^H = \frac{H \cos \psi}{E_c t_i} \quad (44)$$

The effective strains in the corrugated core, in the  $x$ -direction,  $\epsilon_x$ , can be obtained from the integral

$$\epsilon_x = -\frac{1}{\ell} \int_0^{\ell} \epsilon_{xc} ds \quad (45)$$

where  $\epsilon_{xc}$  is the strain in the corrugation leg in the  $x$ -direction due to loading  $H$ , and is given by

$$\epsilon_{xc} = \nu_c \epsilon_s^H \quad (46)$$

Substituting equations (44) and (46) into equation (45) and integrating,

$$\epsilon_x = -\frac{H \nu_c p}{\ell t_c E_c} \left[ 1 - \frac{f}{p} \left( 1 - \frac{t_c}{t_f} \right) \right] \quad (47)$$

The Poisson ratio  $\nu_{xy}$  is then given by

$$\nu_{xy} = -\frac{\epsilon_x}{\epsilon_y} \quad (48)$$

$$= \frac{p^2}{\ell t_c} \frac{\nu_c I_c}{h_c^3 B_y H} \left[ 1 - \frac{f}{p} \left( 1 - \frac{t_c}{t_f} \right) \right] \quad (49)$$

The Poisson ratios  $\nu_{xy}$  and  $\nu_{yx}$  are related as follows:

$$\frac{\nu_{xy}}{E_y} = \frac{\nu_{yx}}{E_x} \left[ 1 - \frac{f}{p} \left( 1 - \frac{t_c}{t_f} \right) \right] \left[ 1 - \frac{f}{\ell} \left( 1 - \frac{t_f}{t_c} \right) \right] \quad (50)$$

If  $t_f$  equals  $t_c$  or if the superplastic deformation is constant volume (that is, if the condition of equation (4) is imposed), then we have the familiar expression

$$\frac{\nu_{xy}}{E_y} = \frac{\nu_{yx}}{E_x} \quad (51)$$

### Evaluation of Poisson Ratio $\nu_{zx}$

The Poisson ratio  $\nu_{zx}$  is associated with loading in the  $x$ -direction only. The effective strain of the corrugated core, in the  $z$ -direction,  $\varepsilon_z$ , can be written

$$\varepsilon_z = -\frac{1}{h_c} \int_0^{\ell} \varepsilon_s \sin \psi \, ds \quad (52)$$

After substituting equations (37) and (40) into equation (52) and integrating,

$$\varepsilon_z = -\frac{\nu_c \sigma_{xc}}{E_c} \quad (53)$$

From equations (37) and (53), the Poisson ratio  $\nu_{zx}$  can be written

$$\nu_{zx} = -\frac{\varepsilon_z}{\varepsilon_x} = \nu_c \quad (54)$$

### Evaluation of Poisson Ratio $\nu_{xz}$

The Poisson ratio  $\nu_{xz}$  is associated with loading in the  $z$ -direction only. From equation (21), the corrugated core strain in the  $z$ -direction,  $\varepsilon_z$ , is given by

$$\varepsilon_z = \frac{\delta_z^F}{h_c} = \frac{F B_z^F}{h_c E_c I_c} \quad (55)$$

In addition, the corrugated core strain in the  $x$ -direction,  $\varepsilon_x$ , is expressed as

$$\varepsilon_x = -\frac{1}{\ell} \int_0^{\ell} \tilde{\varepsilon}_{xc} \, ds \quad (56)$$

where  $\tilde{\varepsilon}_{xc}$  is the strain in the corrugation leg in the  $x$ -direction due to loading in the  $z$ -direction, and is given by

$$\tilde{\varepsilon}_{xc} = \nu_c \varepsilon_s^F \quad (57)$$

where  $\varepsilon_s^F$  is the corrugation leg strain in the s-direction due to loading  $F$ , and is given by

$$\varepsilon_s^F = \frac{F \sin \psi}{E_c t_i} \quad (58)$$

Integrating equation (56) in the light of equations (57) and (58), we have

$$\varepsilon_x = -\frac{\nu_c F h_c}{\ell t_c E_c} \quad (59)$$

The Poisson ratio  $\nu_{xz}$  is then given by

$$\nu_{xz} = -\frac{\varepsilon_x}{\varepsilon_z} = \frac{I_c}{\ell t_c h_c} \frac{\nu_c}{B_z^F} \quad (60)$$

The two Poisson ratios  $\nu_{zx}$  and  $\nu_{xz}$  can be related by the equation

$$\frac{\nu_{xz}}{E_z} = \frac{\nu_{zx}}{E_x} \left[ 1 - \frac{f}{\ell} \left( 1 - \frac{t_f}{t_c} \right) \right] \quad (61)$$

If  $t_f$  equals  $t_c$  or if  $f$  equals 0, then equation (61) becomes

$$\frac{\nu_{xz}}{E_z} = \frac{\nu_{zx}}{E_x} \quad (62)$$

For the superplastic incompressible deformation, equation (61) can be reduced to

$$\frac{\nu_{xz}}{E_z} = \frac{\nu_{zx}}{E_x} \frac{p}{\ell} \frac{t_f}{t_c} \quad (63)$$

## ELASTIC CONSTANTS FOR HONEYCOMB CORE

As shown in figure 5, the honeycomb core is made up of corrugated strips joined together at the corrugation flat segments, with the corrugation axis oriented normal to the sandwich middle surface. Therefore, by taking the coordinate system shown in the figure, the results obtained for the previous case can be applied directly to the honeycomb core if  $t_c$  is set equal to  $t_f$ .

## EFFECT OF FACE SHEETS ON MODULUS OF ELASTICITY $E_z$

The following calculations are presented to evaluate the effect of the face sheets on the stiffness in the  $z$ -direction,  $E_z$ , when bonded to the corrugated core. Let  $\bar{E}_z$  denote the modulus of elasticity in the  $z$ -direction when the deformation of the corrugated core is constrained by the face sheets.

As shown in figure 6, if the corrugation leg is not constrained by the two face sheets and is subjected to loading  $H$  and  $F$ , point 0 will move to  $0_1$ . The horizontal and the vertical components of this displacement are given by equations (27) and (21), respectively.

$$\delta_y^F = \frac{Fh_c^3}{E_c I_c} B_y^F \quad (27)$$

$$\delta_z^F = \frac{Fh_c^3}{E_c I_c} B_z^F \quad (21)$$

If the corrugation leg is constrained by the face sheets, point 0 will move only to point  $0_2$ . This constraint is equivalent to bringing point 0 back from position  $0_1$  to position  $0_2$  by means of horizontal force  $H$ .

The horizontal and vertical components of the displacement  $\overline{0_1 0_2}$  due to  $H$  are given by equations (11) and (16), respectively.

$$\delta_y^H = \frac{Hh_c^3}{E_c I_c} B_y^H \quad (11)$$

$$\delta_z^H = \frac{Hh_c^3}{E_c I_c} B_z^H \quad (16)$$

The horizontal component,  $\bar{\delta}_y$ , of the displacement  $\overline{00_2}$  is due to the compression (neglecting buckling) of the face sheets, and can be written

$$\bar{\delta}_y = \frac{Hp}{2t_s E_c} \quad (64)$$

where  $t_s$  is the thickness of the face sheets. From the relation

$$\bar{\delta}_y = \delta_y^F - \delta_y^H \quad (65)$$

it is possible to express  $H$  in terms of  $F$  with the aid of equations (27) and (11) as follows:

$$H = F \frac{B_y^F}{B_y^H} \frac{1}{1 + \frac{pI_c}{2t_s h_c^3 B_y^H}} \quad (66)$$

The vertical component,  $\bar{\delta}_z$ , of the displacement  $\bar{00}_2$  is given by

$$\bar{\delta}_z = \delta_z^F - \delta_z^H \quad (67)$$

which, with reference to equations (21) and (16), becomes

$$\bar{\delta}_z = \frac{F h_c^3}{E_c I_c} B_z^F \left( 1 - \frac{B_y^F}{B_y^H} \frac{B_z^H}{B_z^F} \frac{1}{1 + \frac{pI_c}{2t_s h_c^3 B_y^H}} \right) \quad (68)$$

Using equations (19), (24), and (30), the modulus of elasticity  $\bar{E}_z$  is then given by

$$\bar{E}_z = \frac{\frac{F}{p}}{\frac{\bar{\delta}_z}{h_c}} \quad (69)$$

$$= \frac{E_z}{1 - \nu_{yz} \nu_{zy} \frac{1}{1 + \frac{pI_c}{2t_s h_c^3 B_y^H}}} \quad (70)$$

indicating that the stiffness of the corrugated core in the  $z$ -direction is greatly enhanced when the core is bonded to the face sheets.

## CORRUGATED CORE BENDING STIFFNESS

The bending stiffness in the  $x$ -direction of the SPF/DB corrugated sandwich core may be written

$$D_x = E_c \bar{I}_c \quad (71)$$

where

$D_x$  bending stiffness in the  $x$ -direction per unit width of a beam cut from the SPF/DB corrugated sandwich core

$\bar{I}_c$  moment of inertia taken about the horizontal centroidal axis of the corrugation cross section per unit width of the corrugation cross section parallel to the  $yz$ -plane, or

$$\begin{aligned} \bar{I}_c = \frac{h_c^3 t_c}{p} \left\{ \frac{1}{4} \frac{f}{h_c} \frac{t_f}{t_c} \left( 1 + \frac{1}{3} \frac{t_f^2}{h_c^2} \right) + \frac{2}{3} \frac{d^3}{h_c^3} \left( \sin^2 \theta + \frac{1}{4} \frac{t_c^2}{d^2} \cos^2 \theta \right) \right. \\ \left. + \frac{R}{h_c} \left[ \frac{\theta}{2} - 2 \frac{R^2}{h_c^2} \sin \theta - \frac{R}{h_c} \left( 2 - 3 \frac{R}{h_c} \right) (\theta - \sin \theta) \right] \right\} \quad (72) \end{aligned}$$

The bending stiffness in the  $y$ -direction of the SPF/DB corrugated core is very small and is of the order of  $E_c I_i$ .

## NUMERICAL RESULTS

In obtaining the numerical values for the effective elastic constants of the SPF/DB corrugated core, it was assumed that  $R$  was equal to  $t_f$  and that the corrugated core material was a titanium alloy 6Al-4V having the following physical properties:

$$E_c = E_{Ti} = 1.1 \times 10^{11} \text{ N/m}^2 \quad (16 \times 10^6 \text{ psi})$$

$$G_c = G_{Ti} = 4.3 \times 10^{10} \text{ N/m}^2 \quad (6.2 \times 10^6 \text{ psi})$$

$$\nu_c = \nu_{Ti} = 0.33$$

$$\rho_c = \rho_{Ti} = 4.47 \text{ gr/cm}^3 \text{ (0.16 lb/in}^3\text{)}$$

where  $\rho_c$  is the density of the core material.

Figure 7 shows the variation of the corrugation angle,  $\theta$ , with the thickness of the diagonal segment,  $t_c$ , after superplastic expansion. It is apparent that  $t_c$  is insensitive to changes in  $t_f/h_c$ .

Figures 8 to 16 present graphs for evaluating the major effective elastic constants for the SPF/DB corrugated core. The elastic constants are plotted against  $p/h_c$ , with  $t_f/h_c$  and  $\theta$  as parameters. Envelopes of optimum points or envelopes of limit points are also shown in the figures. These envelopes correspond to the case when  $f = 0$  (that is, triangular truss core).

Figure 8 shows that  $E_y$  is sensitive to the values of  $t_f$  and  $\theta$ , but relatively insensitive to the change of  $p$  (or  $f$ ), and that  $E_y$  is very small. This indicates that the corrugated core has negligible stiffness in the y-direction.

Figure 9 shows that  $E_z$  is also very small, and is sensitive to the changes of both  $t_f$  and  $p$ , but is insensitive to the change of  $\theta$ . For a given  $\theta$ ,  $E_z$  reaches its maximum (or optimum) value at  $f = 0$ . As will be seen later, the lateral (that is, y-direction) constraint provided by the face sheets will increase the value of  $E_z$  by several orders of magnitude.

The shear modulus  $G_{xy}$  shown in figure 10 is also sensitive to  $\theta$ . As is expected,  $G_{xy}$  increases with increasing values of  $p$  (or  $f$ ).

Figure 11 shows that  $G_{yz}$  is very sensitive to the values of  $p$  (or  $f$ ). For a given  $\theta$ ,  $G_{yz}$  reaches maximum value at  $f = 0$ . Because of the steepness of the curves, a slight increase of  $f$  above 0 drastically reduces the value of  $G_{yz}$ .

Figure 12 shows that  $G_{zx}$  decreases with increasing values of  $p$  (or  $f$ ) and that maximum value for a given  $\theta$  occurs when the corrugation degenerates into a triangular truss core.

The value of Poisson ratio  $\nu_{xy}$ , shown in figure 13, is small. It is sensitive to the values of  $t_f$  and  $\theta$ , and increases as  $p$  increases.

Figure 14 shows the plots of Poisson ratios  $\nu_{yz}$  and  $\nu_{zy}$ . It is apparent that  $\nu_{yz}$  is greater than unity. This is quite common in the truss type of structure, which is not a continuum. For example, if a square truss is pulled diagonally into a rhombic shape, the Poisson ratio will be greater than unity. Both  $\nu_{yz}$  and  $\nu_{zy}$  are sensitive to both  $p$  and  $\theta$ , but insensitive to the value of  $t_f$ .

Figure 15 shows that the value of Poisson ratio  $\nu_{xz}$  is also small. It is quite sensitive to the change of  $t_f$  and less sensitive to the values of  $p$  and  $\theta$ .

Figure 16 presents graphs for evaluating the modulus of elasticity  $\bar{E}_z$ . Because of the constraint of the face sheets,  $\bar{E}_z$  is several orders of magnitude larger than  $E_z$ .  $\bar{E}_z$  is sensitive to the change of  $p$  at low values of  $t_f$ .

Figure 17 shows plots of the bending stiffness,  $D_x$ , of the SPF/DB corrugated core. In the plots,  $D_x$  is normalized by  $D_c = \frac{E_c h_c^3}{12}$  (bending stiffness per unit width of the solid core with height  $h_c$ ). For given values of  $\theta$  and  $t_f$ , the triangular truss core has the lowest bending stiffness.

For comparison, corresponding graphs evaluating the elastic constants for the honeycomb core are also presented (figs. 18 to 26). All the elastic constants have been normalized and may be used for any material, except for  $G_{yz}$ ,  $\nu_{xy}$ , and  $\nu_{xz}$ , which are for titanium only. For a material other than titanium,  $G_{yz}$ ,  $\nu_{xy}$ , and  $\nu_{xz}$  (figs. 22, 24, and 26) must be multiplied by  $\frac{E}{G} \frac{G_{Ti}}{E_{Ti}}$ ,  $\frac{\nu}{\nu_{Ti}}$ , and  $\frac{\nu}{\nu_{Ti}}$ , respectively.

## COMPARISON WITH HONEYCOMB CORE

This section compares the stiffness of the SPF/DB titanium alloy corrugated core with that of the honeycomb (aluminum or titanium) core when both types of sandwich core have the same density.

Let  $( )_{SP}$  and  $( )_{HC}$  denote, respectively, the quantities associated with the SPF/DB corrugated core and the honeycomb core. The densities,  $\rho$ , of these two types of sandwich core may be written

$$\rho_{SP} = \left( \frac{t_f}{h_c} \right)_{SP} \rho_{Ti} \quad (73)$$



$$\rho_{HC} = \left( \frac{t_c \ell}{p h_c} \right)_{HC} \rho_c \quad (74)$$

where  $\rho_c$  is the density of the honeycomb core material. From the condition  $\rho_{SP} = \rho_{HC}$ , equations (73) and (74) may be related to find the geometric parameter  $t_f/h_c$  for the SPF/DB core as follows:

$$\left( \frac{t_f}{h_c} \right)_{SP} = \left( \frac{t_c \ell}{p h_c} \right)_{HC} \frac{\rho_c}{\rho_{Ti}} \quad (75)$$

A typical honeycomb core for application to high speed aircraft is characterized by the following geometric parameters:

$$t_c = t_f \approx R, \quad \theta \approx 60^\circ \quad (76)$$

$$\left( \frac{f}{h_c} \right)_{HC} = 0.4053 \quad (77)$$

$$\left( \frac{\ell}{h_c} \right)_{HC} = 1.5600 \quad (78)$$

$$\left( \frac{t_c}{h_c} \right)_{HC} = 0.0147 \quad (79)$$

$$\left( \frac{p}{h_c} \right)_{HC} = 0.9825 \quad (80)$$

For the aluminum honeycomb core, the material properties are:

$$E_c = E_{Al} = 6.8948 \times 10^{10} \text{ N/m}^2 \quad (10 \times 10^6 \text{ psi})$$

$$G_c = G_{Al} = 2.7579 \times 10^{10} \text{ N/m}^2 \quad (4 \times 10^6 \text{ psi})$$

$$\nu_c = \nu_{Al} = 0.36$$

$$\rho_c = \rho_{Al} = 2.77 \text{ gr/cm}^3 \quad (0.100 \text{ lb/in}^3)$$

Using the numerical values given above, equation (75) yields the following geometric parameters for the SPF/DB corrugated core corresponding to

$$\left(\frac{t_f}{h_c}\right)_{HC} = 0.0147. \text{ When the honeycomb core is aluminum,}$$

$$\left(\frac{t_f}{h_c}\right)_{SP} = 0.0146 \quad (81)$$

When the honeycomb core is titanium,

$$\left(\frac{t_f}{h_c}\right)_{SP} = 0.02334 \quad (82)$$

From figures 18, 21, and 23 the three major elastic constants for the honeycomb core,  $E_x$ ,  $G_{xy}$ , and  $G_{zx}$ , may be replotted against  $t_f/h_c$  for  $\theta = 60^\circ$  and  $p/h_c = 0.9825$  (eq. (80)). This is shown in figure 27.

Likewise, from figures 16, 11, and 12, the optimum values of the corresponding elastic constants for the SPF/DB corrugated core,  $\bar{E}_z$ ,  $G_{yz}$ , and  $G_{zx}$ , may be replotted against  $t_f/h_c$  for  $\theta = 60^\circ$  (fig. 28).

Because of the different orientations of the coordinate axes of the two types of sandwich cores,  $E_x$ ,  $G_{xy}$ , and  $G_{zx}$  (honeycomb core moduli) should be compared respectively with their counterparts,  $\bar{E}_z$ ,  $G_{yz}$ , and  $G_{zx}$  (SPF/DB corrugated core moduli).

Because  $(E_x)_{HC}$  is insensitive to the existence of the face sheets, it is used to compare with  $(\bar{E}_z)_{SP}$ , which is insensitive to the change of thickness of the face sheets.

Given that  $E_c = E_{Al}$  and  $G_c = G_{Al}$  for the aluminum honeycomb core and that  $E_c = E_{Ti}$  and  $G_c = G_{Ti}$  for the titanium honeycomb core, figures 27 and 28 allow the comparisons between the elastic constants as shown in tables 1 and 2.

From the tables, it becomes apparent that the stiffness in the sandwich thickness direction of the SPF/DB corrugated core is lower than that of the honeycomb core (aluminum or titanium). The transverse shear stiffness of the SPF/DB corrugated core is greater than that of the honeycomb core.

## CONCLUDING REMARKS

In this report the formulae and related graphs are developed to evaluate the major effective elastic constants for a superplastically formed/diffusion-bonded (SPF/DB) corrugated sandwich core. Assuming uniform thickness of the corrugation leg, the formulae were used to evaluate the effective elastic constants for a honeycomb sandwich core.

A comparison of the stiffness of the two types of sandwich core was made under conditions of equal sandwich core density. It was found that the stiffness in the thickness direction of the optimum SPF/DB corrugated core (that is, triangular truss core) was lower than that of the honeycomb core, and that the former had a higher transverse shear stiffness than the latter. Alternatively, for the same transverse shear stiffness, the SPF/DB corrugated core had lower core density than the honeycomb core, but its thickness stiffness was lower than that of the honeycomb core.

For the SPF/DB corrugated sandwich core, it was found that increasing the length of the crest or trough increased the bending stiffness but reduced the transverse shear stiffness.

Dryden Flight Research Center  
National Aeronautics and Space Administration  
Edwards, Calif., June 27, 1979

## REFERENCES

1. Pulley, John: Evaluation of Low-Cost Titanium Structure for Advanced Aircraft. NASA CR-145111, 1976.
2. Ueng, Charles E. S.: Superplastically Formed New Sandwich Cores. Transportation Eng. J., American Soc. Civil Eng., vol. 104, July 1978, pp. 437-447.
3. Ueng, C. E. S.; Underwood, E. E.; and Liu, T. L.: Shear Modulus of Superplastically Formed Sandwich Cores. Trends in Computerized Structural Analysis and Synthesis. Pergamon Press, 1978, pp. 393-397.
4. Libove, Charles; and Hubka, Ralph E.: Elastic Constants for Corrugated-Core Sandwich Plates. NACA TN 2289, 1951.
5. Roark, Raymond J.: Formulas for Stress and Strain. Third ed. McGraw-Hill Book Co., Inc., 1954.

TABLE 1.—COMPARISON BETWEEN ELASTIC CONSTANTS FOR  
ALUMINUM HONEYCOMB CORE AND SPF/DB TITANIUM CORRUGATED CORE  
[ $\rho_{SP} = \rho_{HC}$ ]

Aluminum honeycomb core	SPF/DB titanium corrugated core	$( )_{SP} / ( )_{HC}$
$\frac{t_f}{h_c} = 0.0147, \theta = 60^\circ$	$\frac{t_f}{h_c} = 0.0146, \theta = 60^\circ, f = 0$	----
$E_x = 14.4790 \times 10^8 \text{ N/m}^2$ ( $2.1 \times 10^5 \text{ psi}$ )	$\bar{E}_z = 8.2737 \times 10^8 \text{ N/m}^2$ ( $1.2 \times 10^5 \text{ psi}$ )	0.57
$G_{xy} = 2.4821 \times 10^8 \text{ N/m}^2$ ( $3.6 \times 10^4 \text{ psi}$ )	$G_{yz} = 2.7358 \times 10^8 \text{ N/m}^2$ ( $3.968 \times 10^4 \text{ psi}$ )	1.10
$G_{zx} = 2.5924 \times 10^8 \text{ N/m}^2$ ( $3.76 \times 10^4 \text{ psi}$ )	$G_{zx} = 4.7022 \times 10^8 \text{ N/m}^2$ ( $6.82 \times 10^4 \text{ psi}$ )	1.81

TABLE 2.—COMPARISON BETWEEN ELASTIC CONSTANTS FOR  
TITANIUM HONEYCOMB CORE AND SPF/DB TITANIUM CORRUGATED CORE  
[ $\rho_{SP} = \rho_{HC}$ ]

Titanium honeycomb core	SPF/DB titanium corrugated core	$( )_{SP} / ( )_{HC}$
$\frac{t_f}{h_c} = 0.0147, \theta = 60^\circ$	$\frac{t_f}{h_c} = 0.02334, \theta = 60^\circ, f = 0$	----
$E_x = 23.1664 \times 10^8 \text{ N/m}^2$ ( $3.36 \times 10^5 \text{ psi}$ )	$\bar{E}_z = 13.4586 \times 10^8 \text{ N/m}^2$ ( $1.9520 \times 10^5 \text{ psi}$ )	0.58
$G_{xy} = 3.8473 \times 10^8 \text{ N/m}^2$ ( $5.58 \times 10^4 \text{ psi}$ )	$G_{yz} = 4.5740 \times 10^8 \text{ N/m}^2$ ( $6.8340 \times 10^4 \text{ psi}$ )	1.22
$G_{zx} = 4.0182 \times 10^8 \text{ N/m}^2$ ( $5.8280 \times 10^4 \text{ psi}$ )	$G_{zx} = 7.5663 \times 10^8 \text{ N/m}^2$ ( $1.0974 \times 10^5 \text{ psi}$ )	1.88

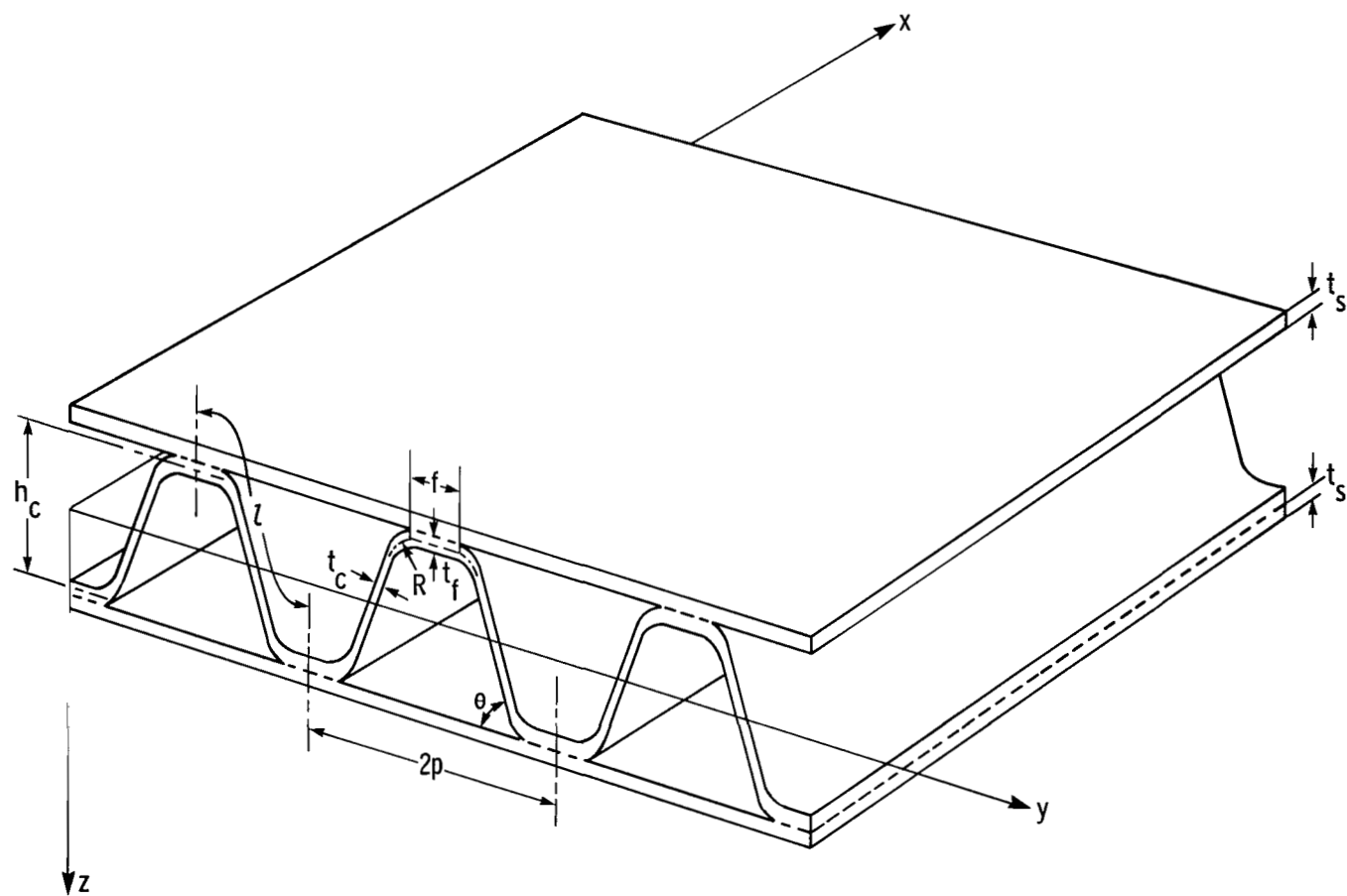


Figure 1. Geometry of superplastically formed/diffusion-bonded corrugated core sandwich plate.

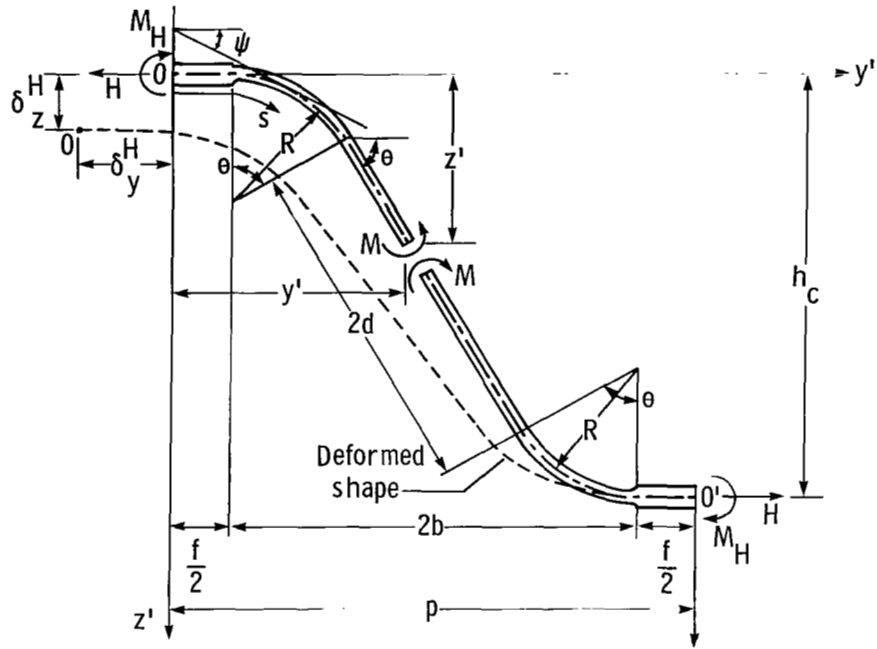


Figure 2. Free body diagram of corrugation leg under horizontal loading.  $M_H = \frac{1}{2} H h_c$ .

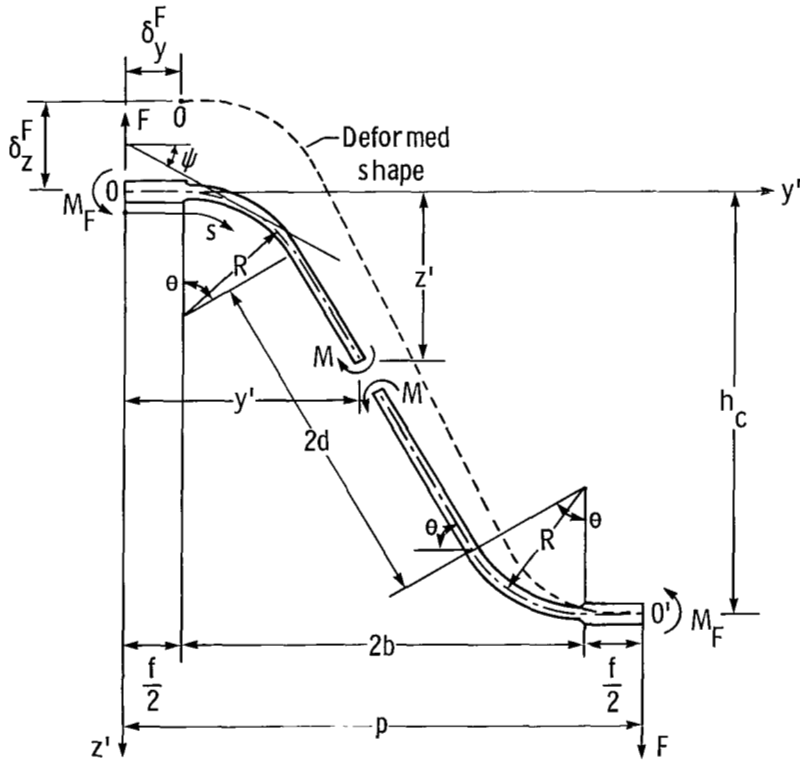


Figure 3. Free body diagram of corrugation leg under vertical loading.  $M_F = \frac{1}{2} F p$ .

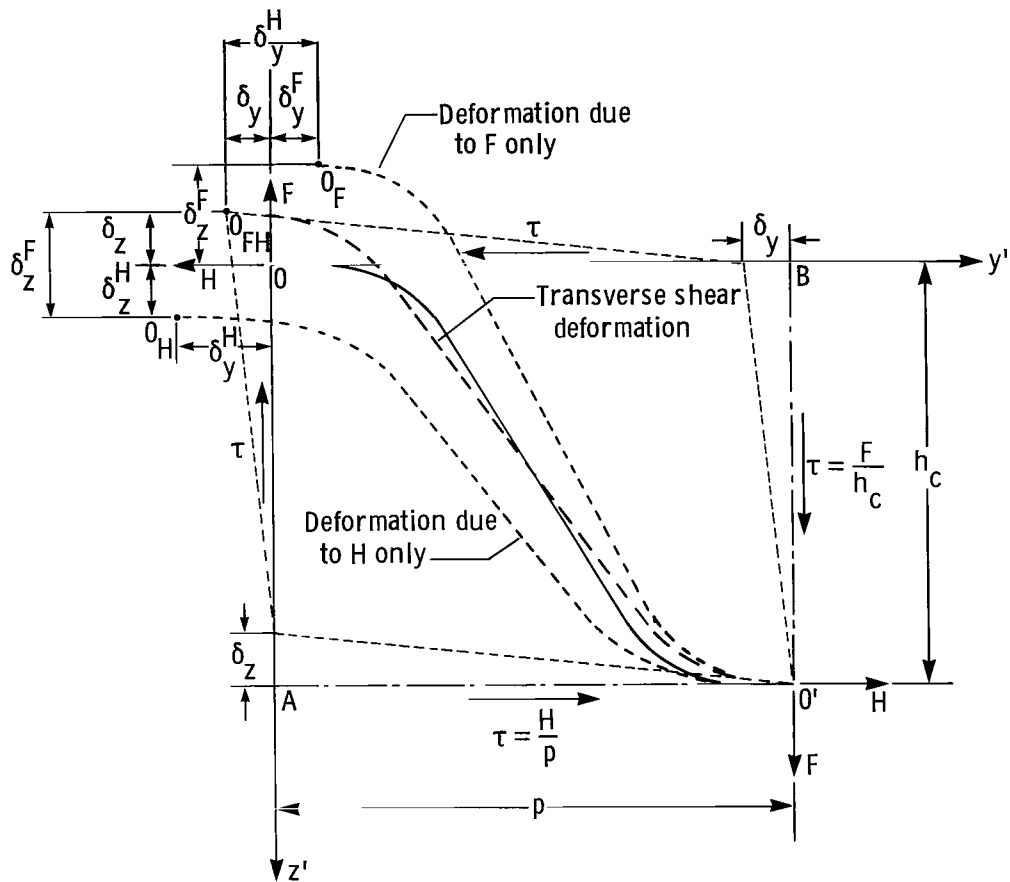


Figure 4. Transverse shear deformation of the corrugated core unit element.

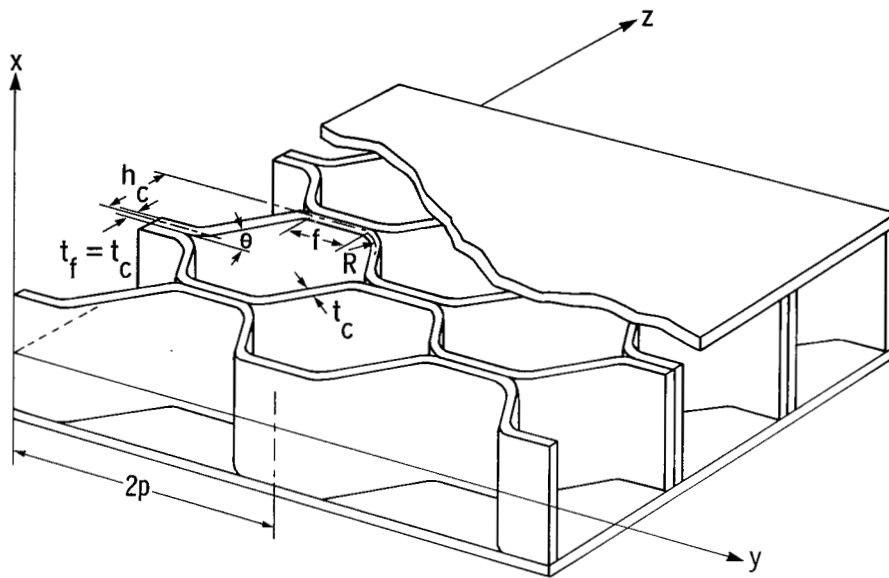


Figure 5. Geometry of honeycomb core sandwich plate.

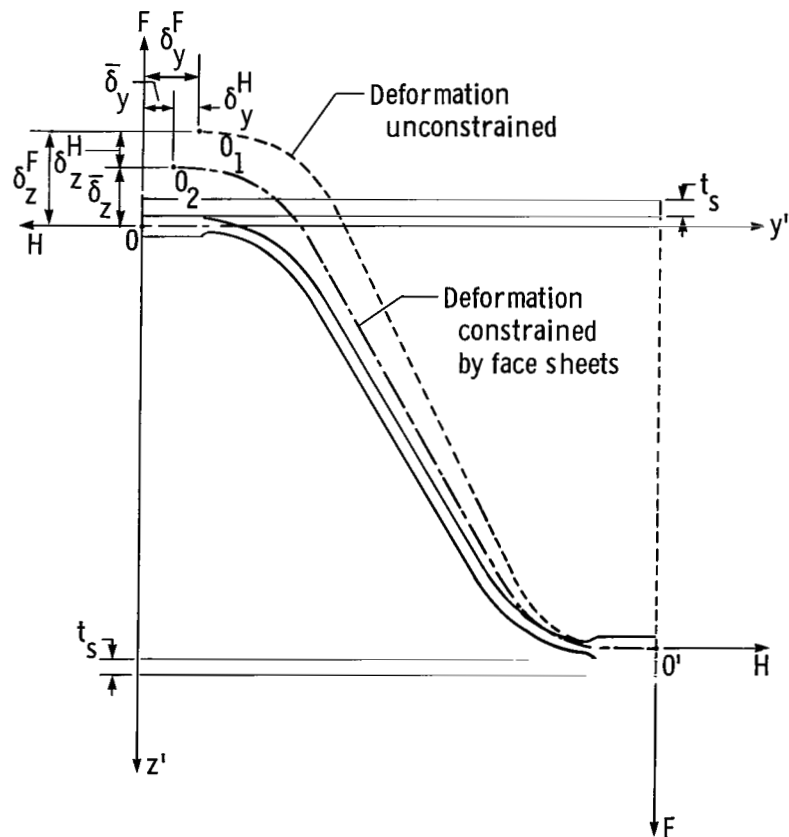


Figure 6. Constrained deformation of corrugation leg.



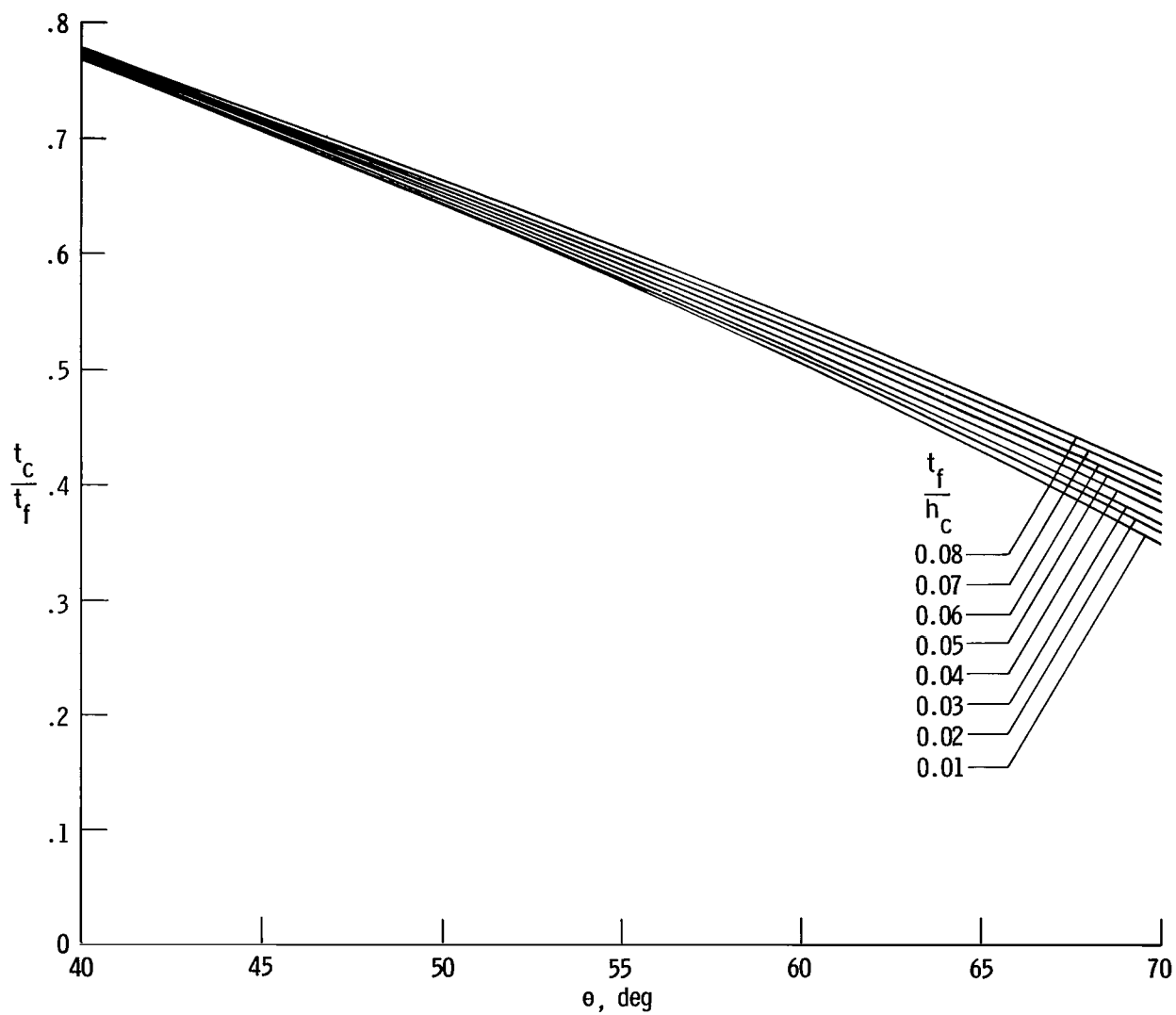


Figure 7. Corrugation leg straight diagonal segment thickness versus corrugation angle.  $R = t_f$ .

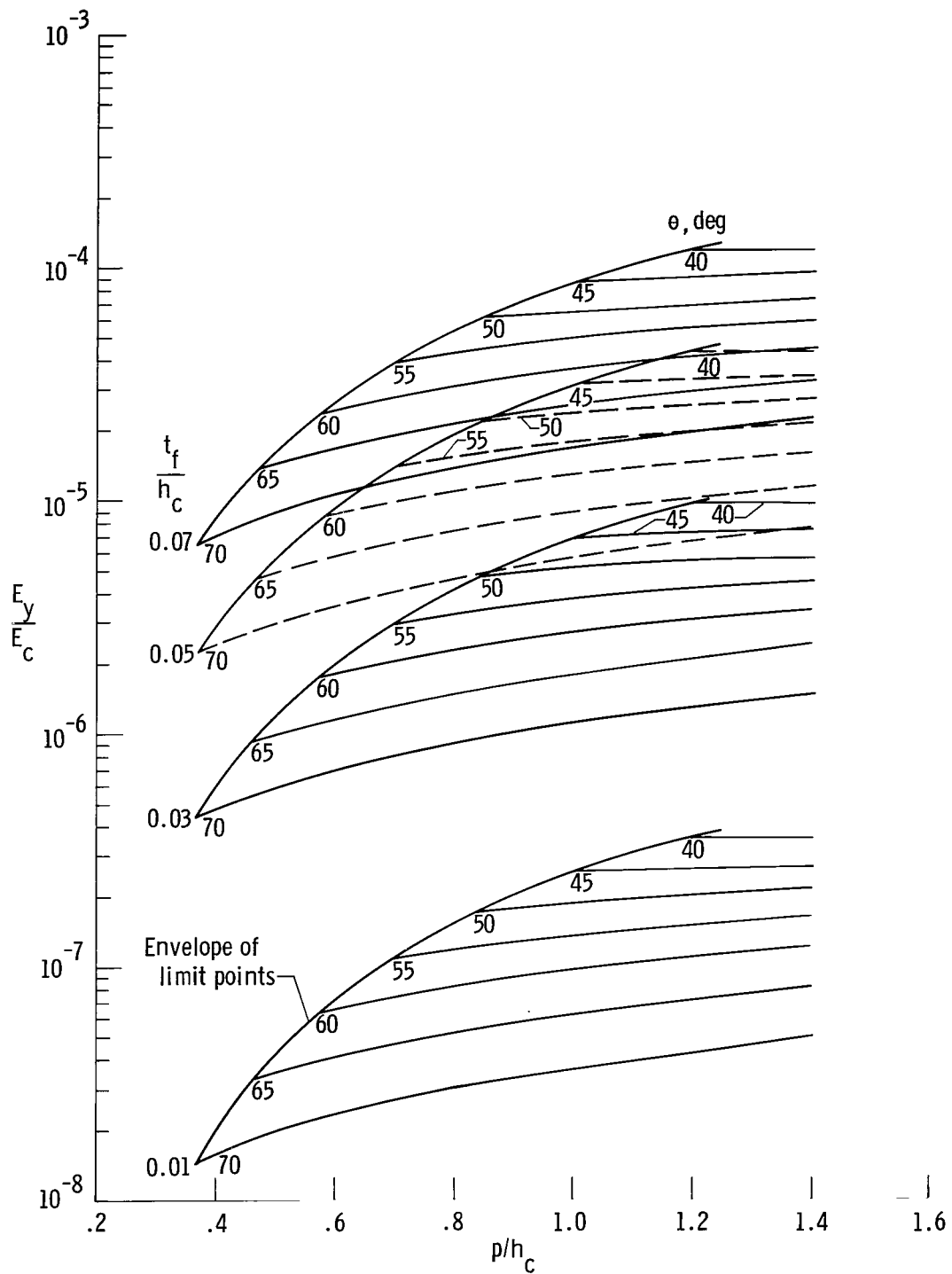


Figure 8. Modulus of elasticity  $E_y$  for SPF/DB corrugated core.  $R = t_f$ .

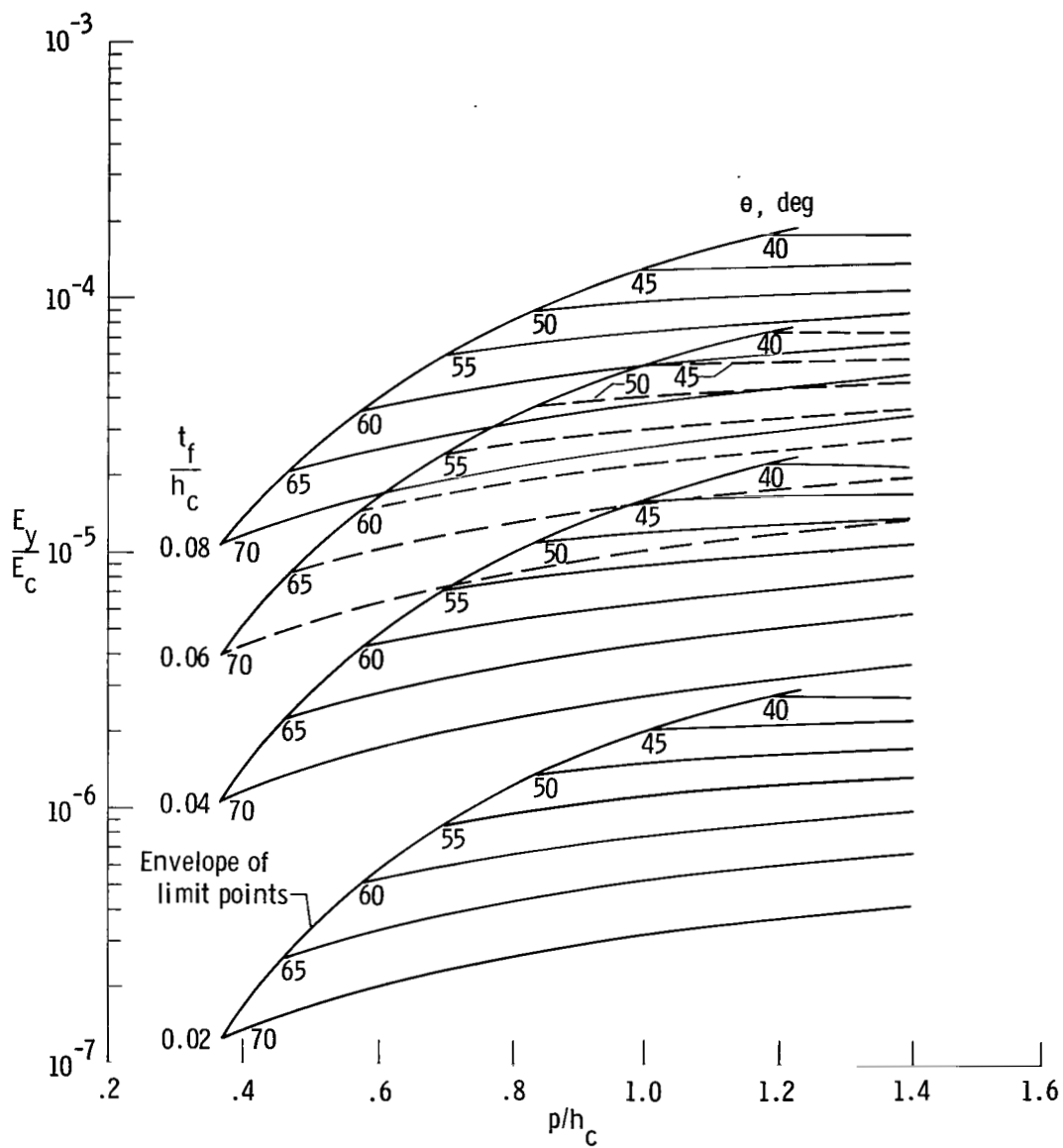


Figure 8. Concluded.

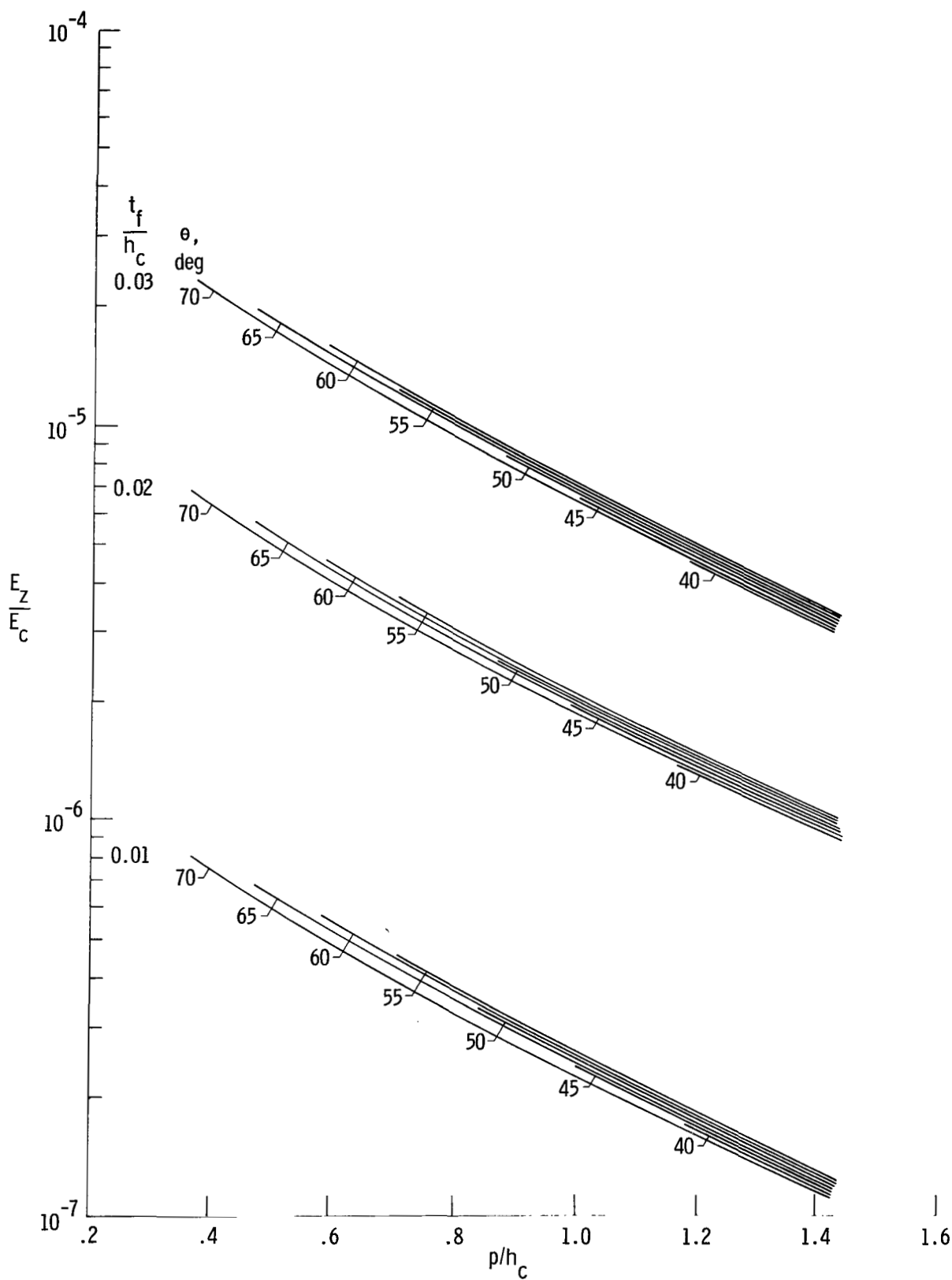


Figure 9. Modulus of elasticity  $E_z$  for SPF/DB corrugated core.  $R = t_f$ .

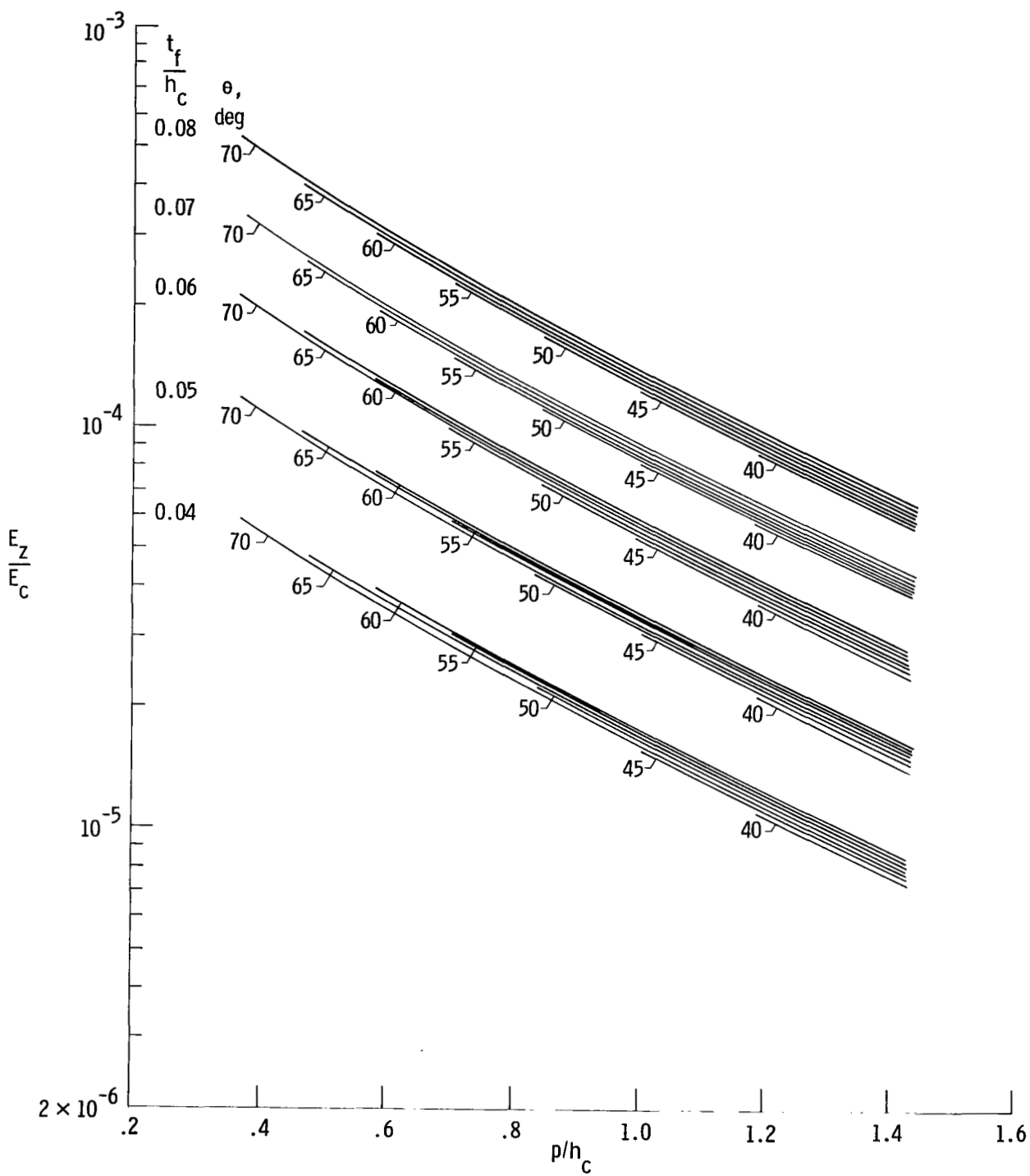


Figure 9. Concluded.

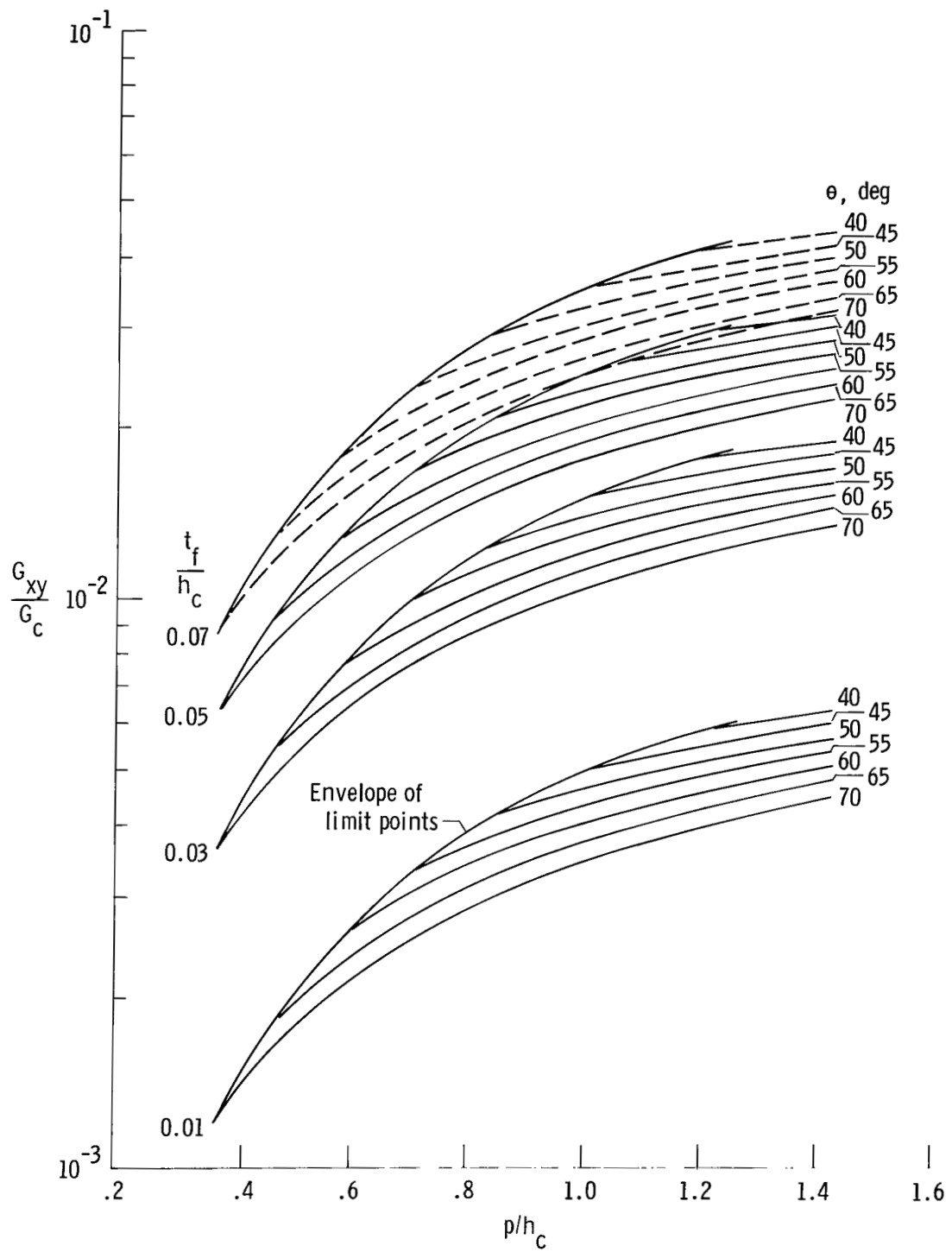


Figure 10. Shear modulus  $G_{xy}$  for SPF/DB corrugated core.  
 $R = t_f$ .

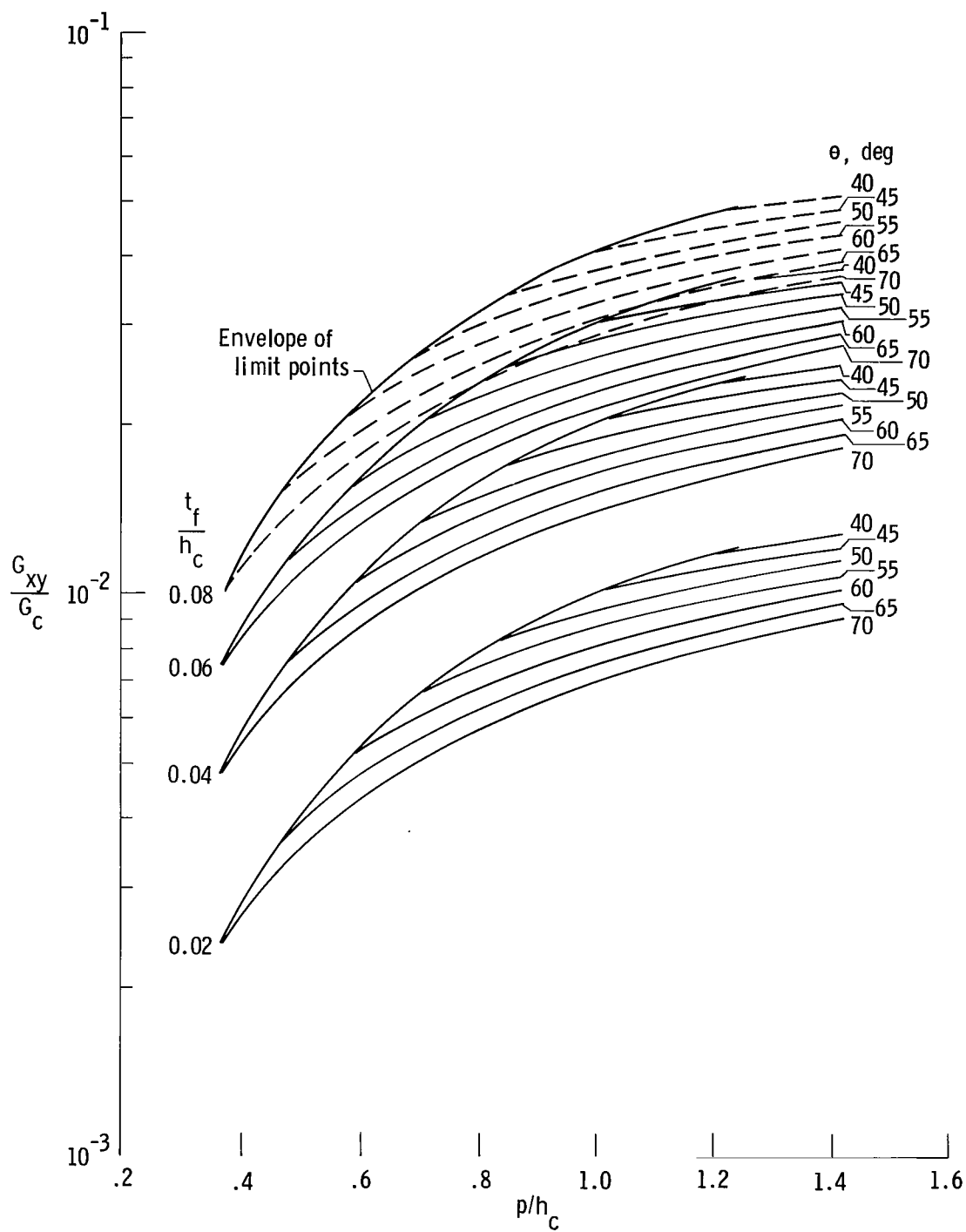


Figure 10. Concluded.

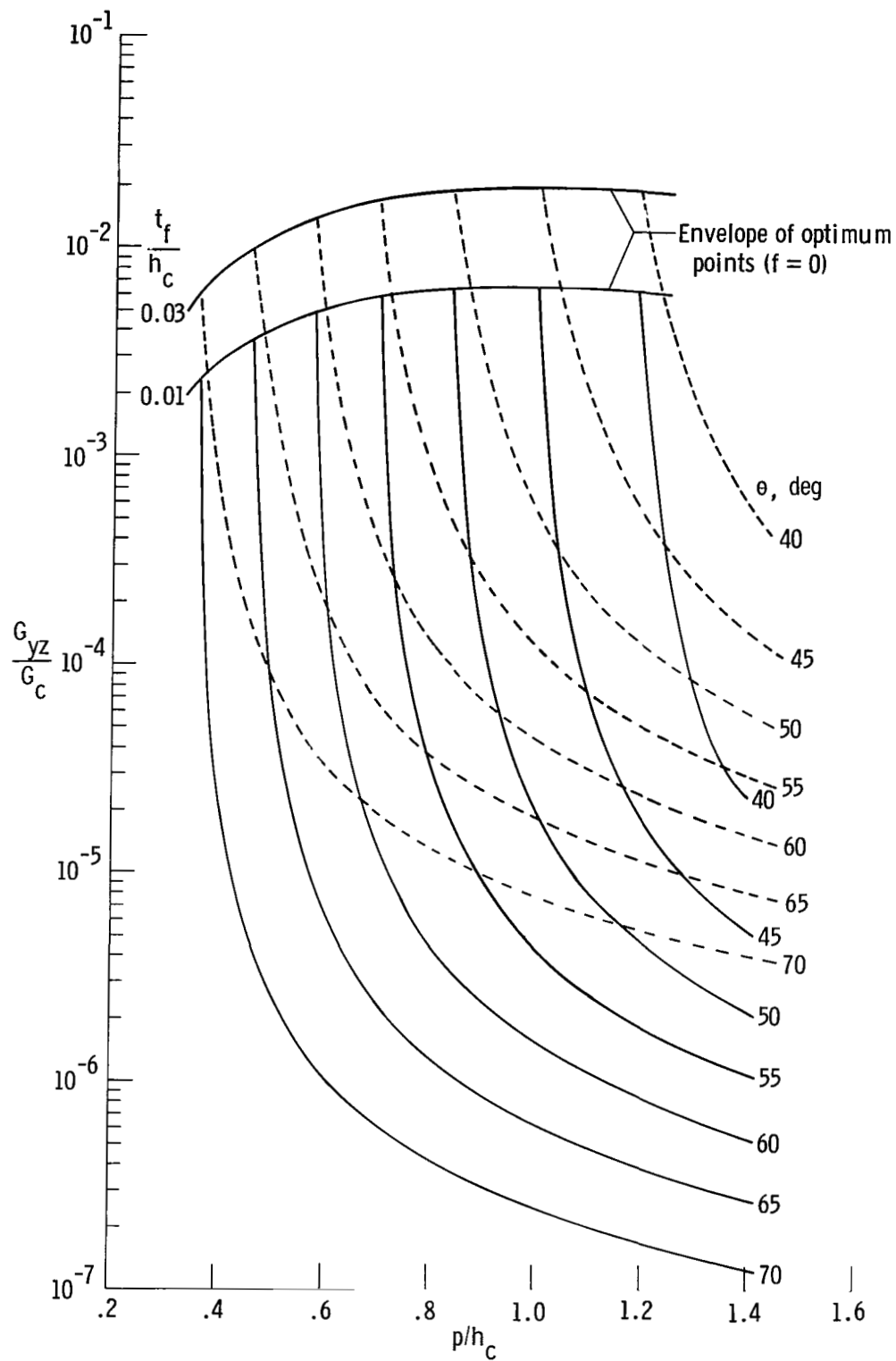


Figure 11. Shear modulus  $G_{yz}$  for SPF/DB corrugated titanium core.  $R = t_f$ .



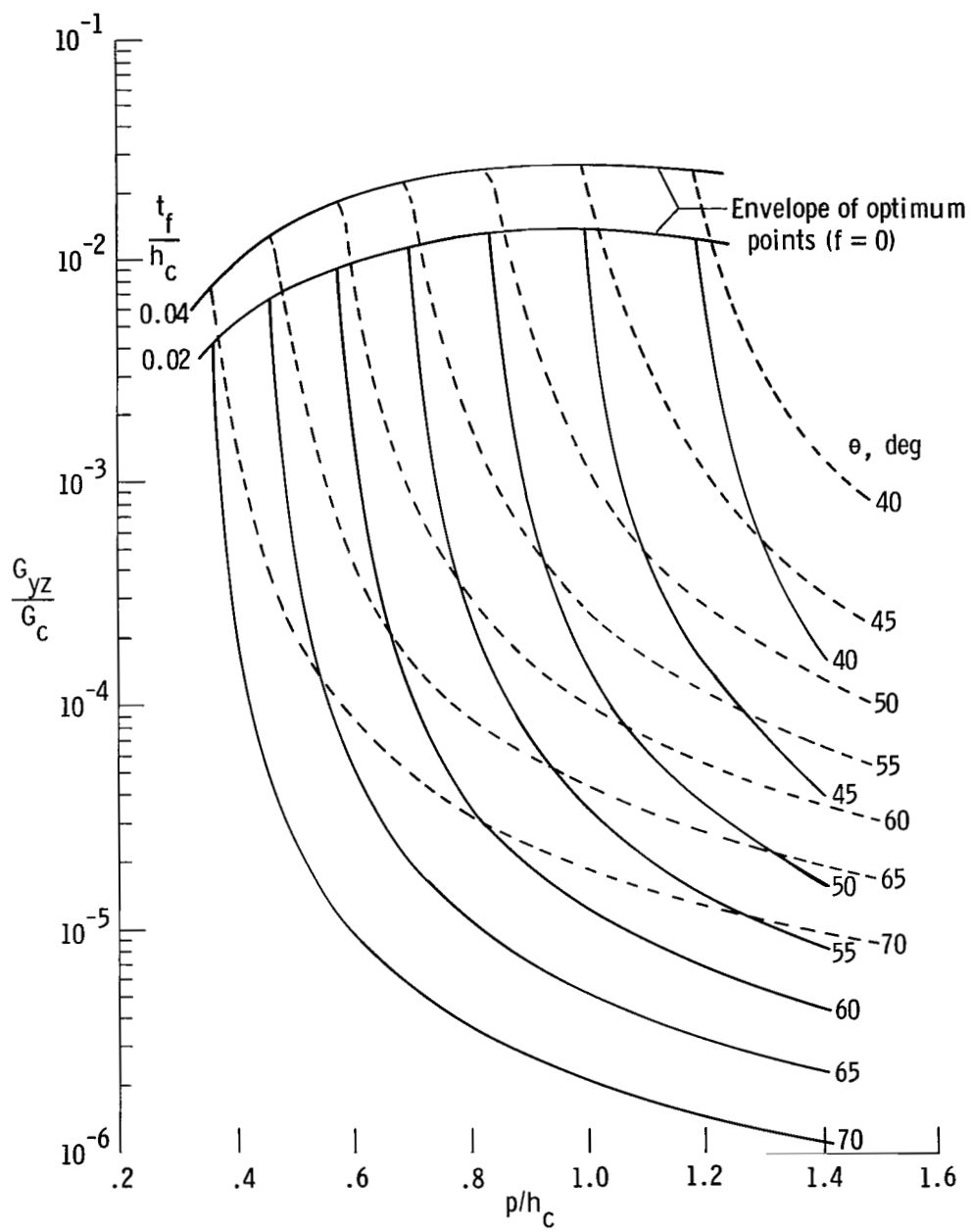


Figure 11. Continued.

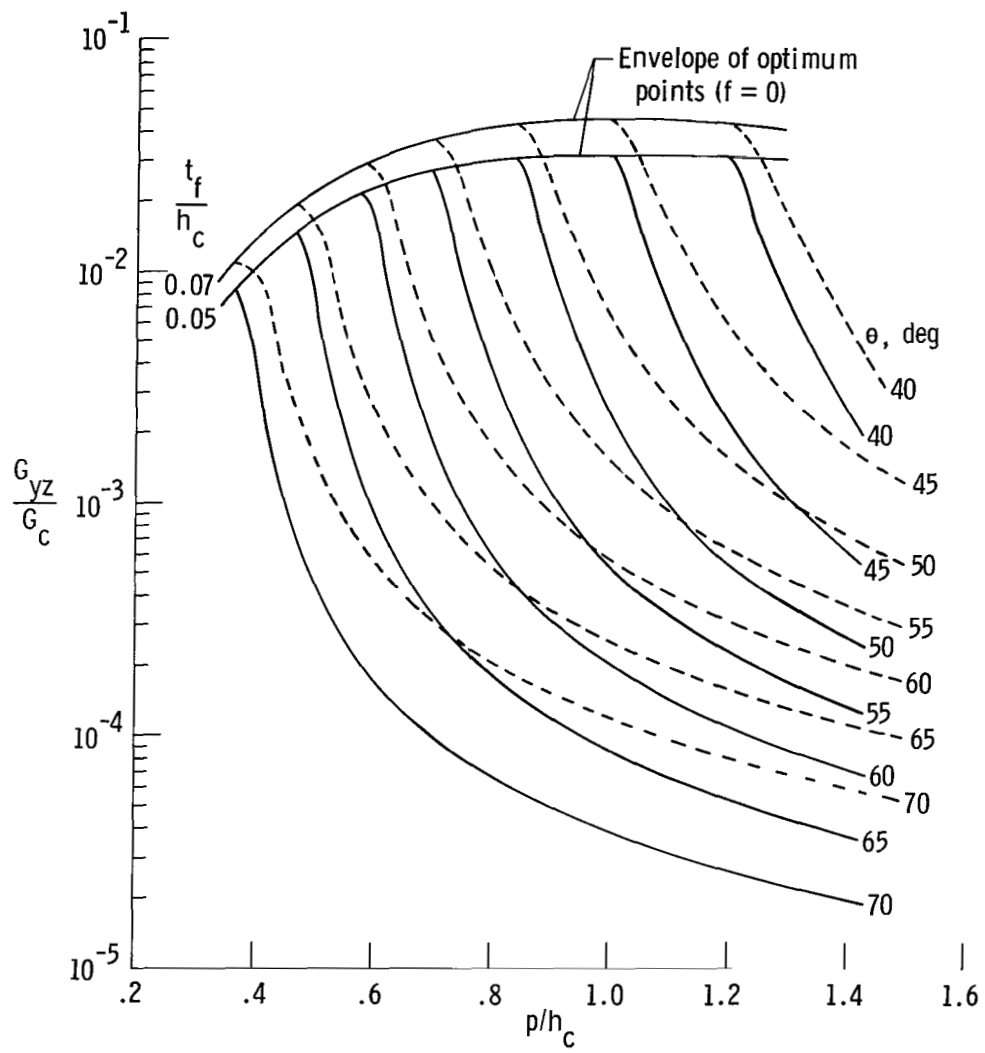


Figure 11. Continued.

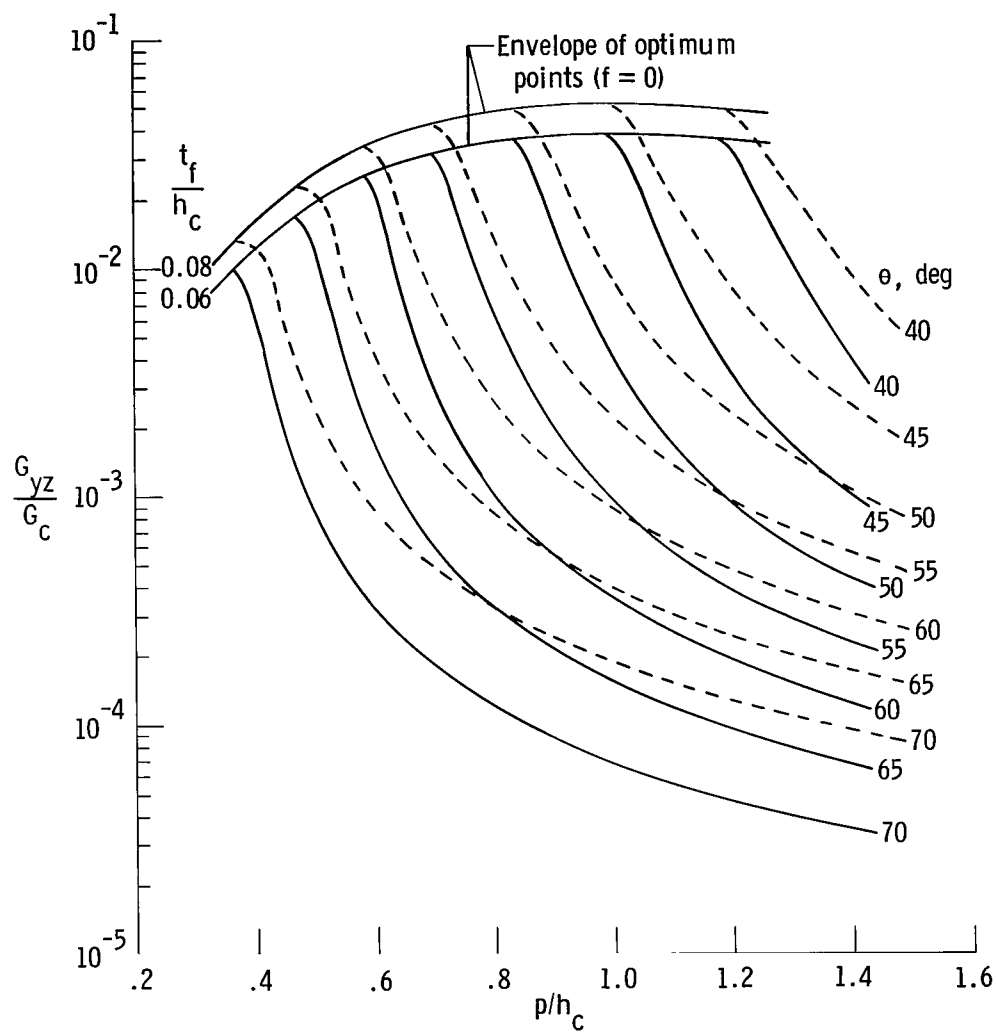


Figure 11. Concluded.

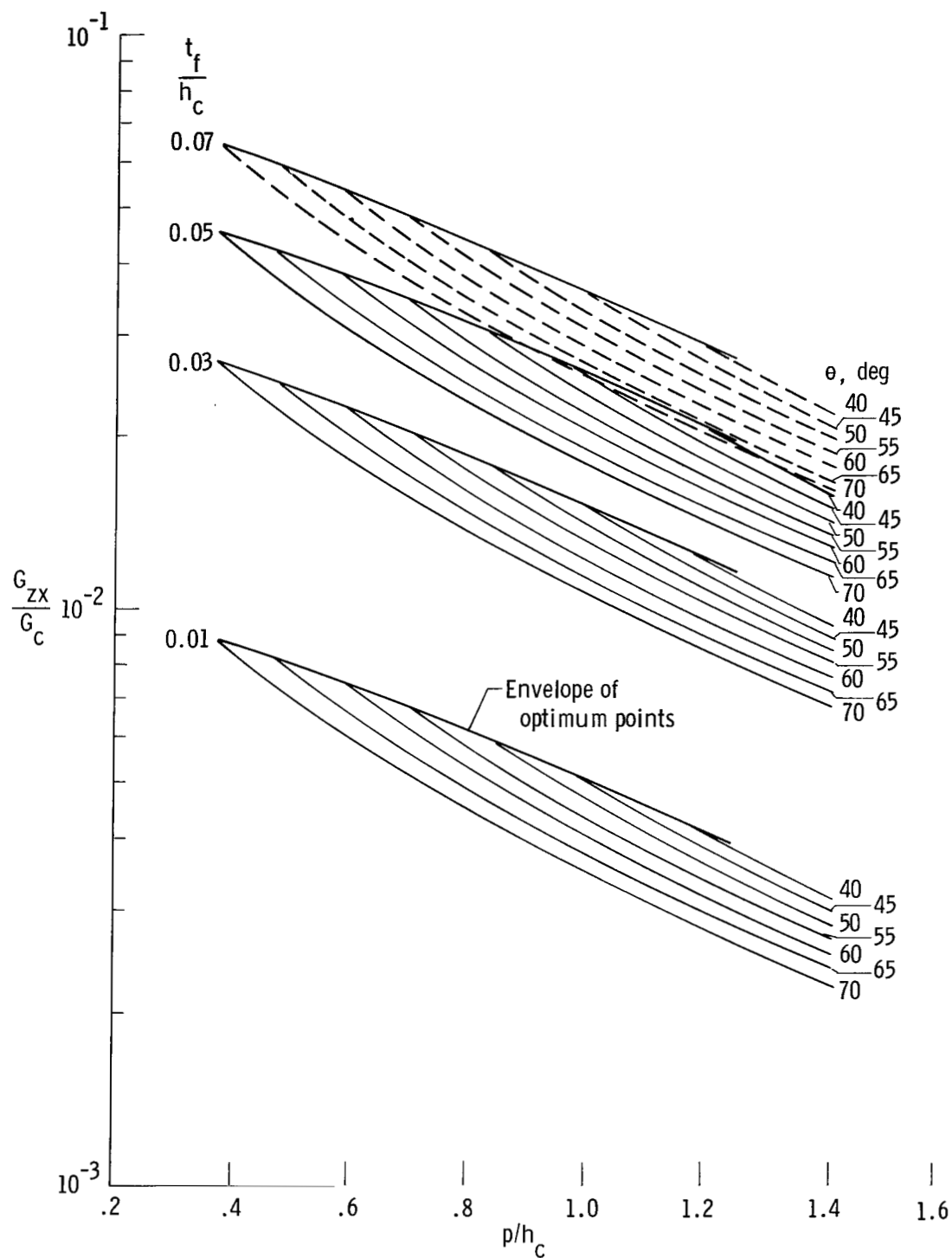


Figure 12. Shear modulus  $G_{zx}$  for SPF/DB corrugated core.  $R = t_f$ .

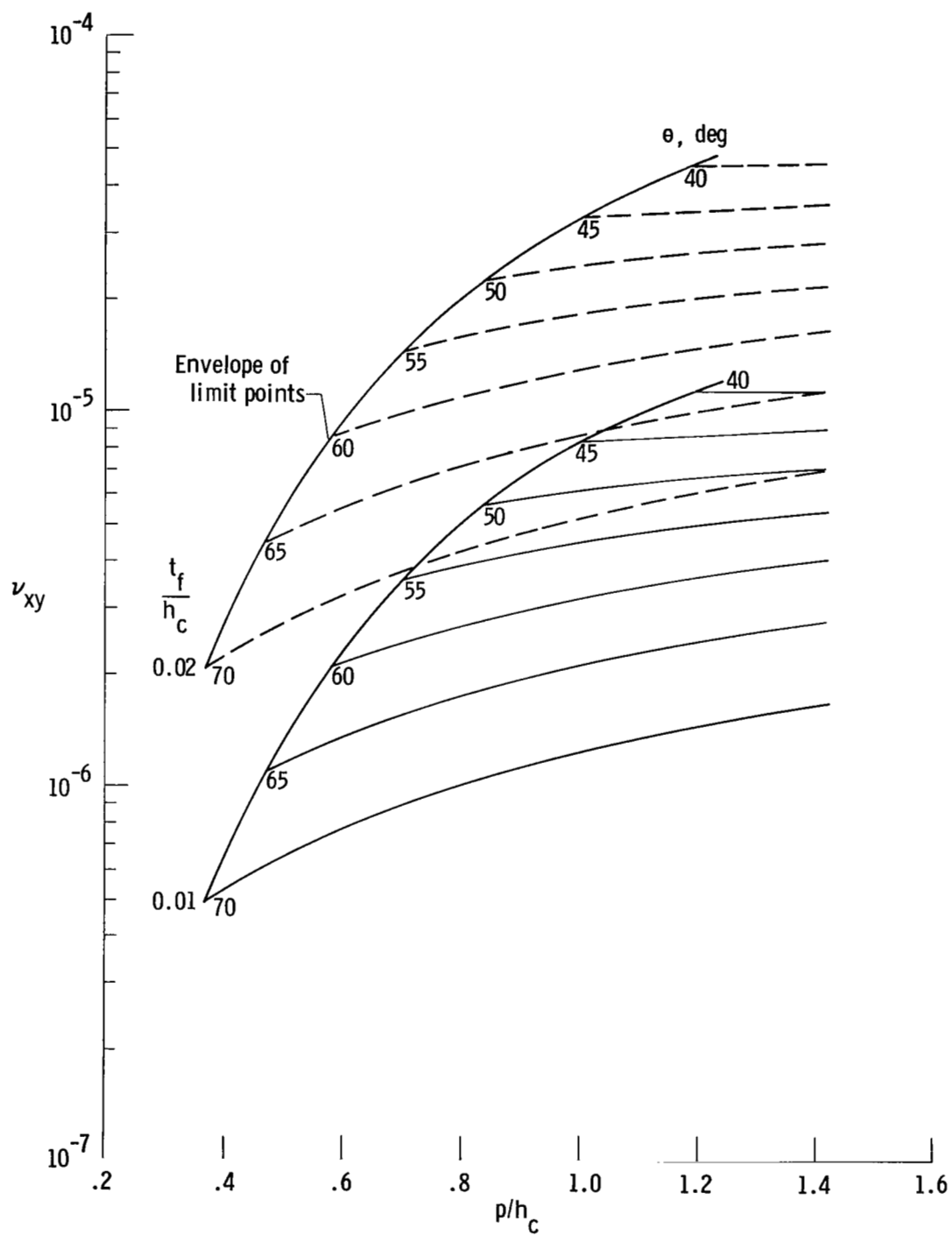


Figure 13. Poisson ratio  $\nu_{xy}$  for SPF/DB corrugated core.  $R = t_f$ .

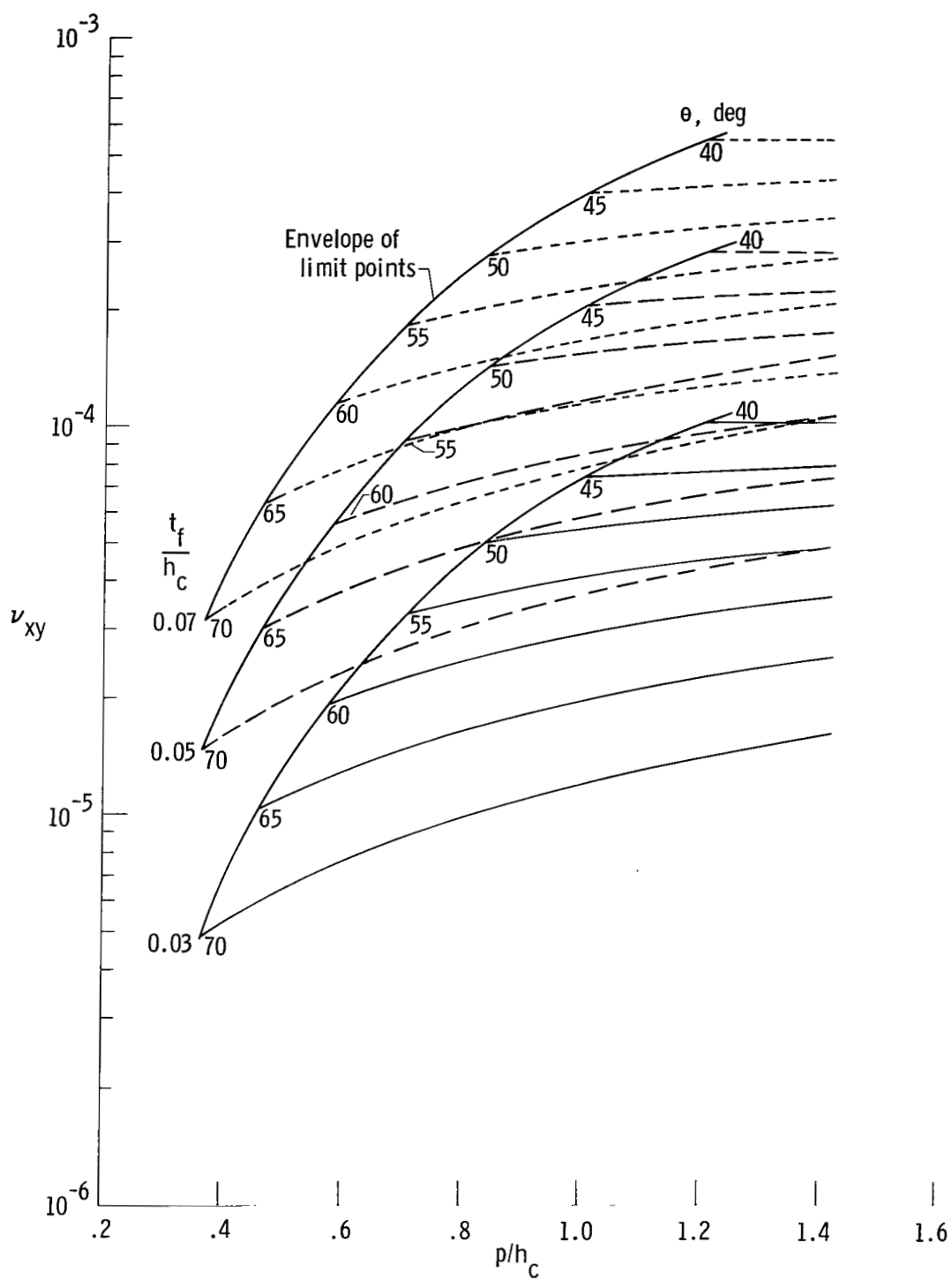


Figure 13. Continued.

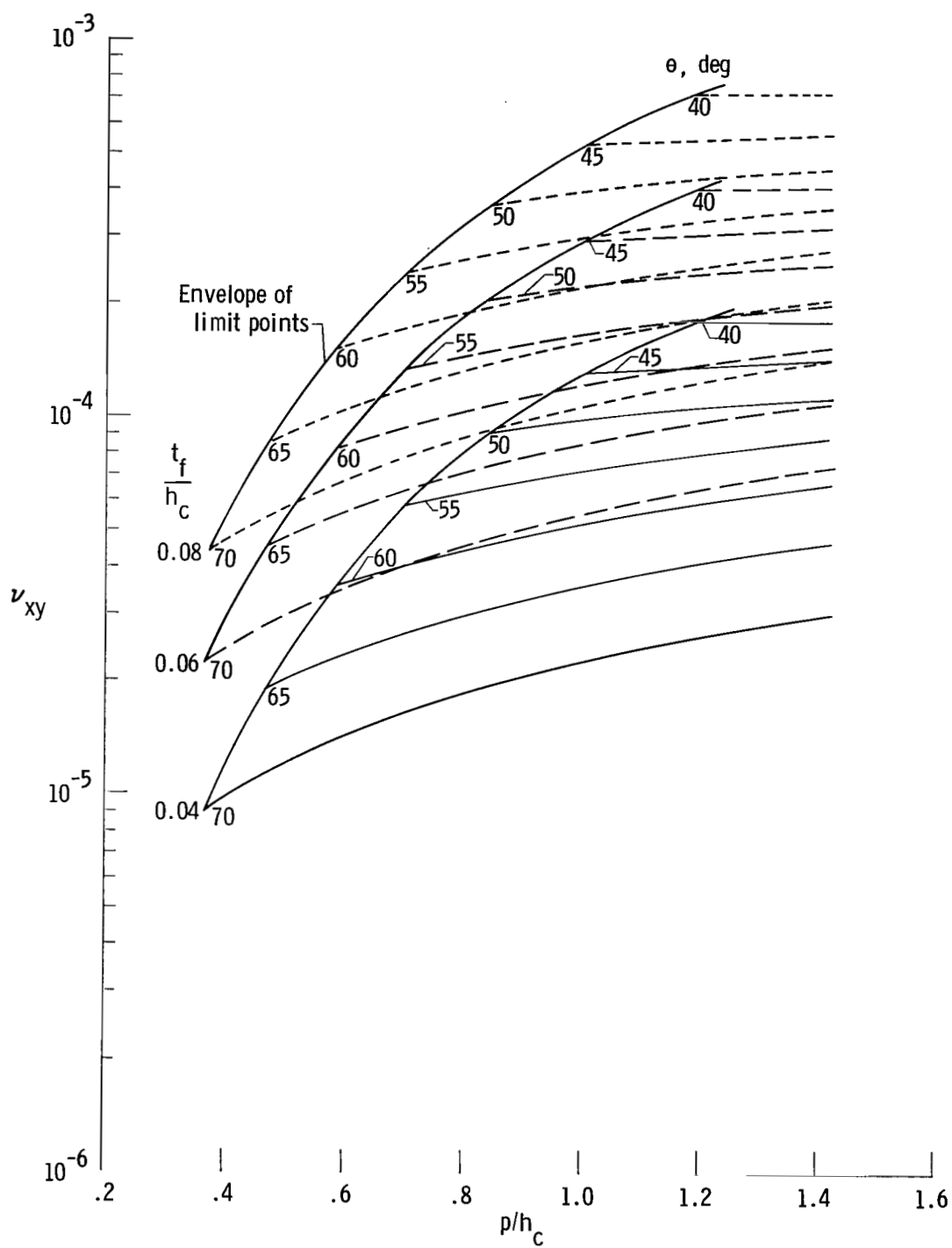


Figure 13. Concluded.

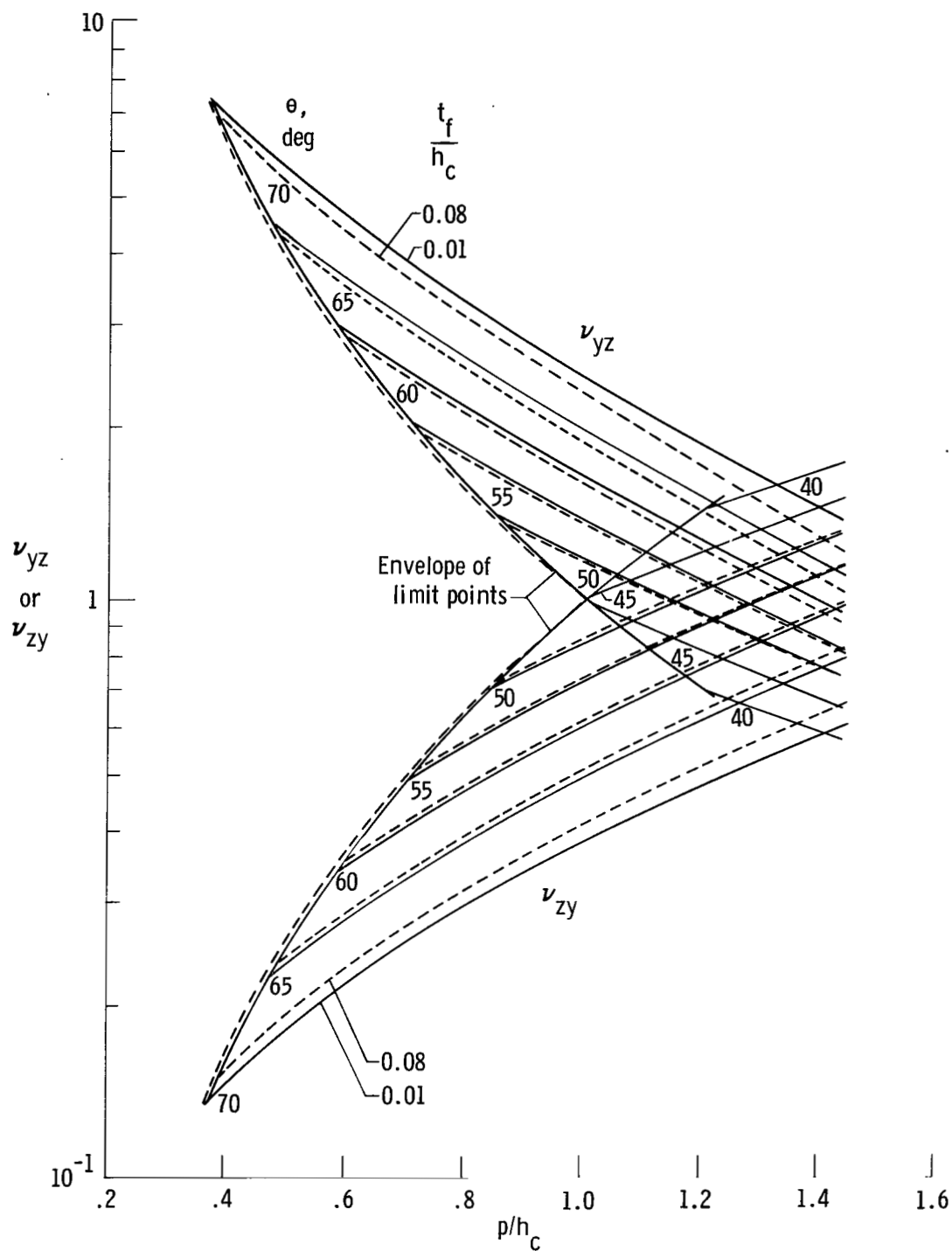


Figure 14. Poisson ratios  $\nu_{yz}$  and  $\nu_{zy}$  for SPF/DB corrugated core.  $R = t_f$ .



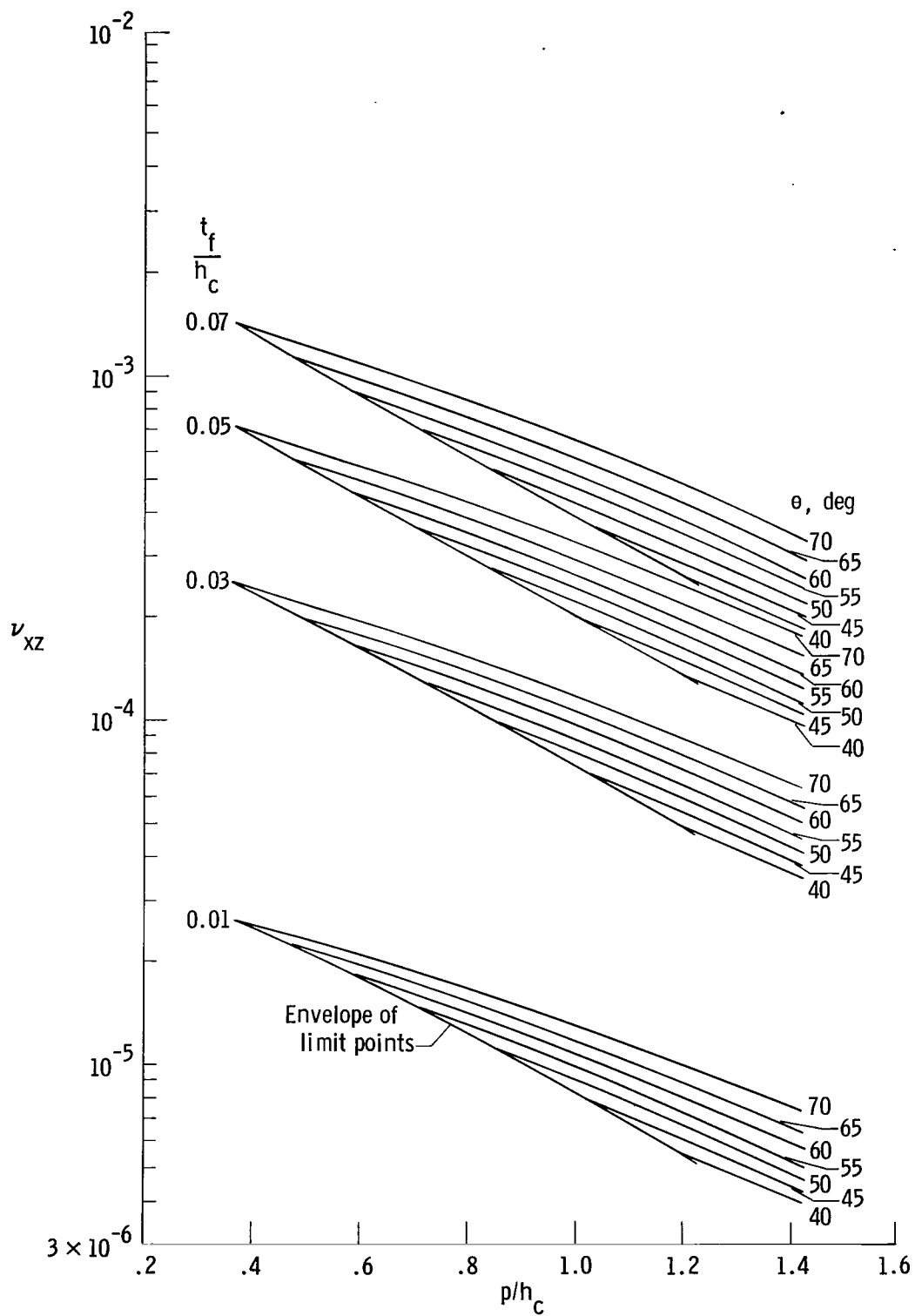


Figure 15. Poisson ratio  $\nu_{xz}$  for SPF/DB corrugated core.  $R = t_f$ .

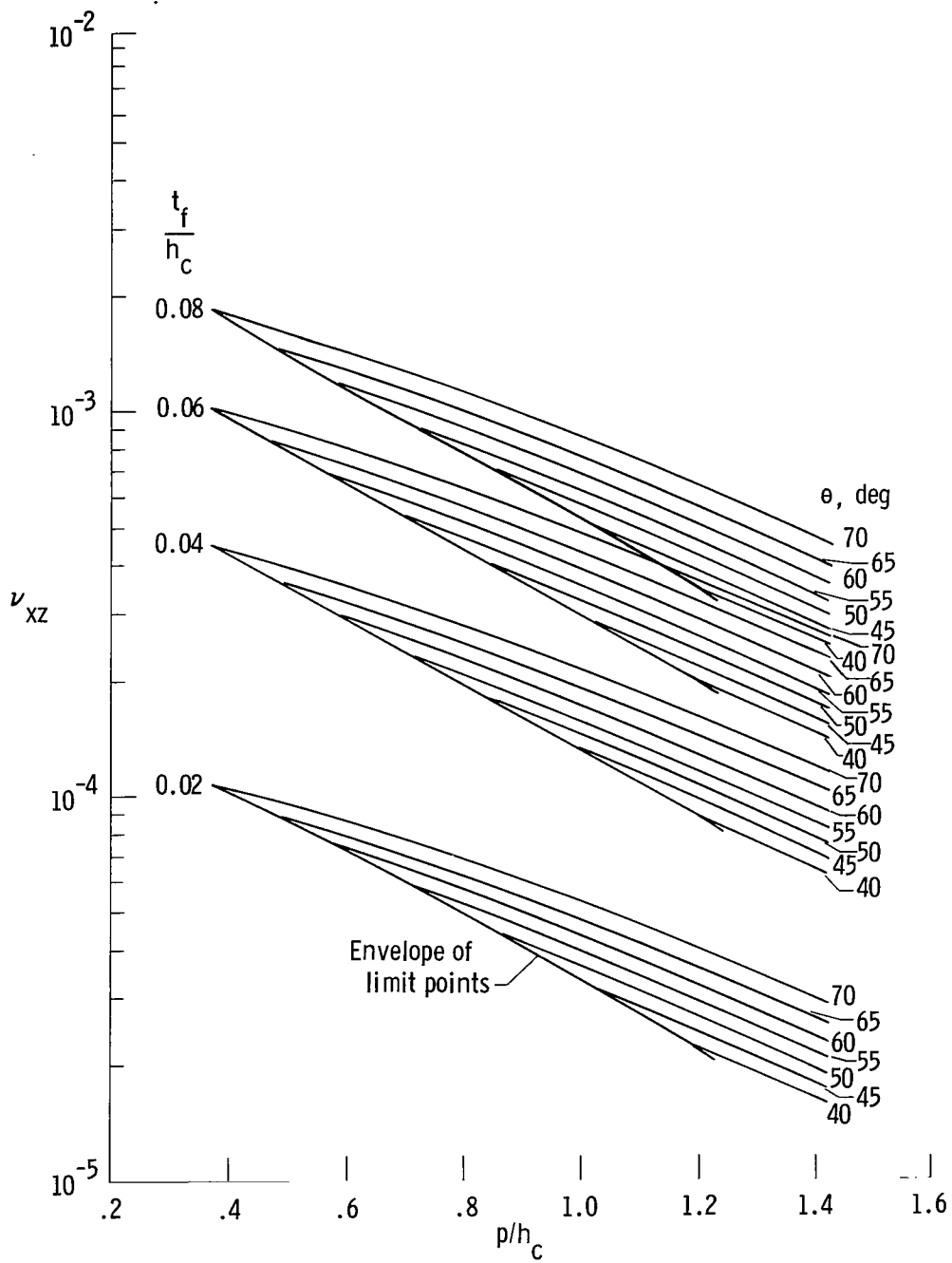


Figure 15. Concluded.

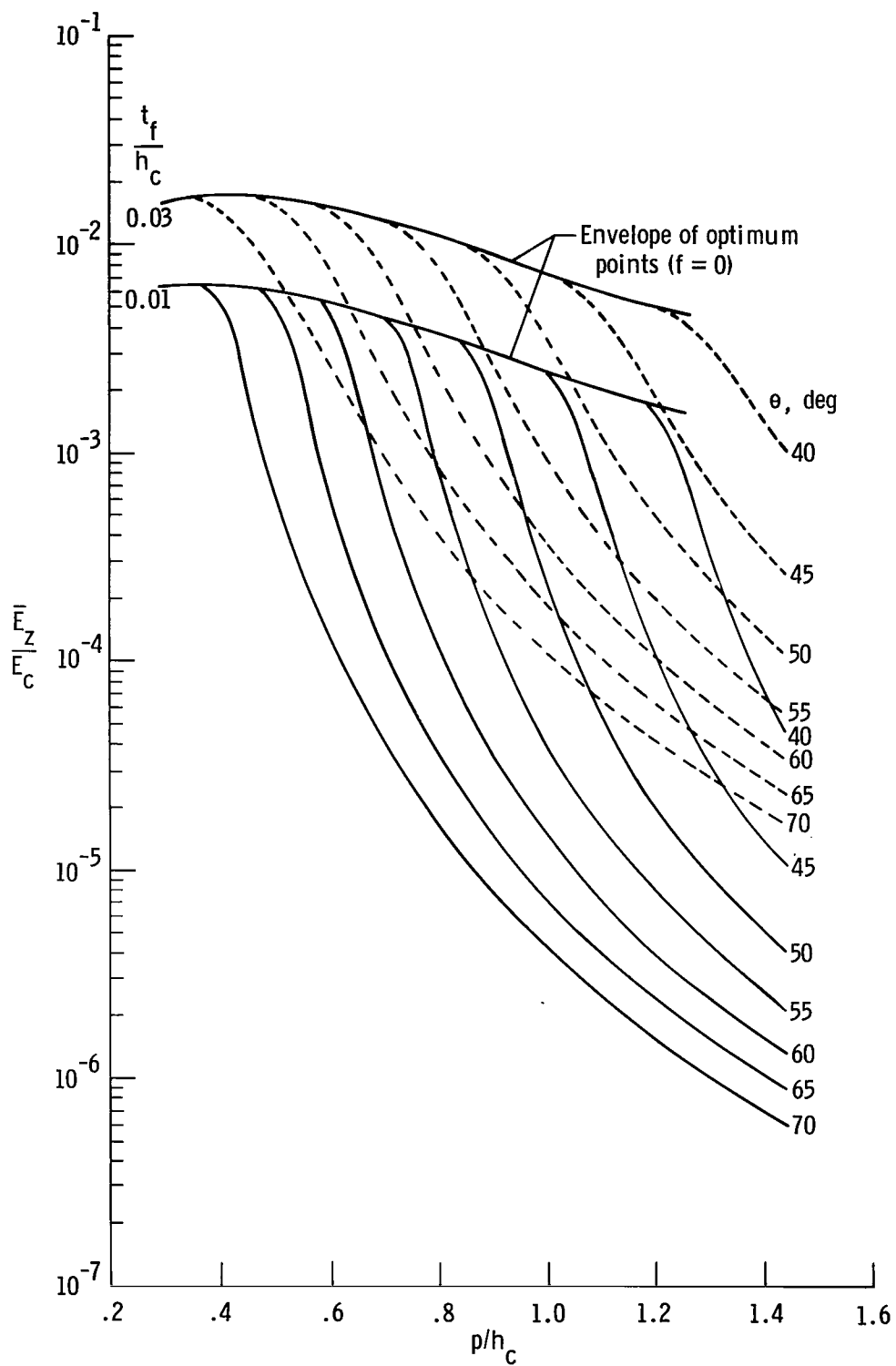


Figure 16. Modulus of elasticity  $\bar{E}_Z$  for SPF/DB corrugated core.  $R = t_f$ .

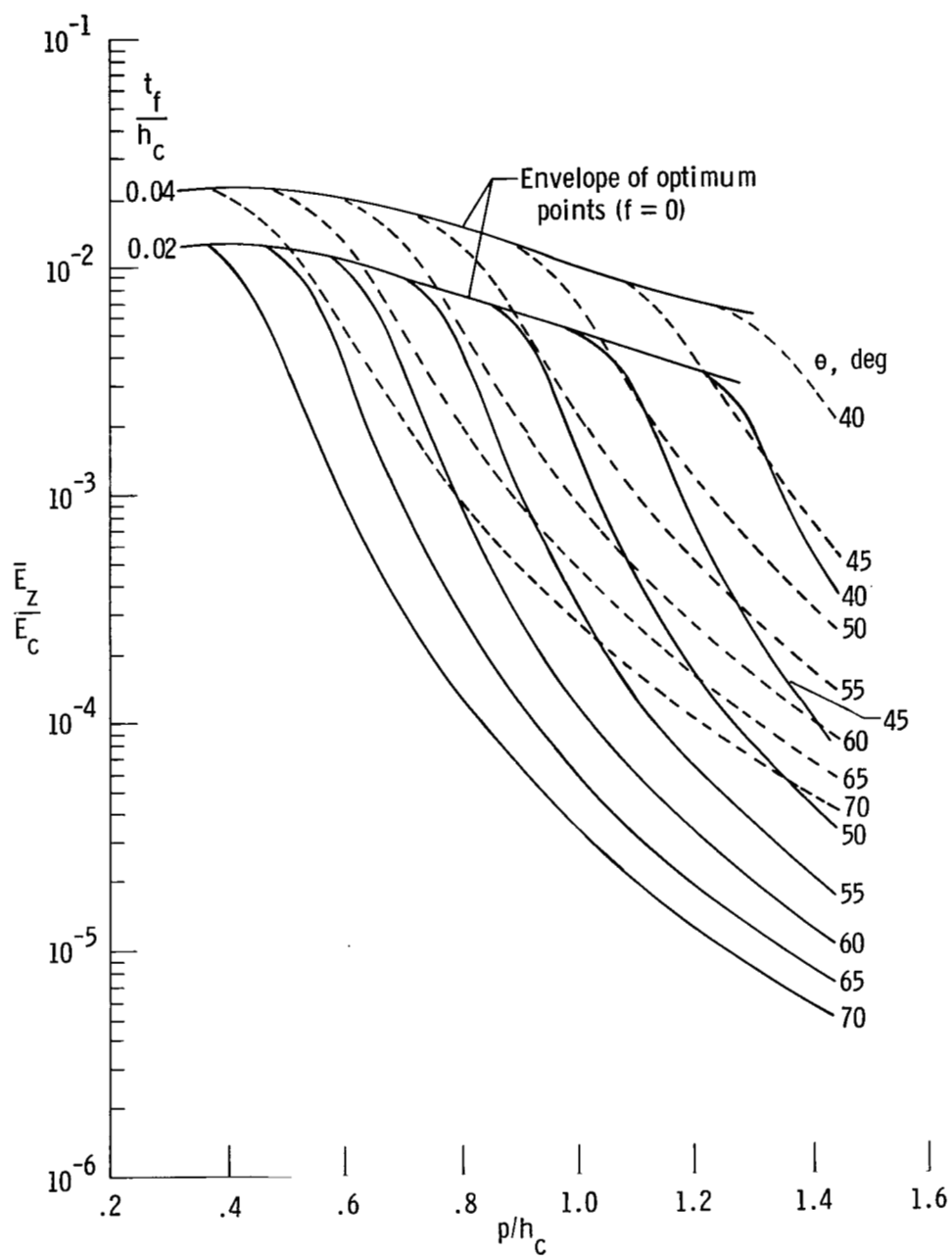


Figure 16. Continued.

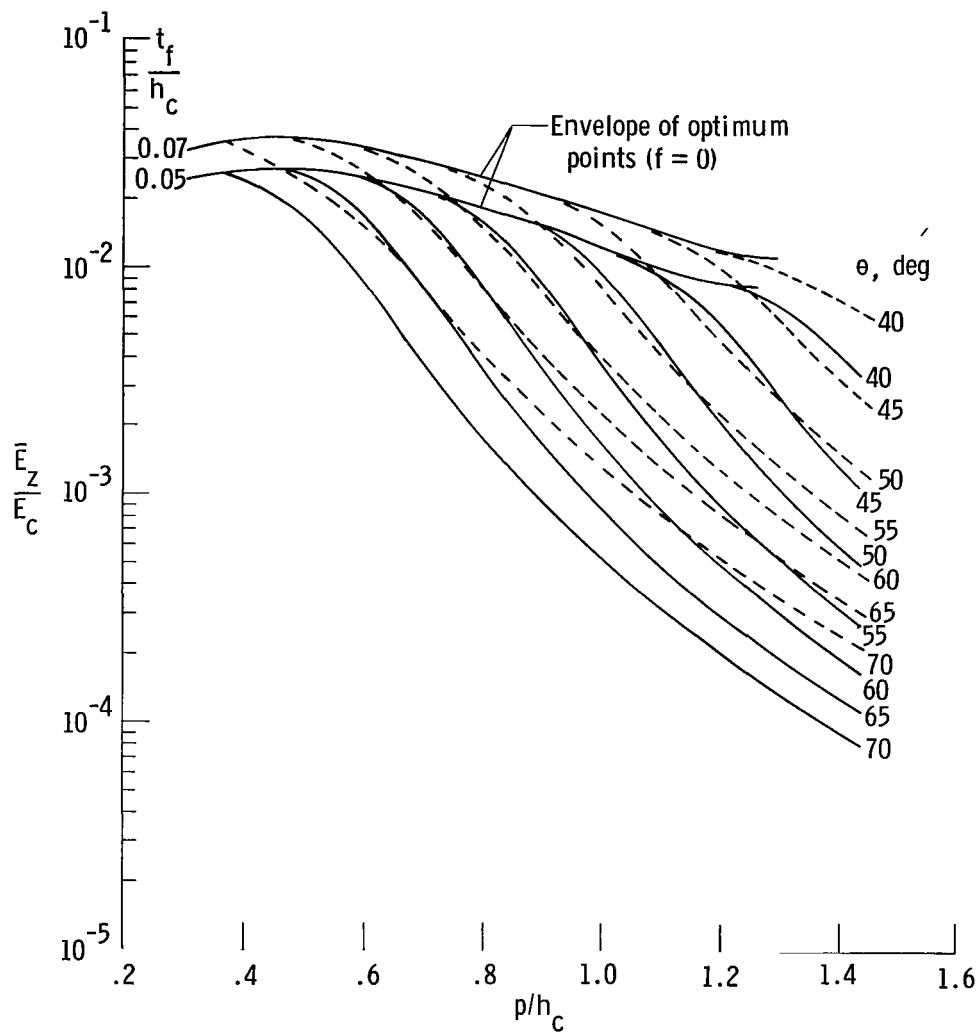


Figure 16. Continued.

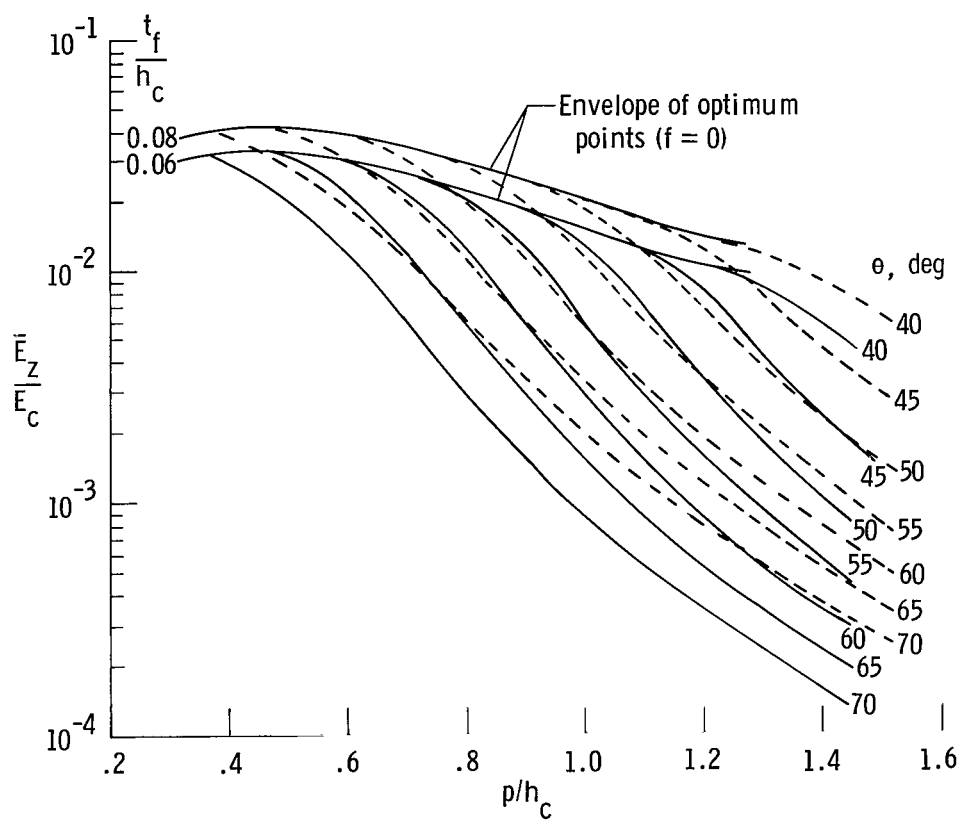


Figure 16. Concluded.

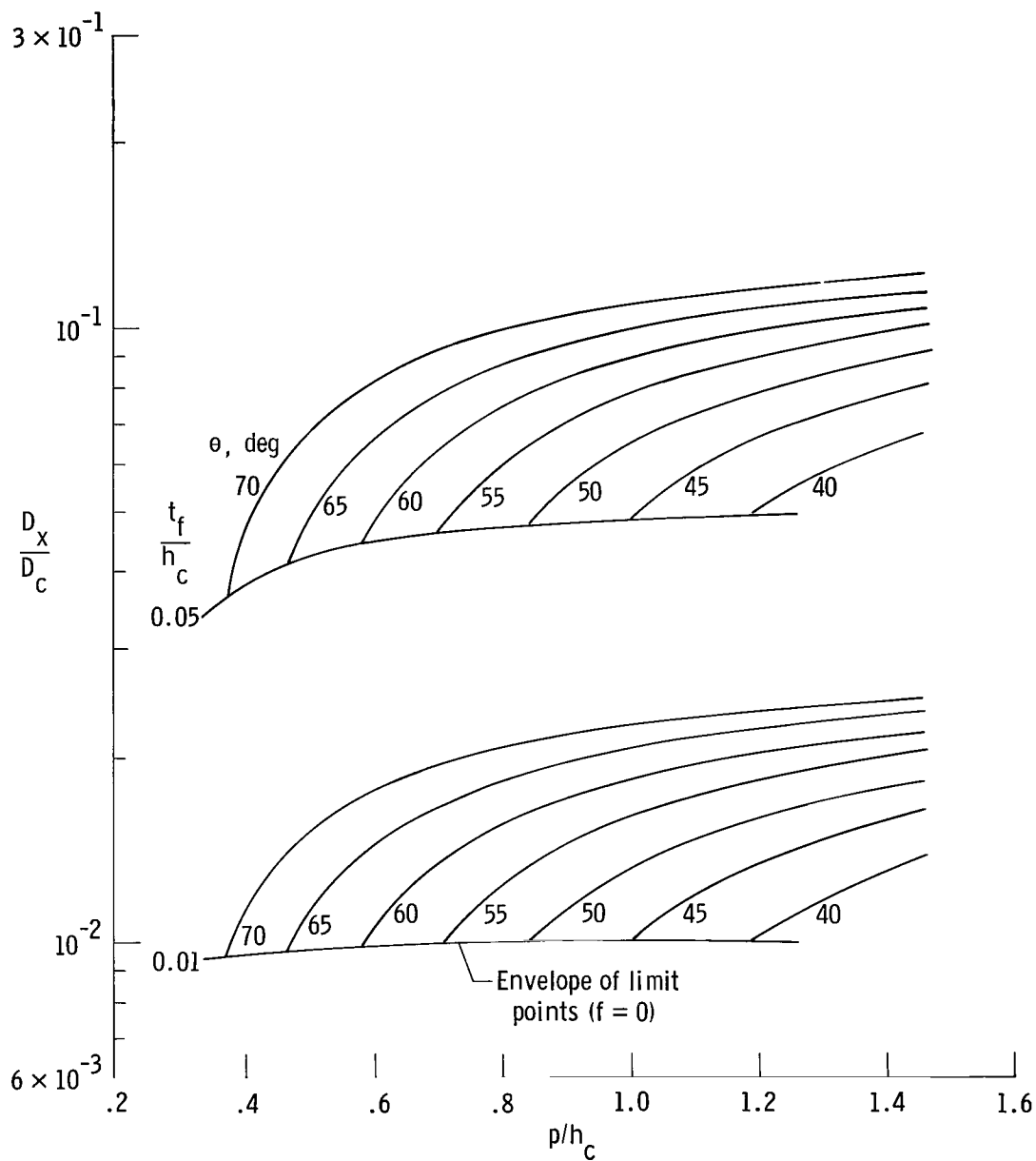


Figure 17. Bending stiffness  $D_x$  for SPF/DB corrugated sandwich core.  $R = t_f$ ;  $D_C = E_C h_C^3 / 12$ .

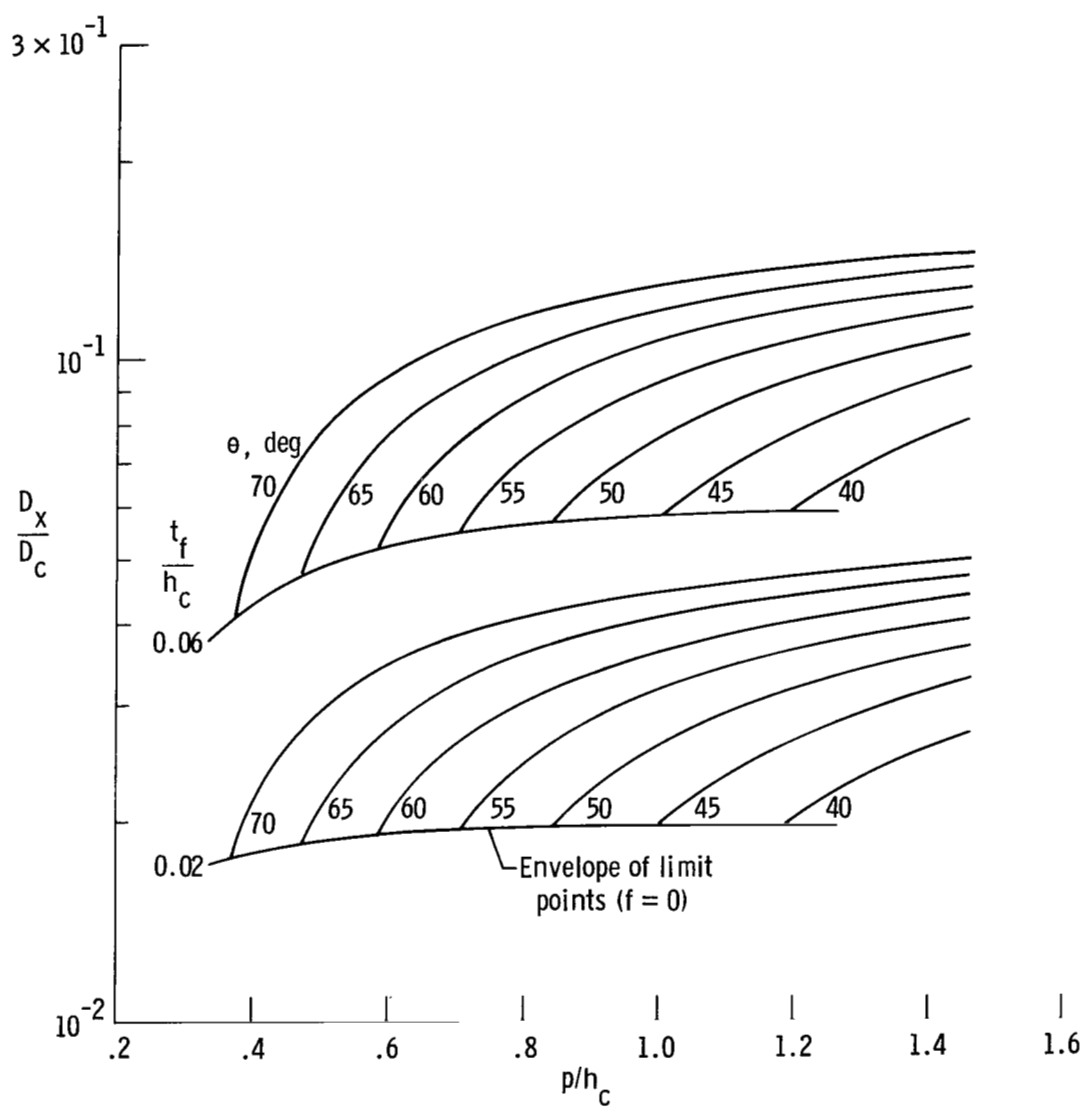


Figure 17. Continued.



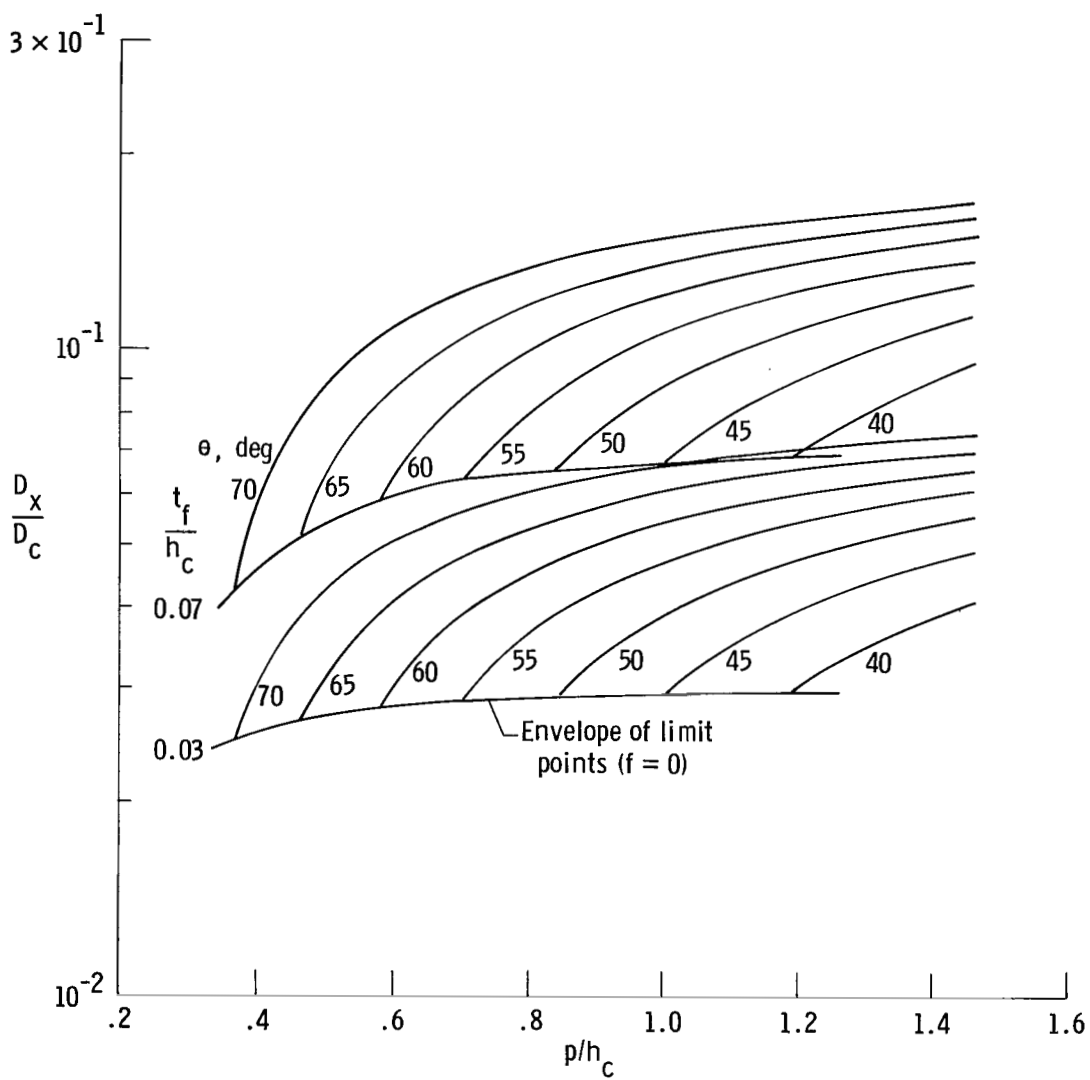


Figure 17. Continued.

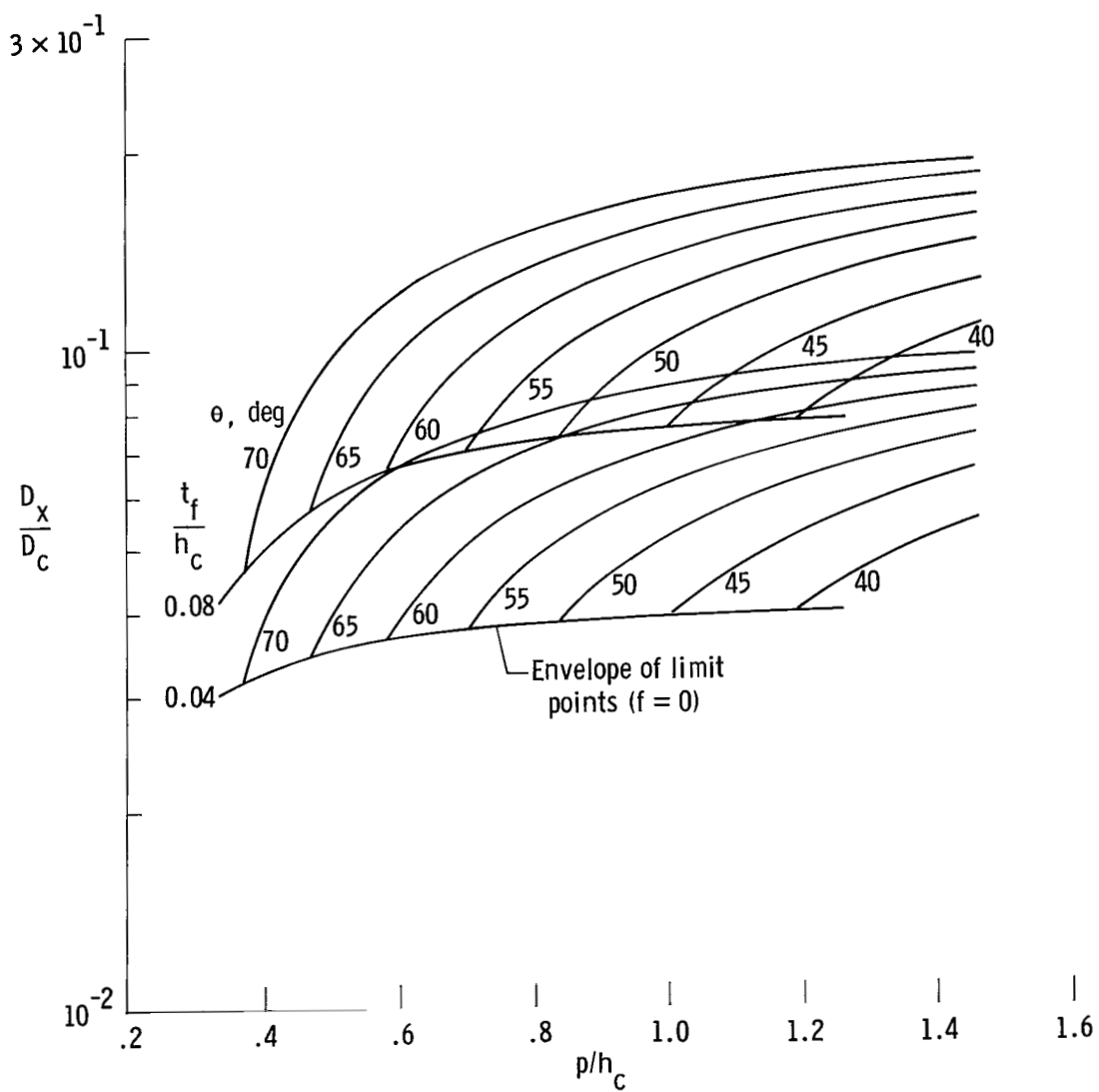


Figure 17. Concluded.

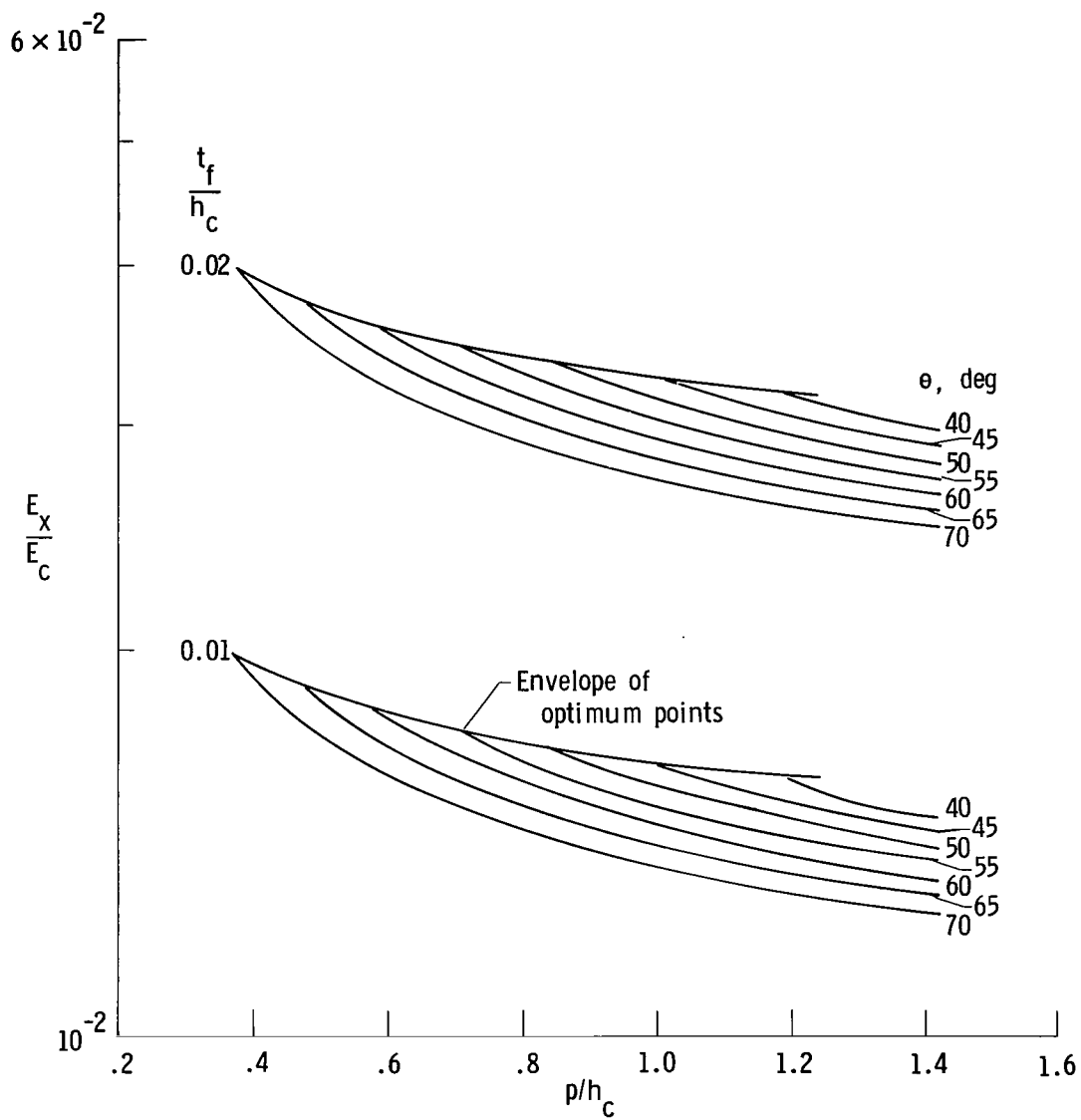


Figure 18. Modulus of elasticity  $E_x$  for honeycomb core.  $R = t_c = t_f$ .

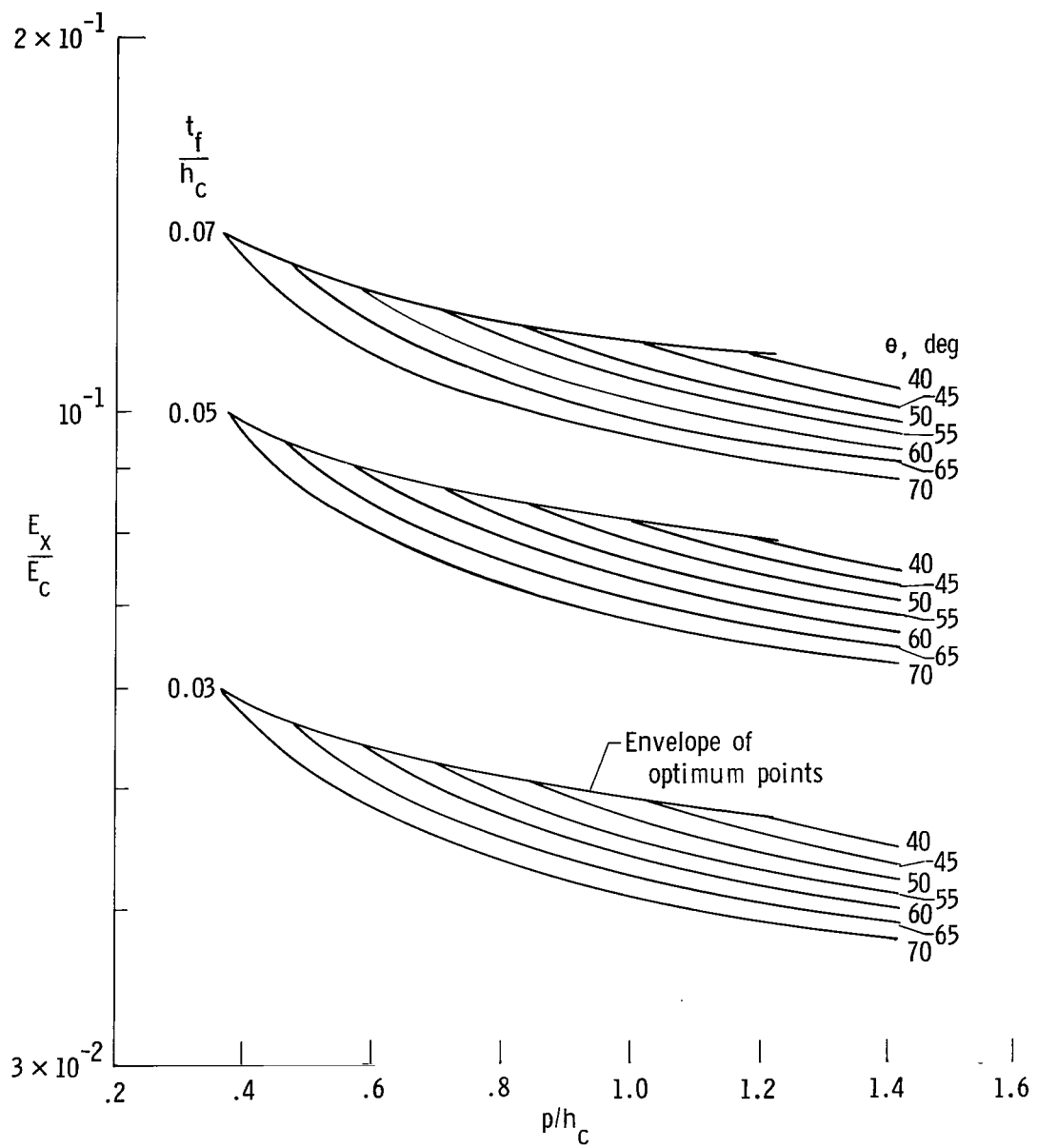


Figure 18. Continued.

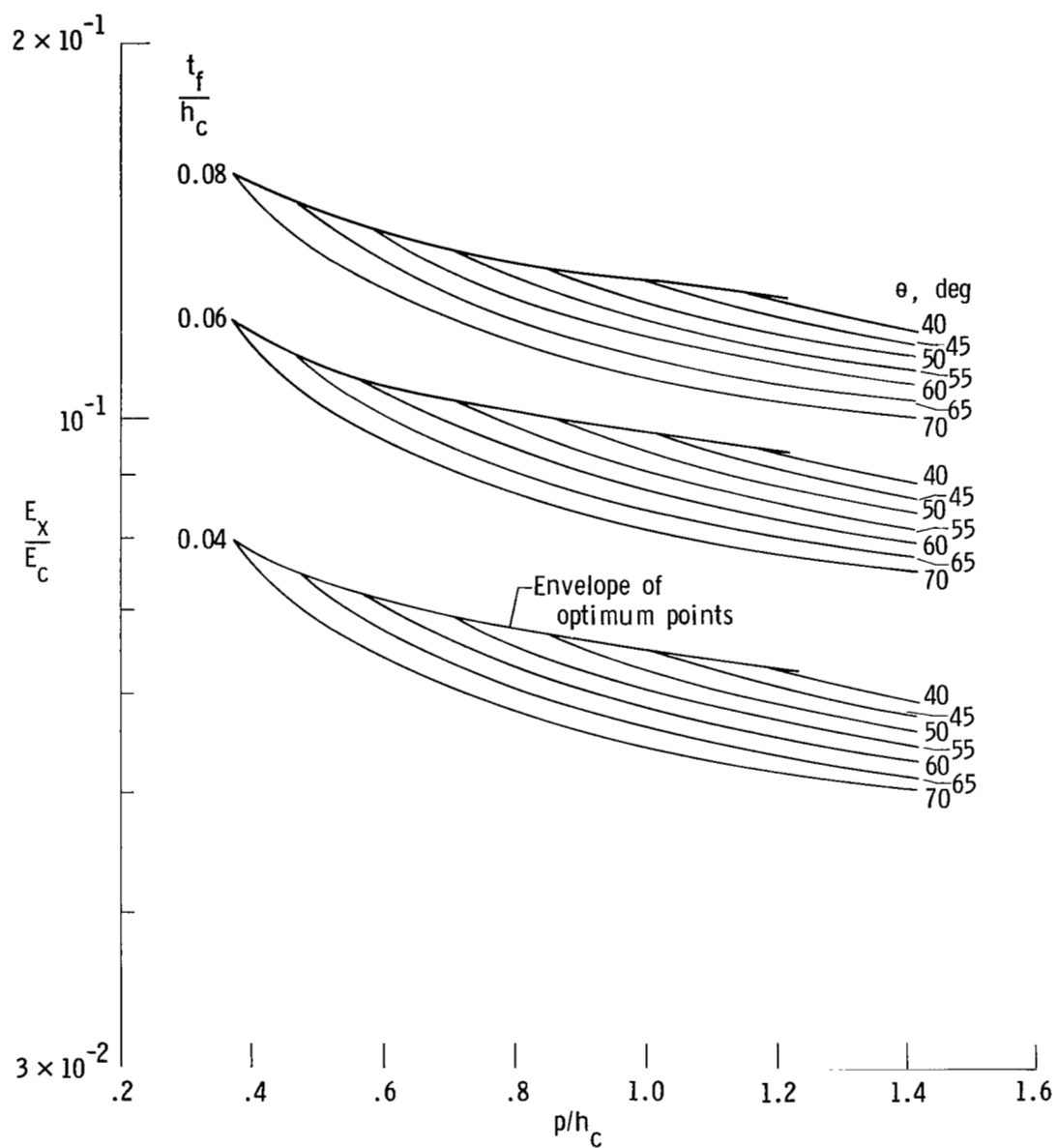


Figure 18. Concluded.

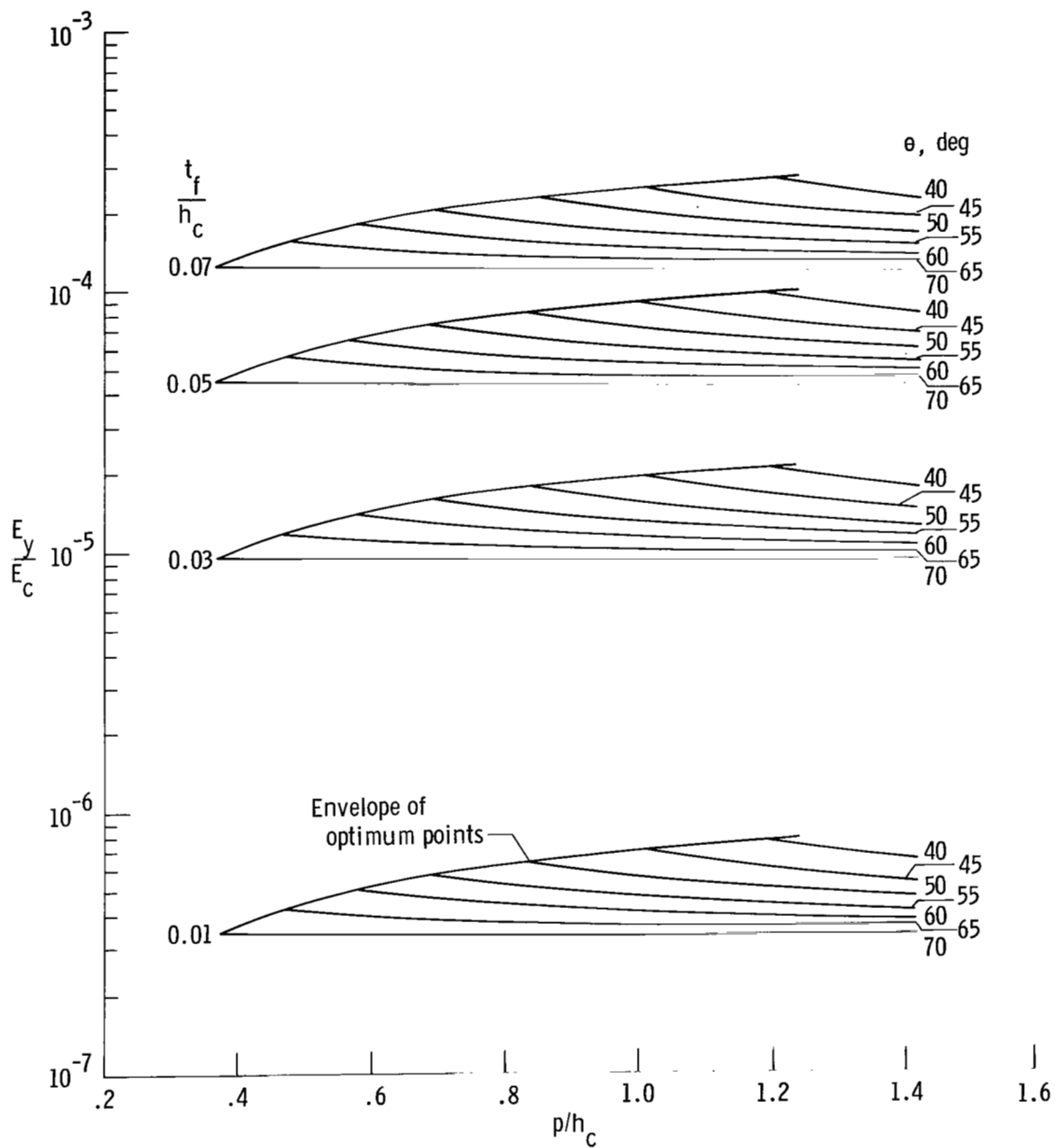


Figure 19. Modulus of elasticity  $E_y$  for honeycomb core.  $R = t_c = t_f$ .

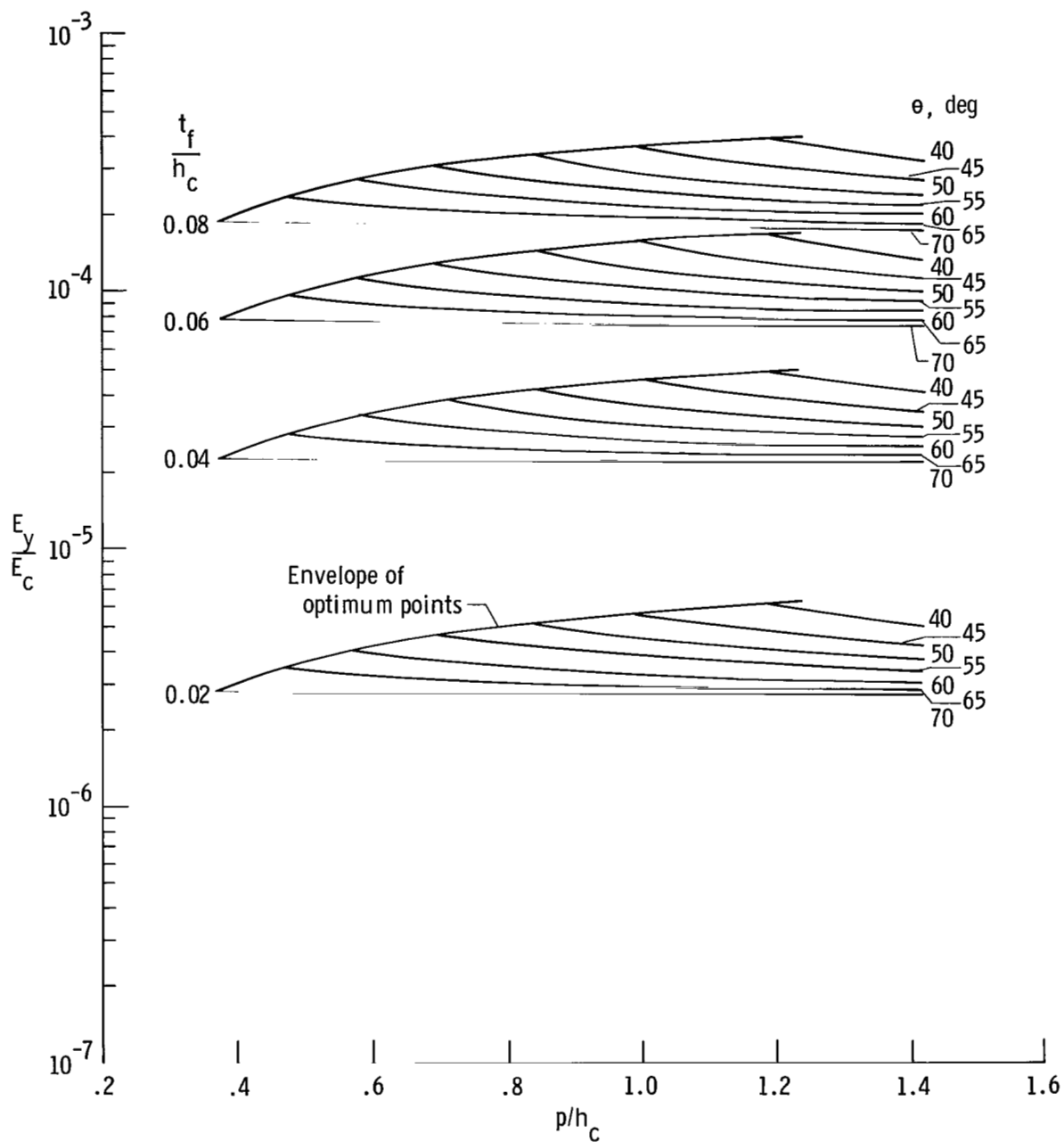


Figure 19. Concluded.

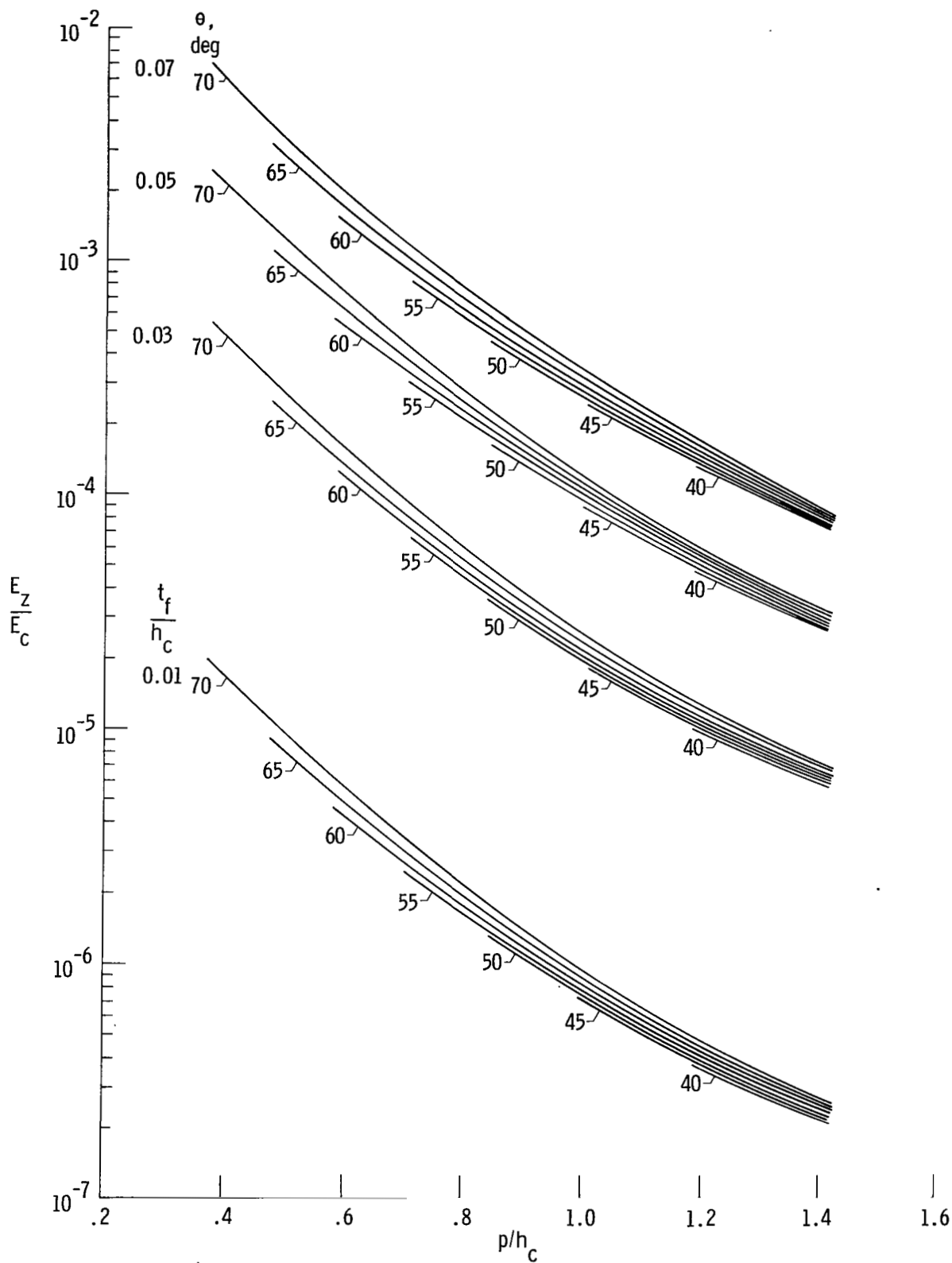


Figure 20. Modulus of elasticity  $E_z$  for honeycomb core.  $R = t_c = t_f$ .



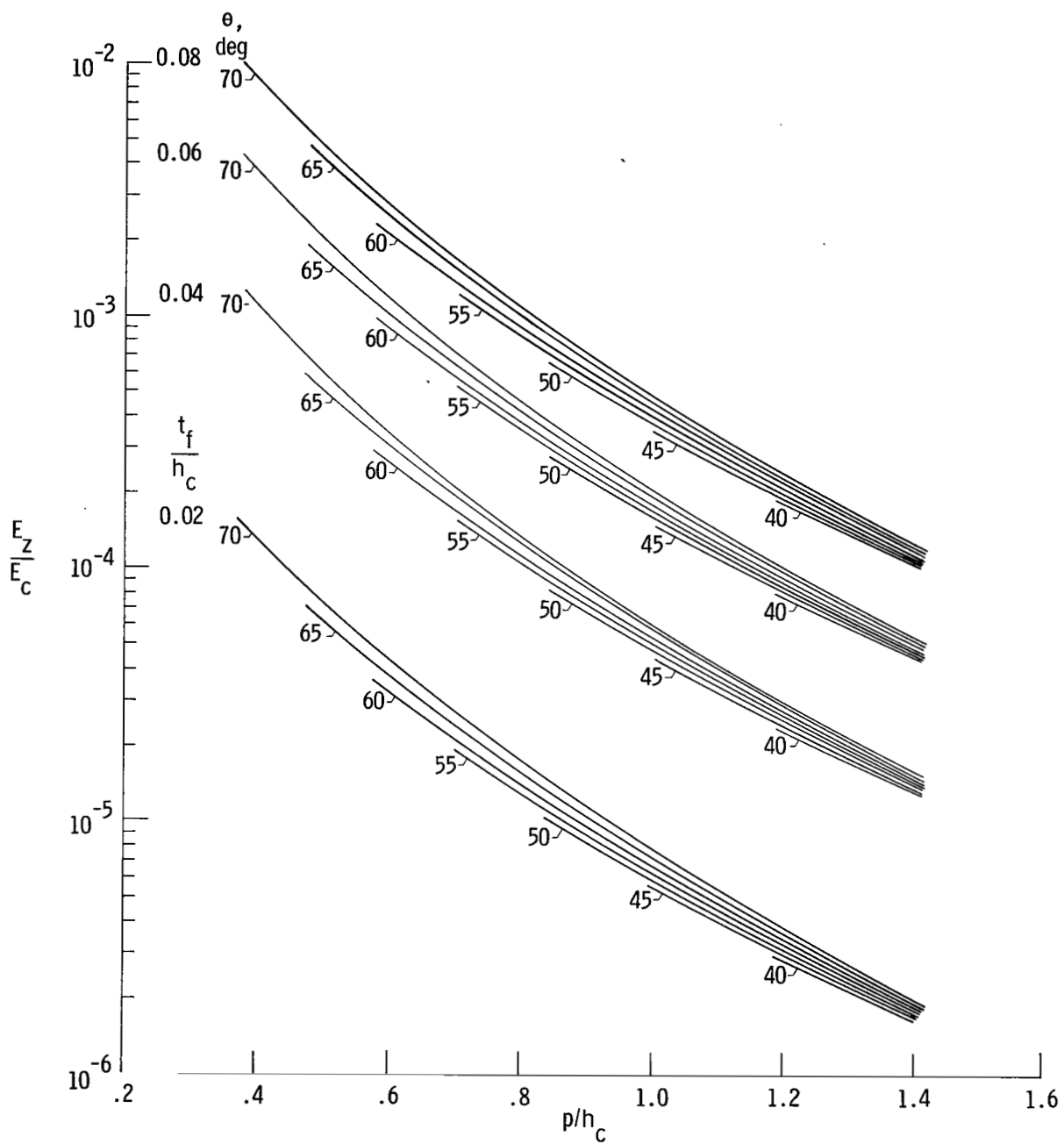


Figure 20. Concluded.

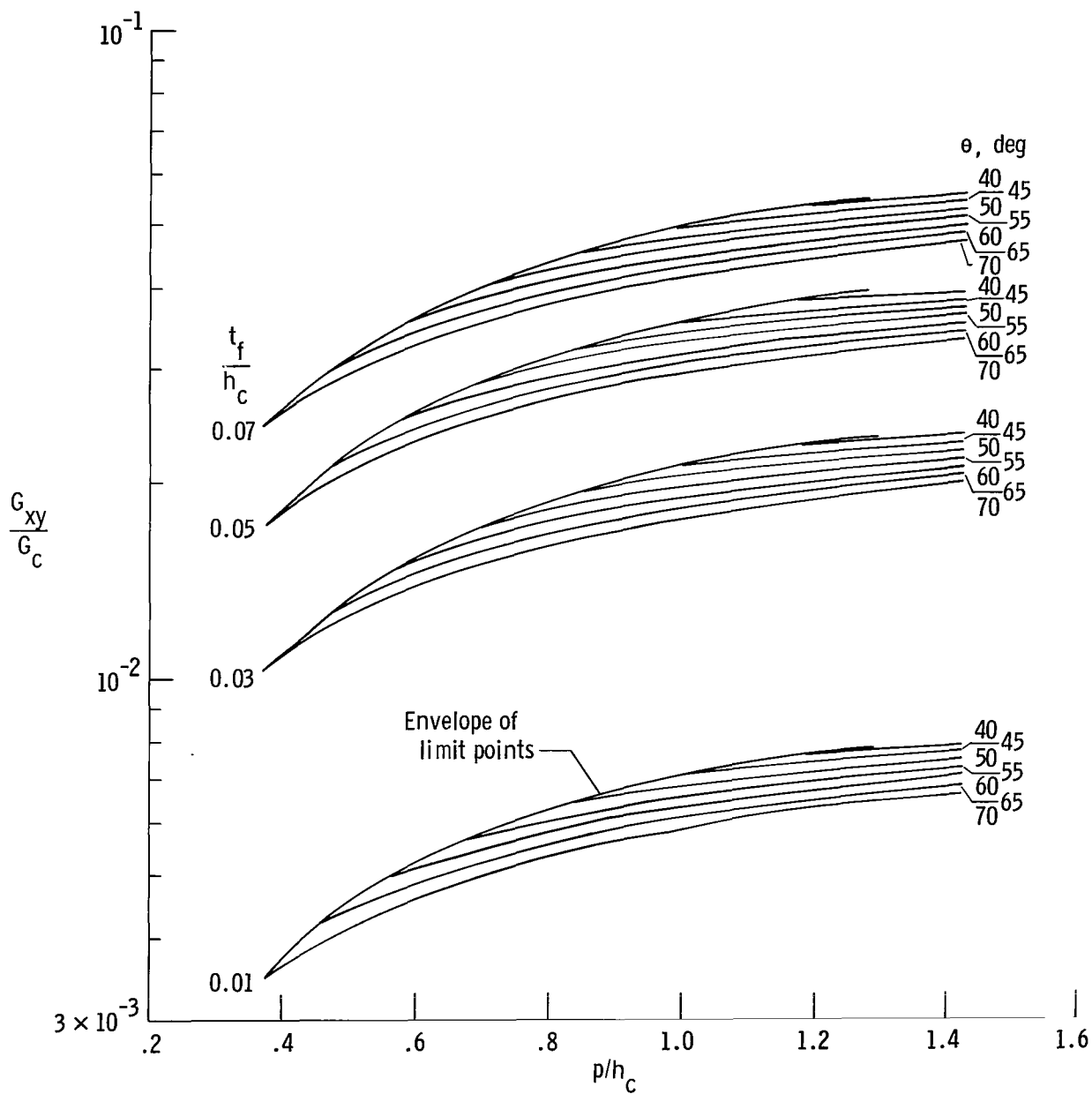


Figure 21. Shear modulus  $G_{xy}$  for honeycomb core.  $R = t_c = t_f$ .

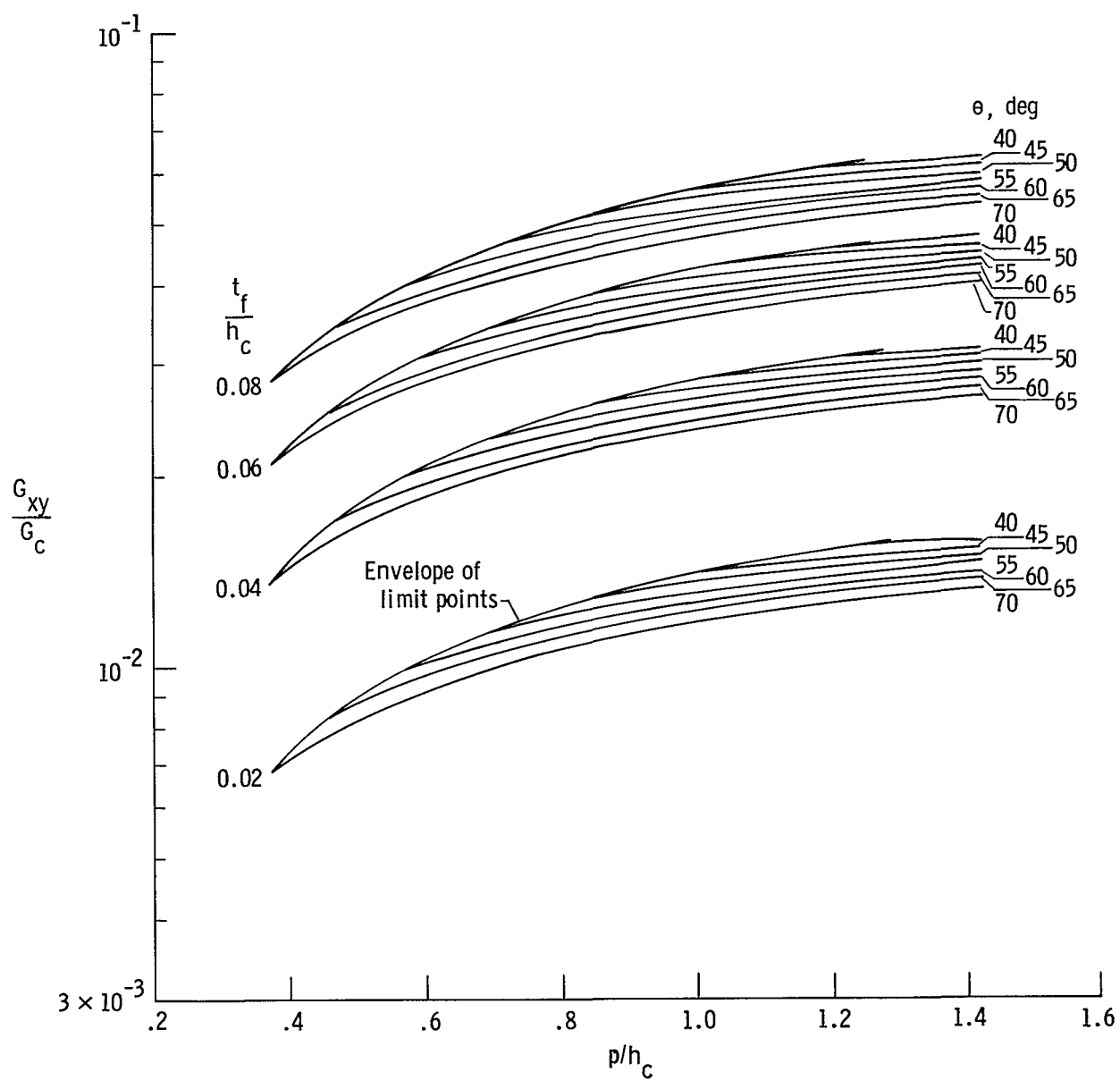


Figure 21. Concluded.

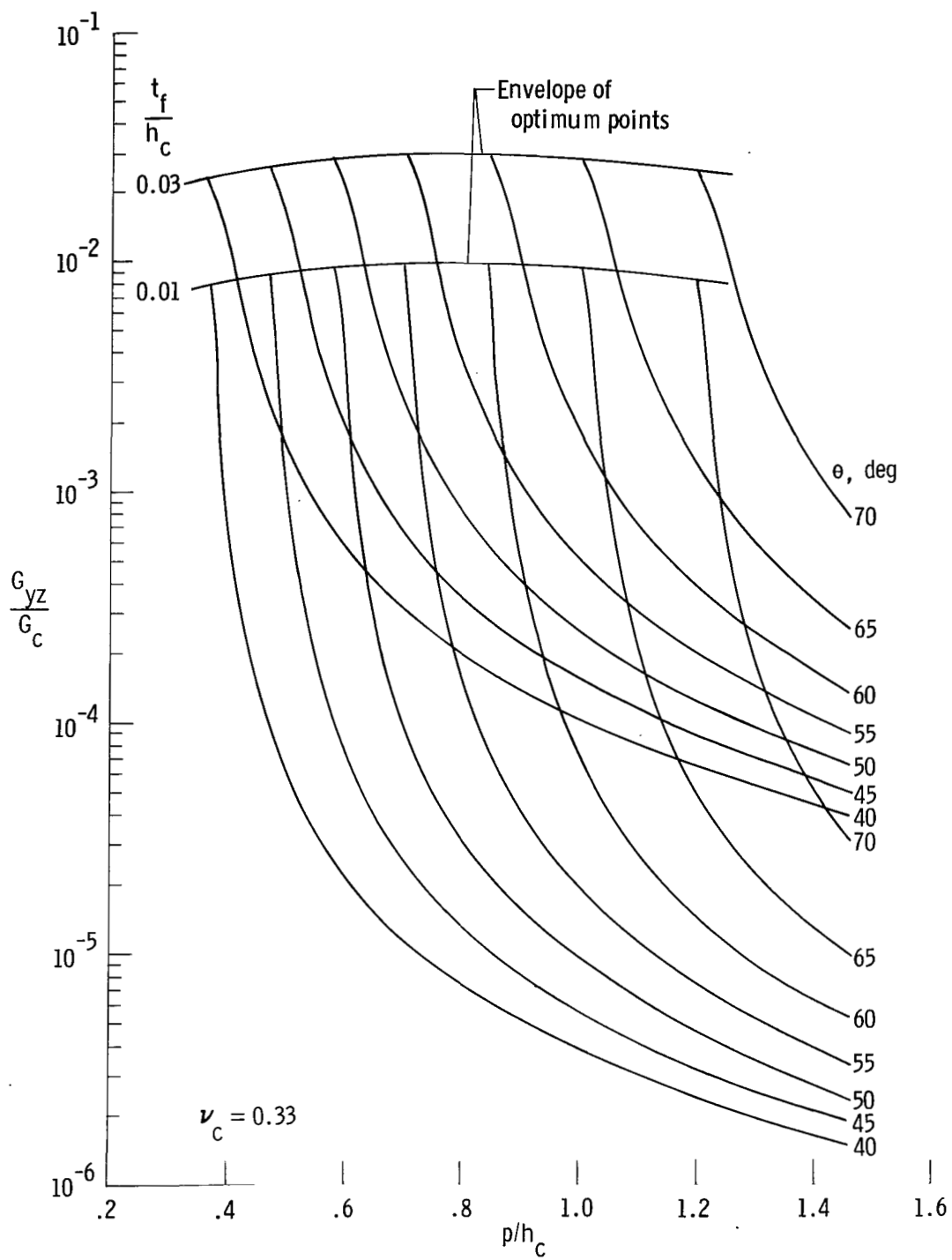


Figure 22. Shear modulus  $G_{yz}$  for honeycomb core.  
 $R = t_c = t_f$ .

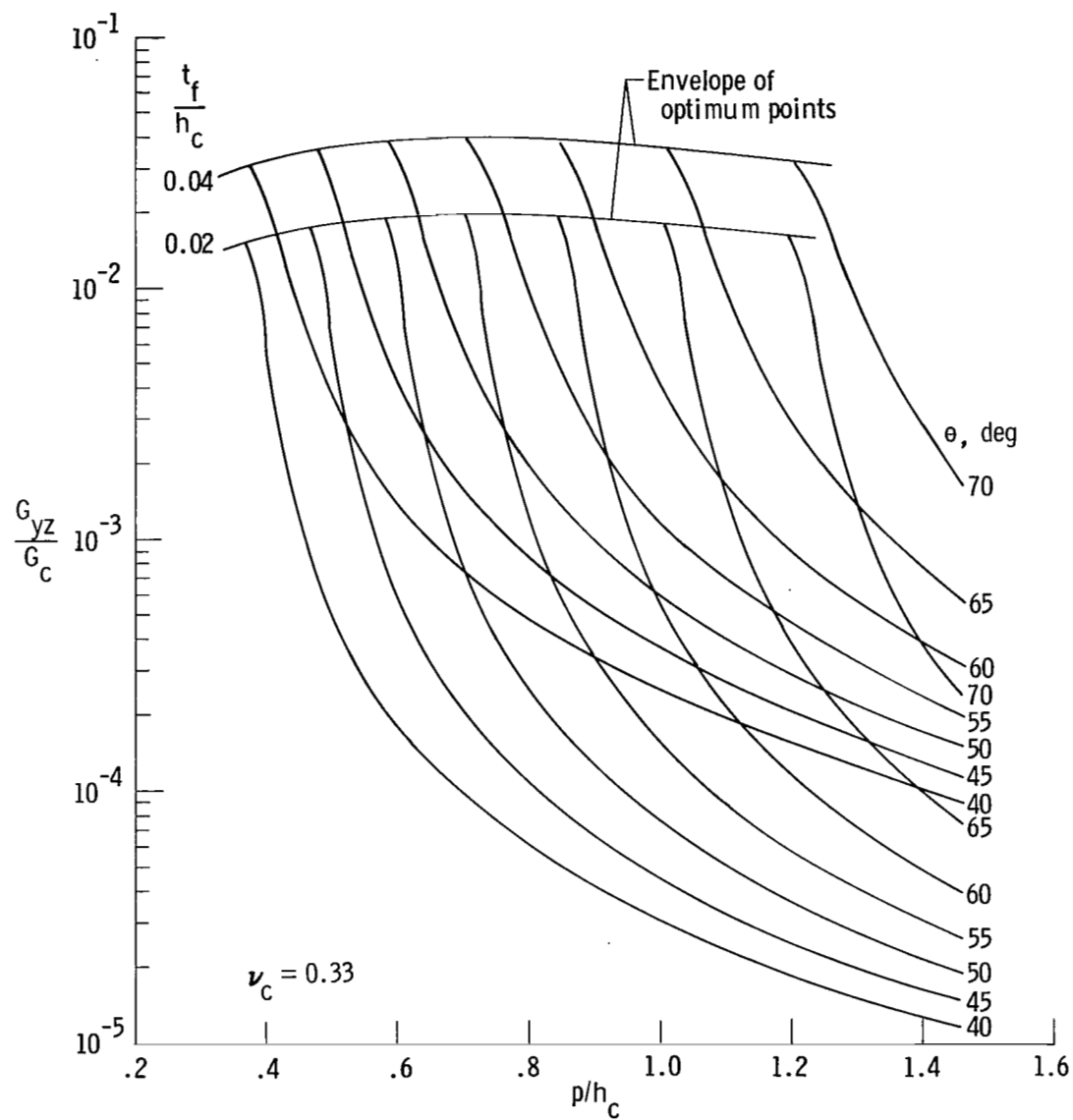


Figure 22. Continued.

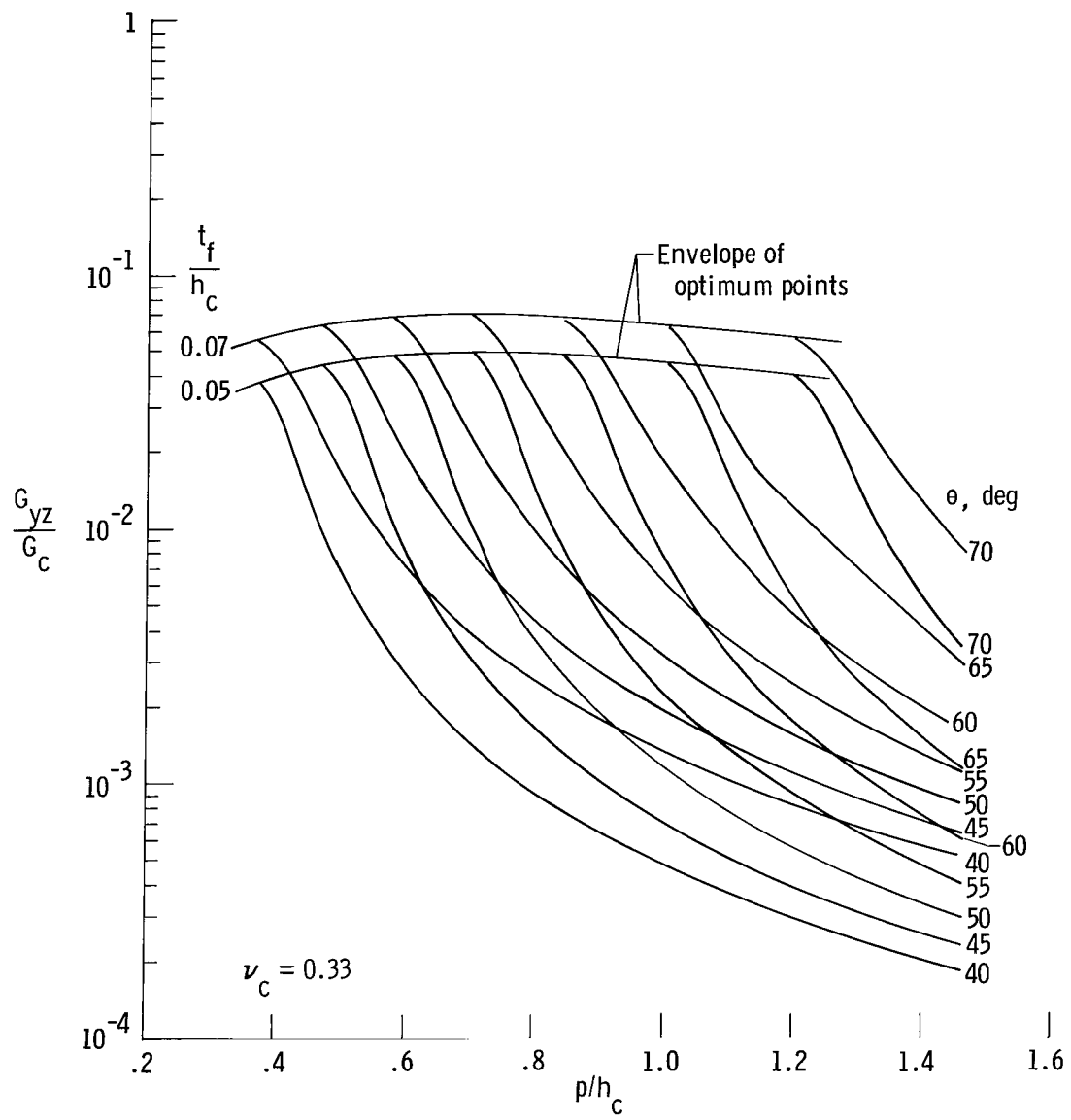


Figure 22. Continued.

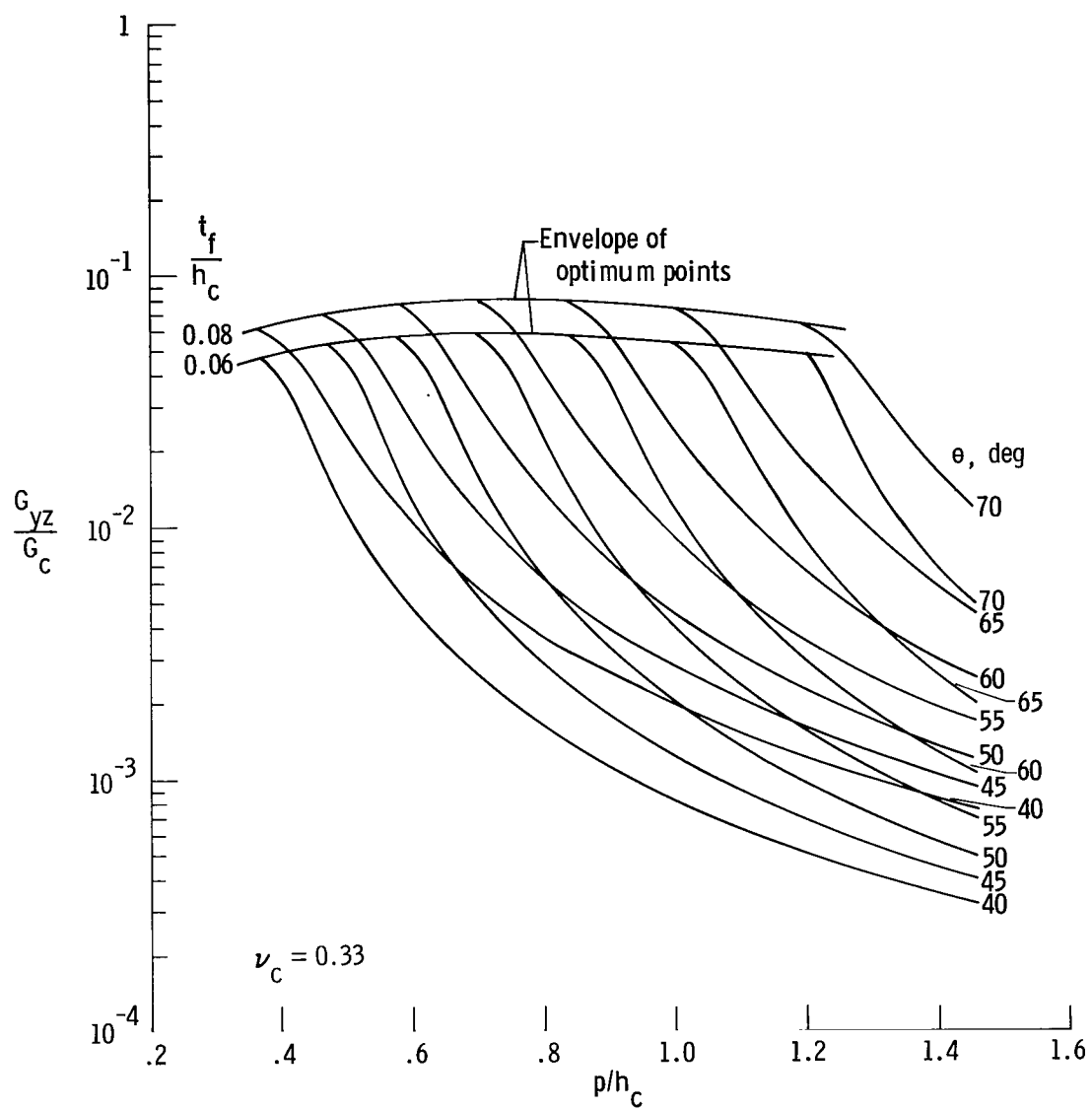


Figure 22. Concluded.

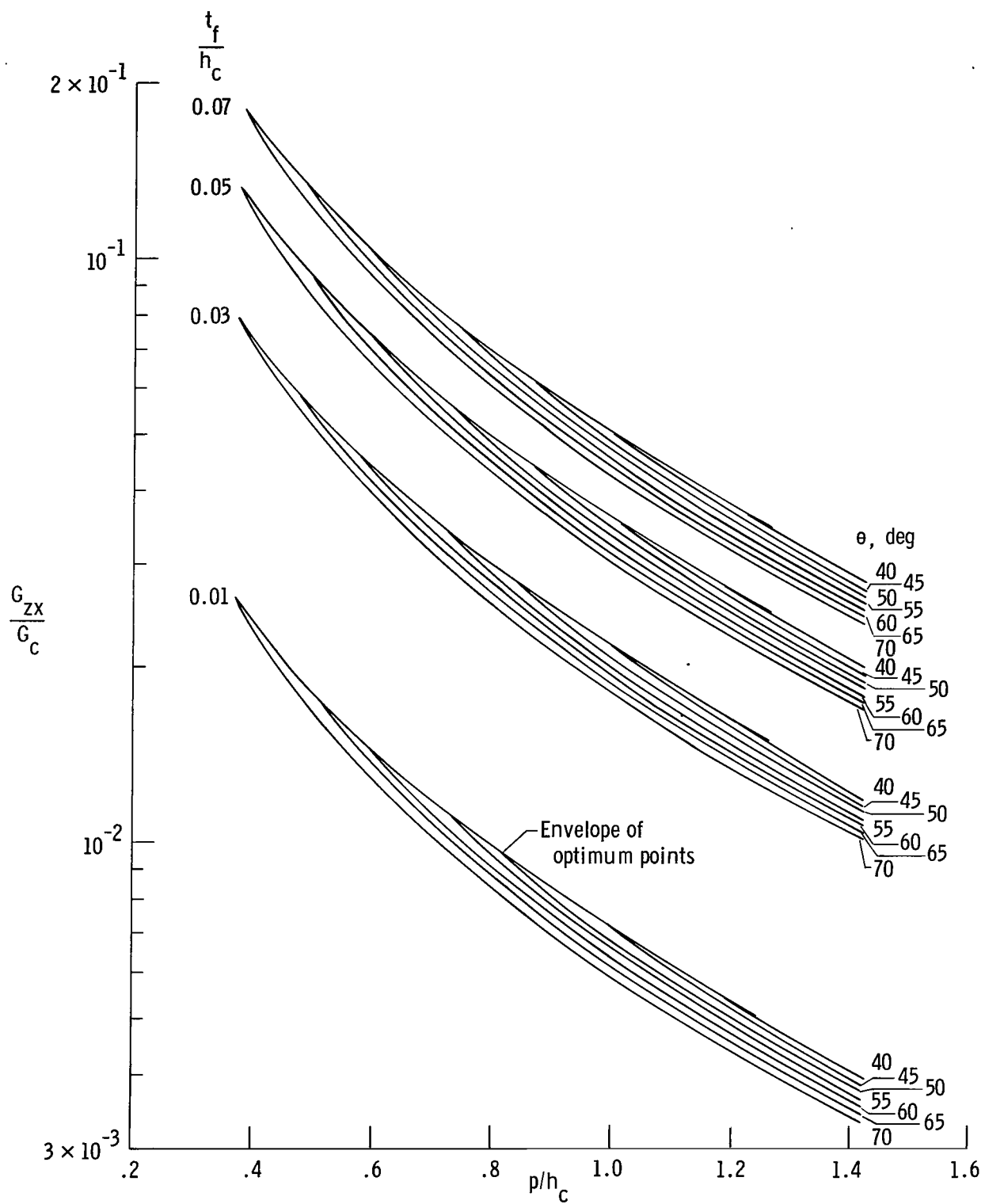


Figure 23. Shear modulus  $G_{ZX}$  for honeycomb core.  $R = t_C = t_f$ .



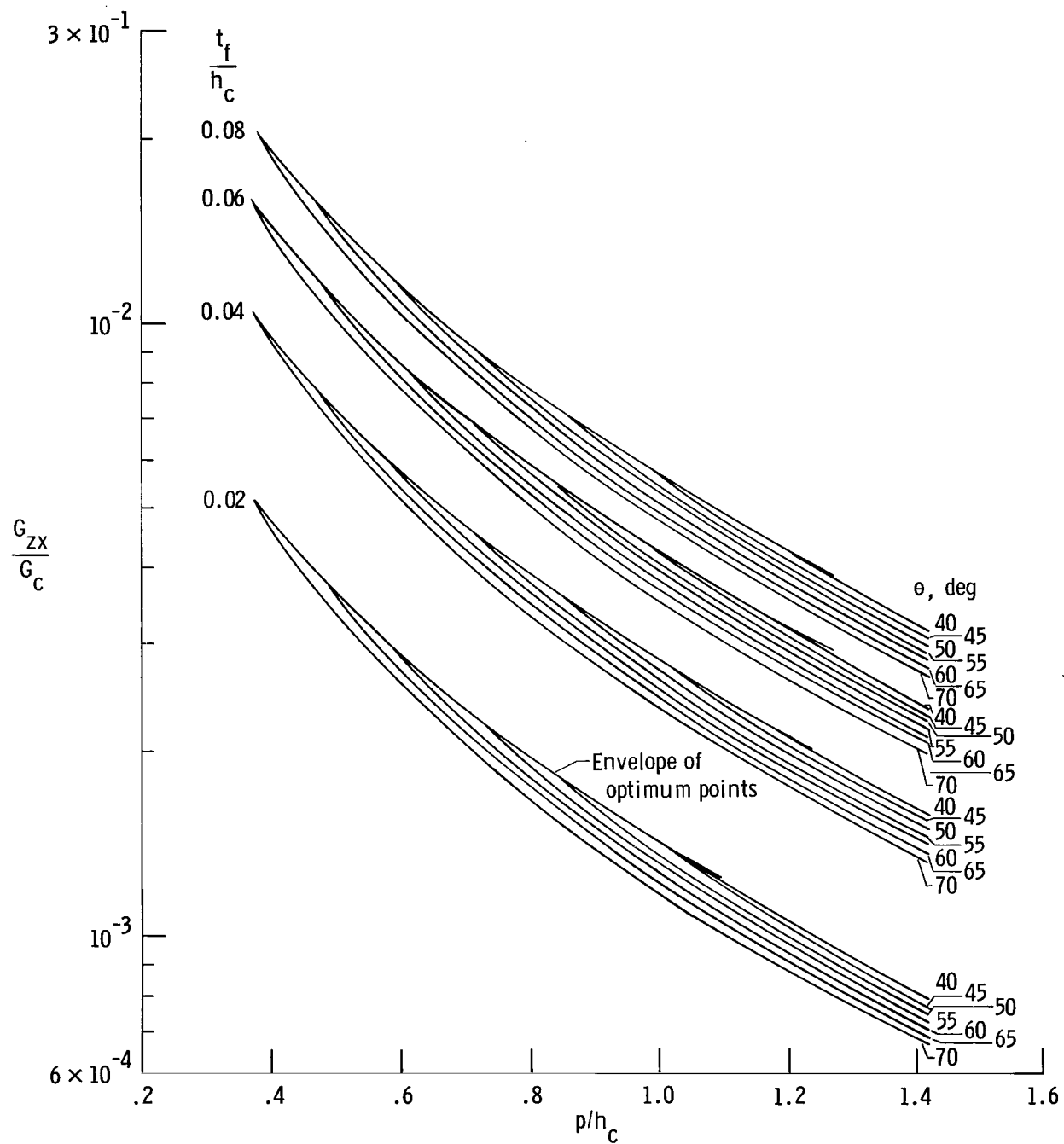


Figure 23. Concluded.

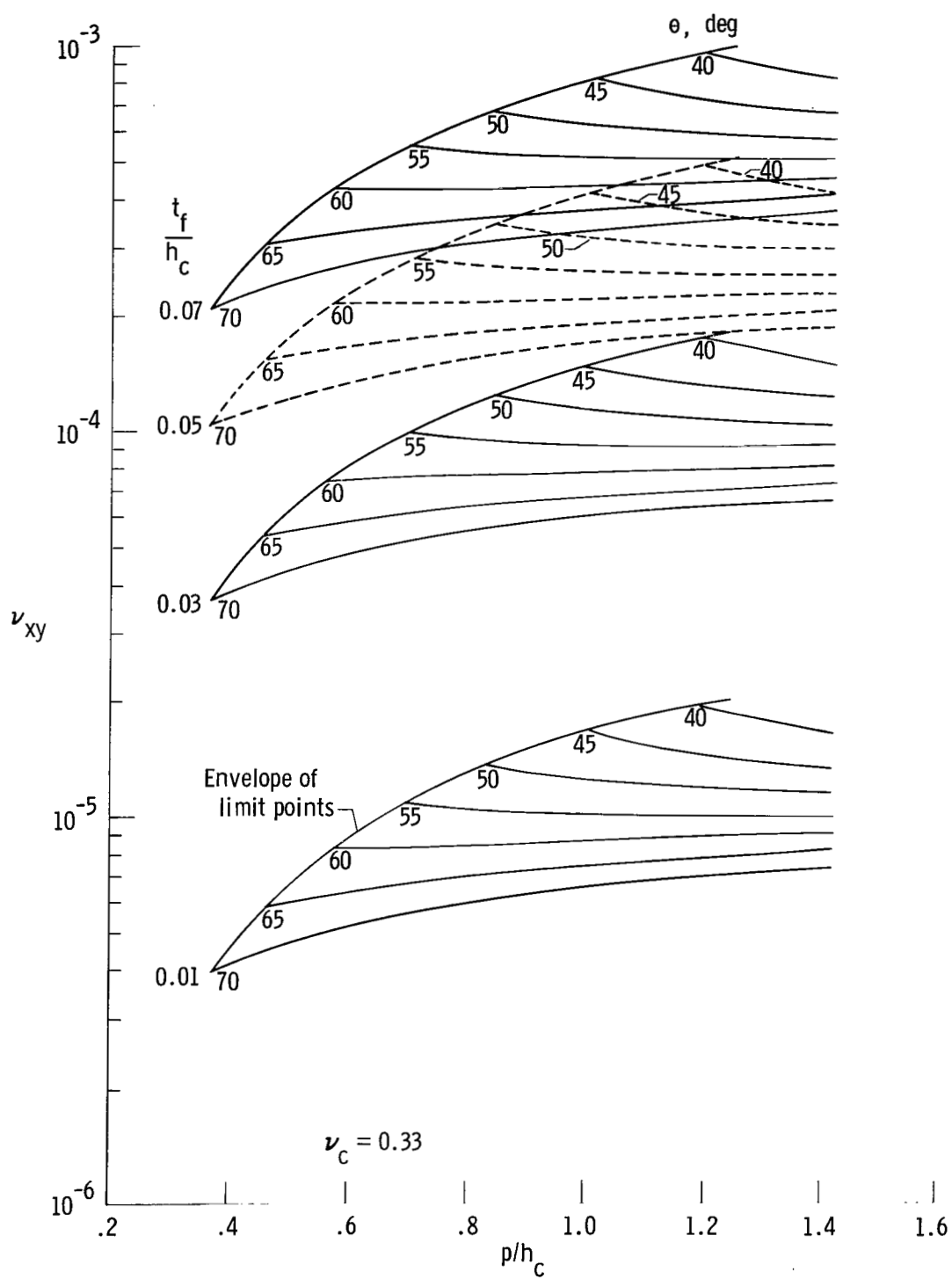


Figure 24. Poisson ratio  $\nu_{xy}$  for honeycomb core.  $R = t_c = t_f$ .

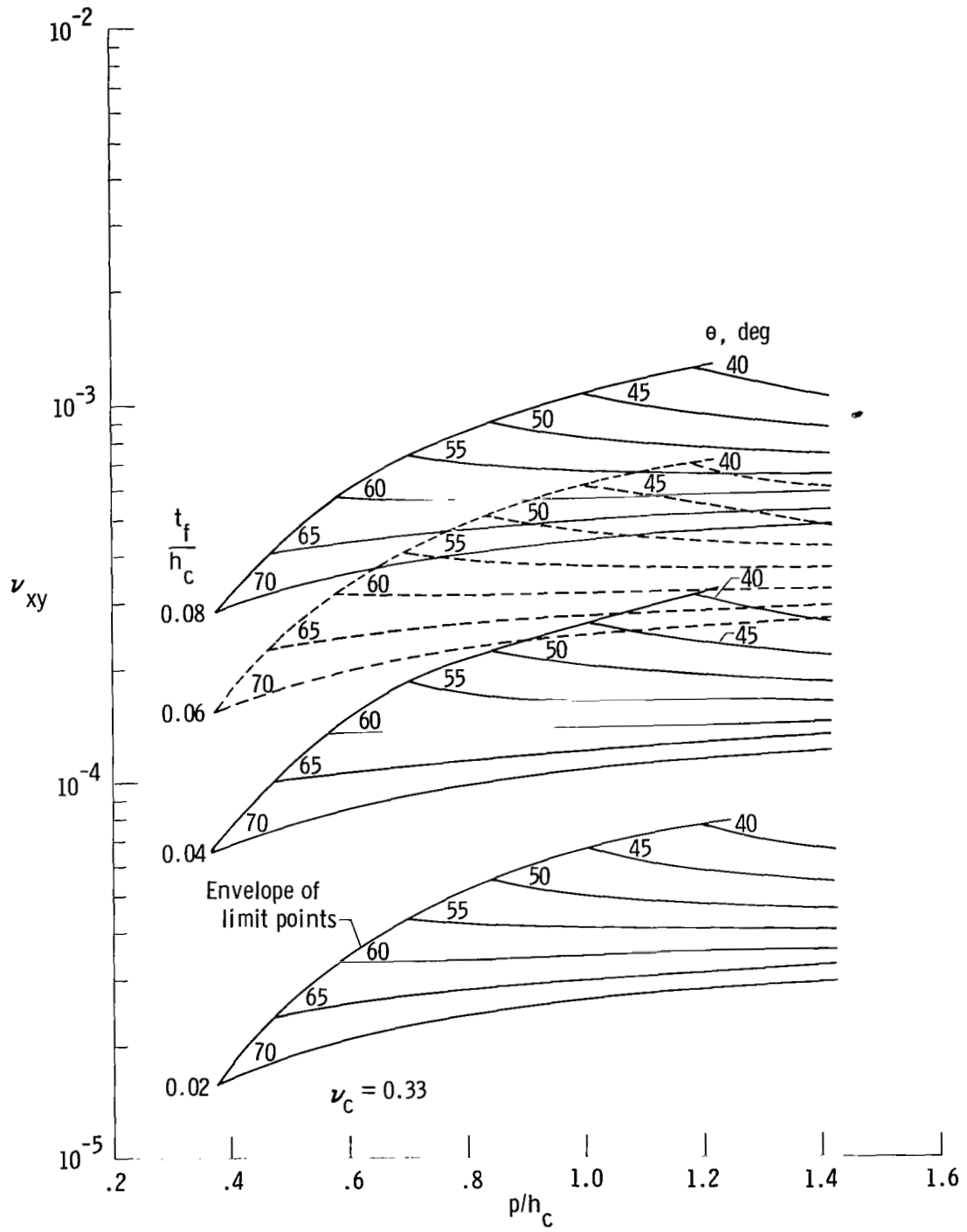


Figure 24. Concluded.

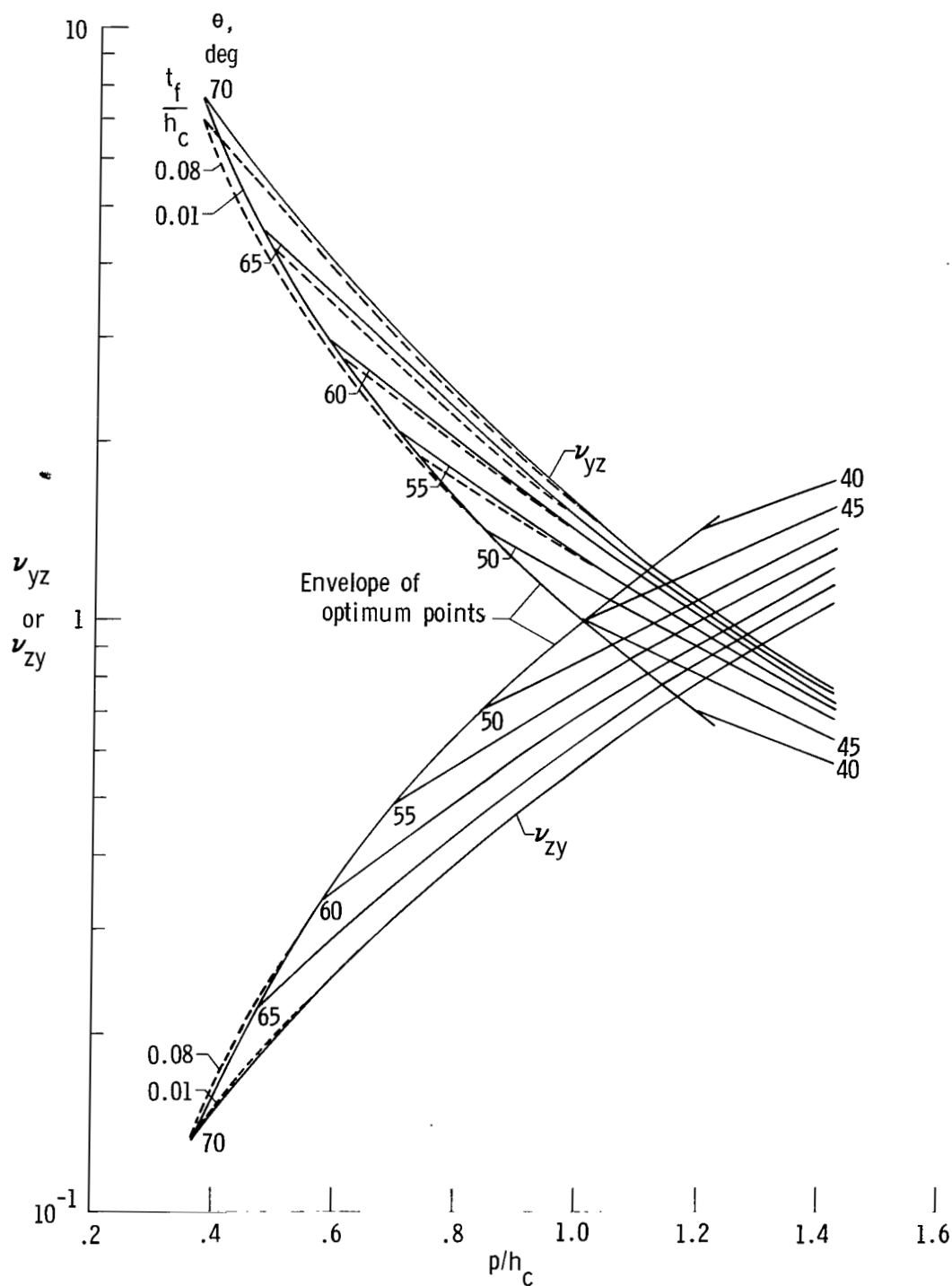


Figure 25. Poisson ratios  $\nu_{yz}$  and  $\nu_{zy}$  for honeycomb core.  $R = t_c = t_f$ .

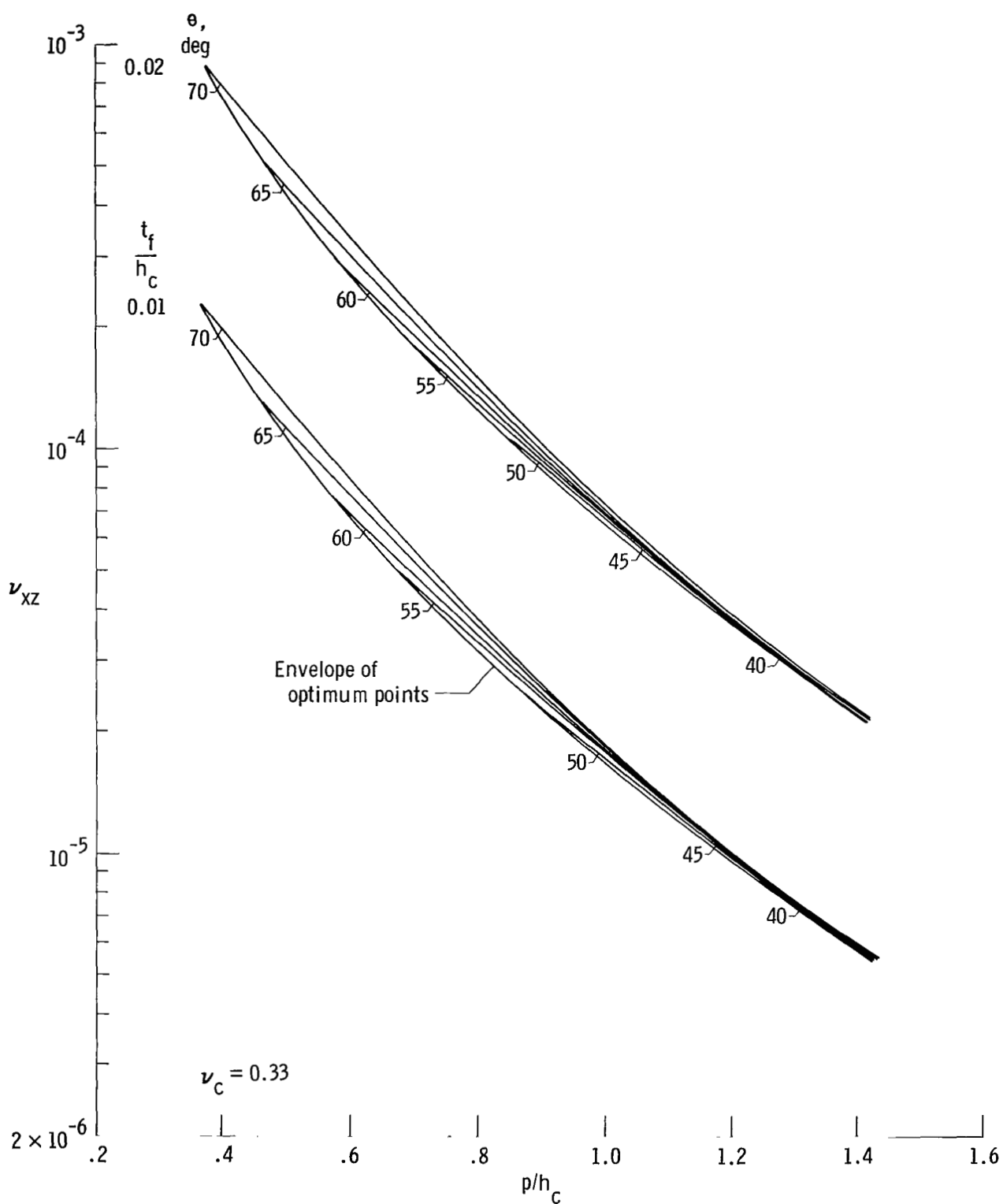


Figure 26. Poisson ratio  $\nu_{xz}$  for honeycomb core.  $R = t_c = t_f$ .

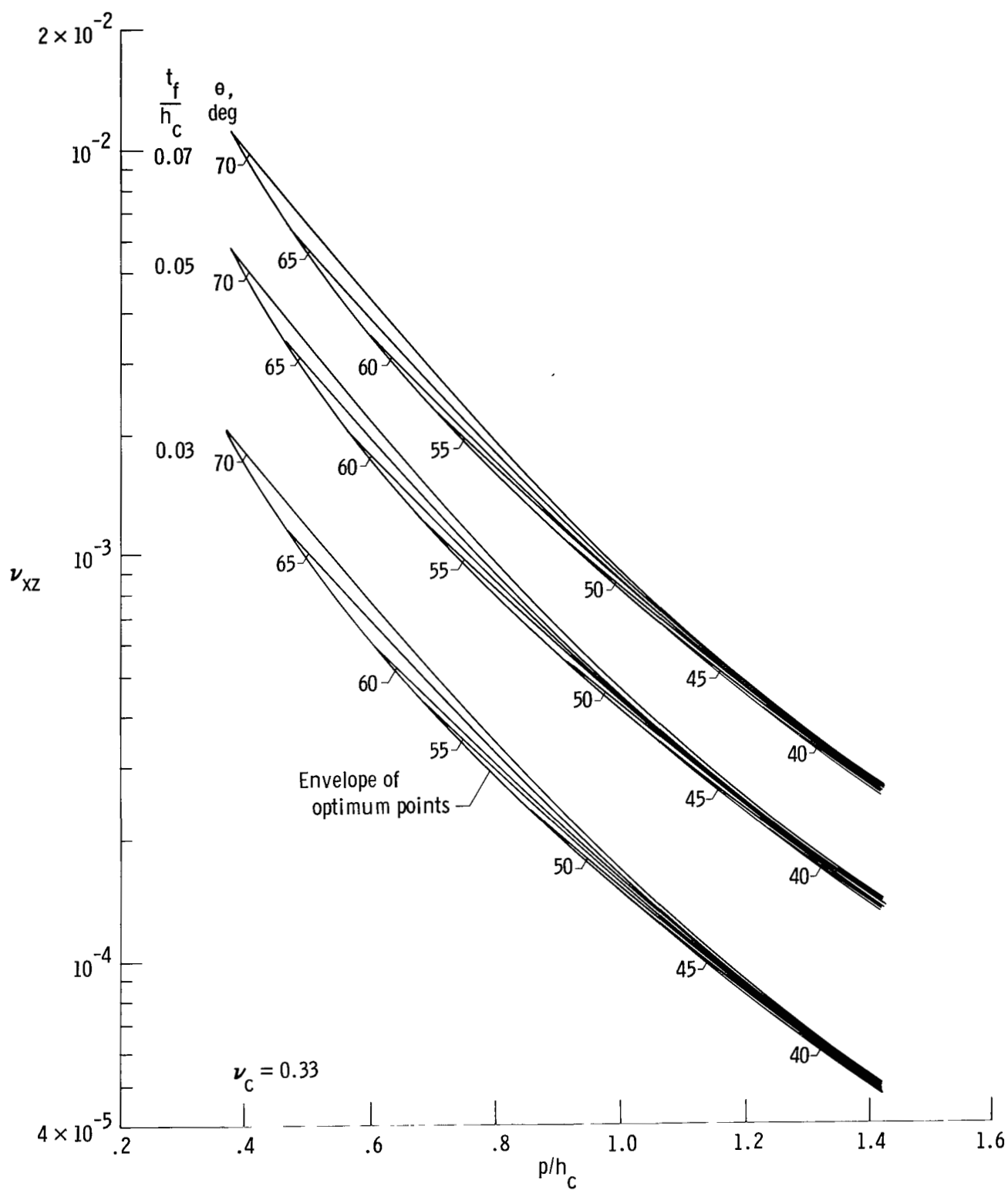


Figure 26. Continued.

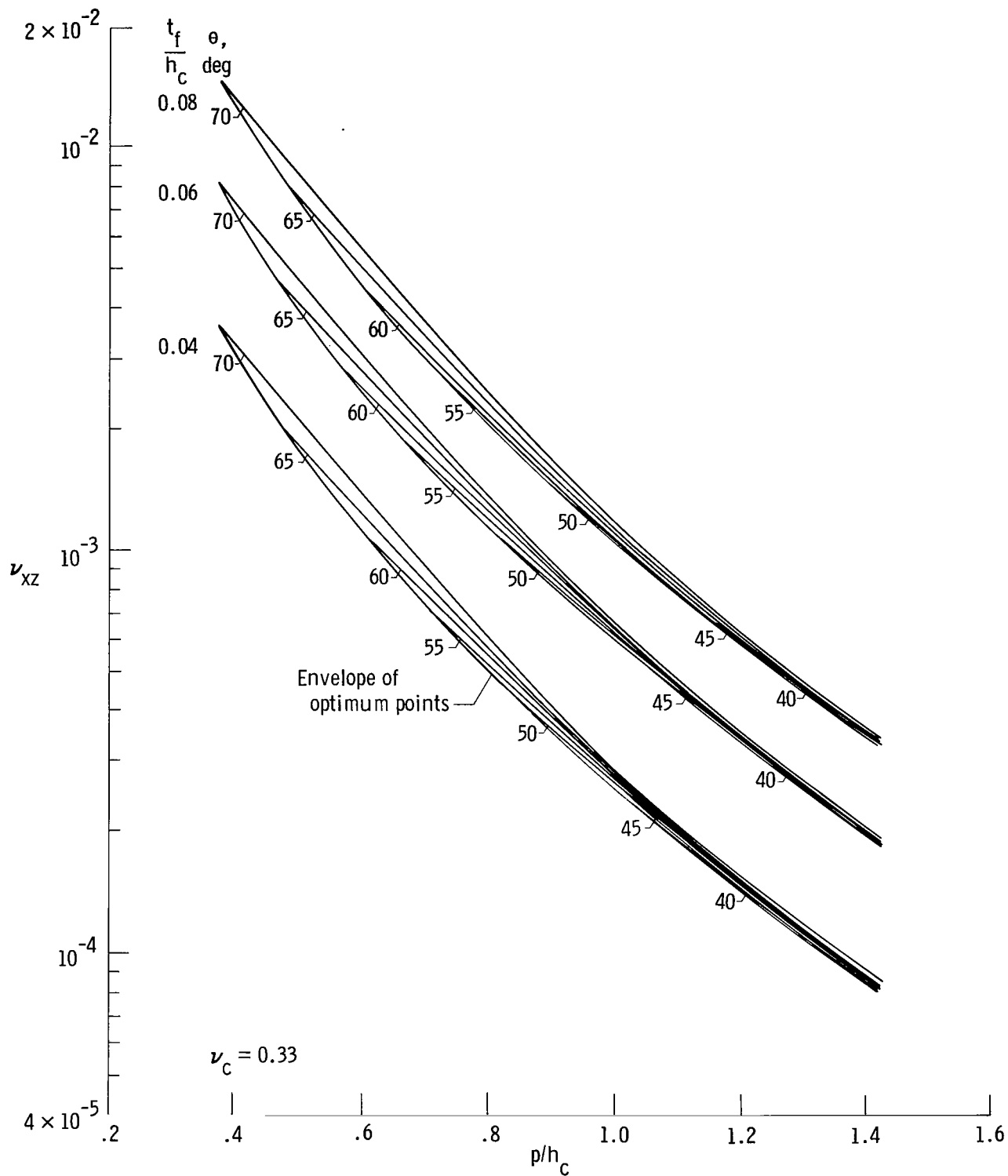


Figure 26. Concluded.

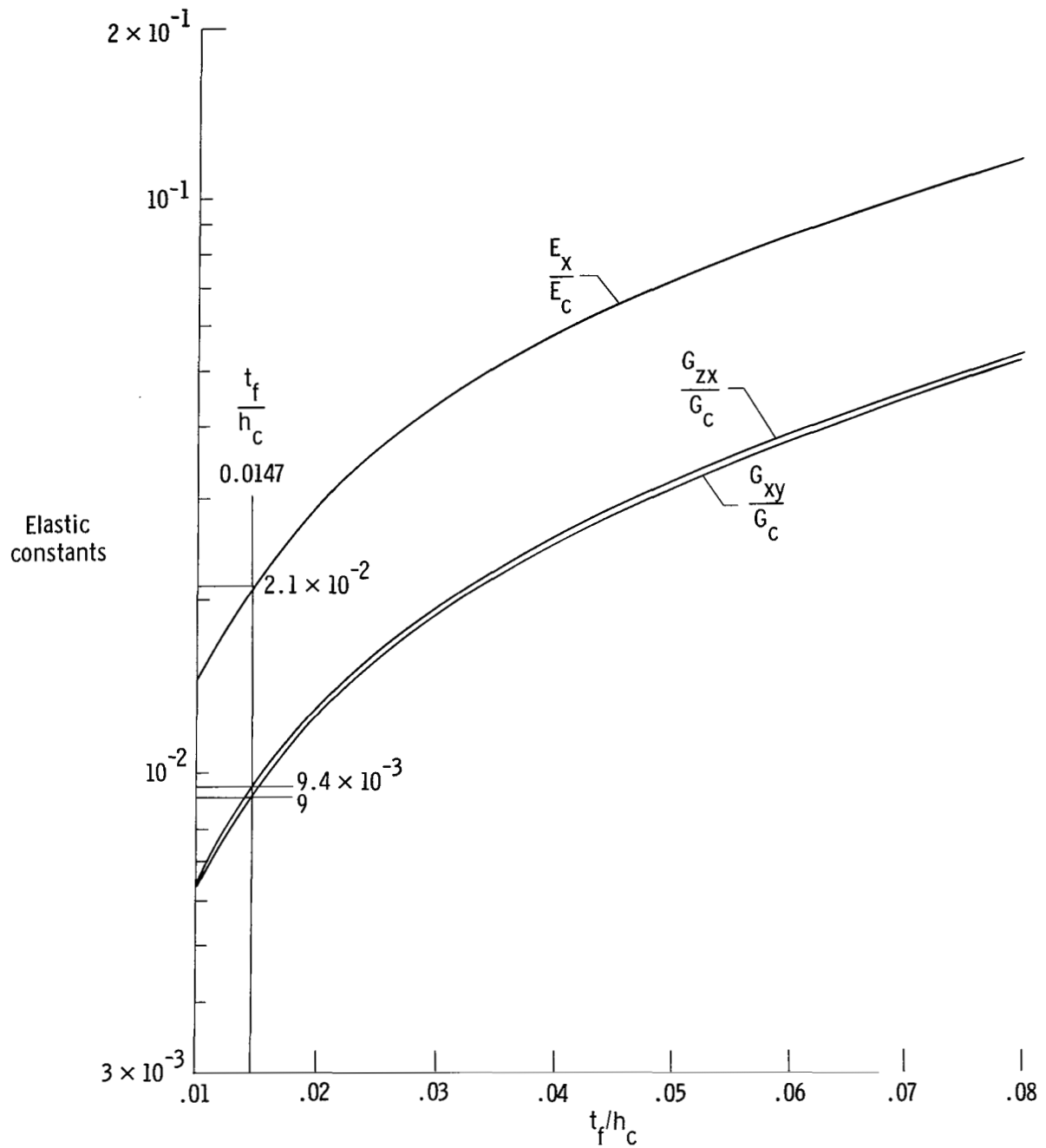


Figure 27. Variations of elastic constants with  $t_f/h_c$  for honeycomb core.  $p/h_c = 0.9825$ ;  $\theta = 60^\circ$ ;  $R = t_c = t_f$ .



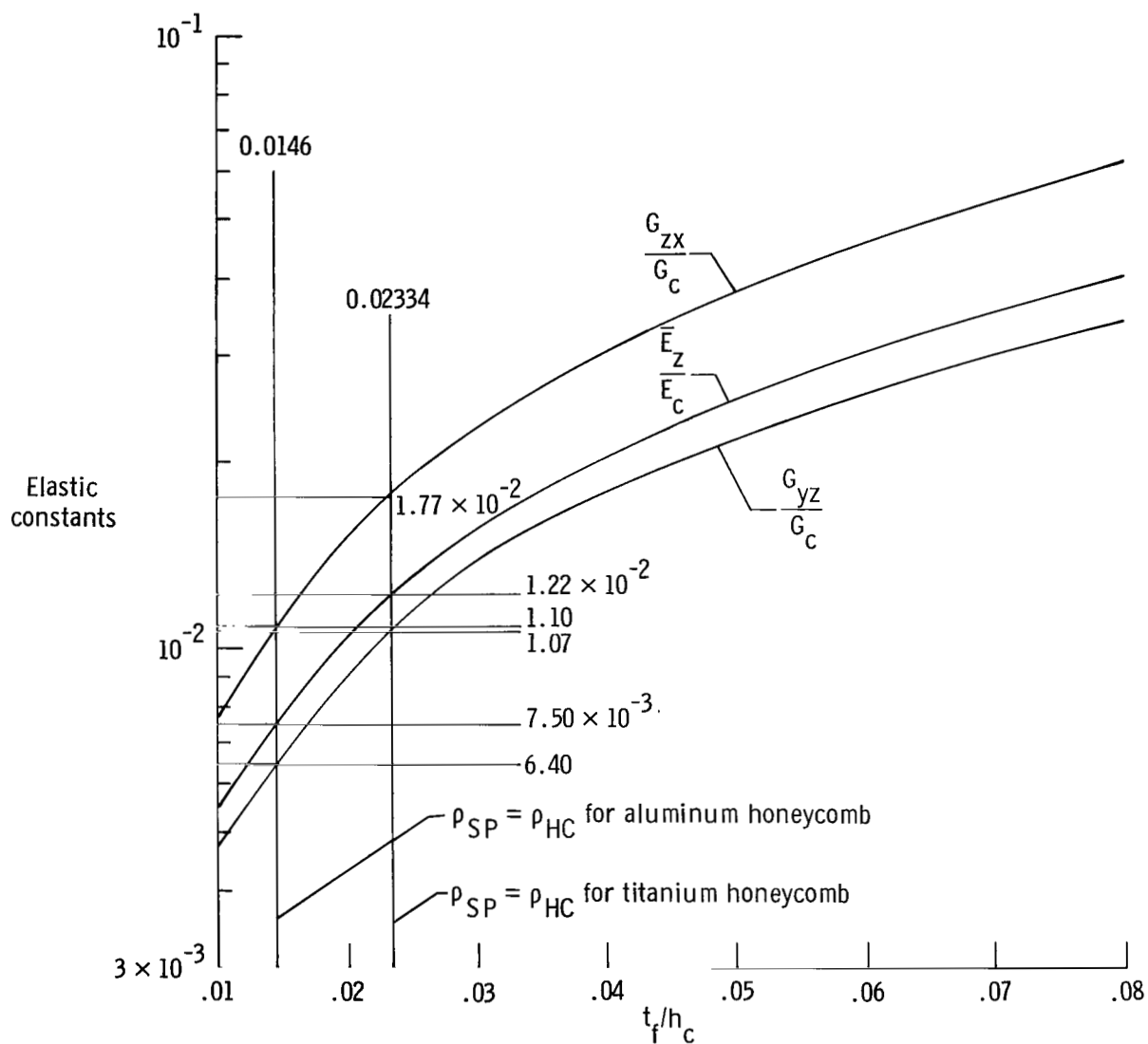


Figure 28. Variations of elastic constants with  $t_f/h_c$  for SPF/DB corrugated sandwich core.  $f = 0$ ;  $\theta = 60^\circ$ ;  $R = t_f$ .

1. Report No. <b>NASA TP-1562</b>		2. Government Accession No.		3. Recipient's Catalog No.	
4. Title and Subtitle <b>ELASTIC CONSTANTS FOR SUPERPLASTICALLY FORMED/DIFFUSION-BONDED CORRUGATED SANDWICH CORE</b>				5. Report Date <b>May 1980</b>	
				6. Performing Organization Code	
7. Author(s) <b>William L. Ko</b>				8. Performing Organization Report No. <b>H-1094</b>	
9. Performing Organization Name and Address <b>NASA Dryden Flight Research Center P.O. Box 273 Edwards, California 93523</b>				10. Work Unit No.	
12. Sponsoring Agency Name and Address <b>National Aeronautics and Space Administration Washington, D.C. 20546</b>				11. Contract or Grant No.	
				13. Type of Report and Period Covered <b>Technical Paper</b>	
				14. Sponsoring Agency Code	
15. Supplementary Notes  This report is an expanded version of "Elastic Constants for Superplastically Formed/Diffusion-Bonded Sandwich Structures" by the same author (AIAA Paper No. 79-0756).					
16. Abstract  <p>This paper presents formulae and associated graphs for evaluating the effective elastic constants for a superplastically formed/diffusion-bonded (SPF/DB) corrugated sandwich core.</p> <p>The results were used in the comparison of structural stiffnesses of the above sandwich core and a honeycomb core under conditions of equal sandwich core density.</p> <p>It was found that the stiffness in the thickness direction of the optimum SPF/DB corrugated core (that is, triangular truss core) was lower than that of the honeycomb core, and that the former had higher transverse shear stiffness than the latter.</p>					
17. Key Words (Suggested by Author(s)) <b>Stiffness Structural properties</b>				18. Distribution Statement <b>Unclassified-Unlimited</b>	
				Category: 39	
19. Security Classif. (of this report) <b>Unclassified</b>		20. Security Classif. (of this page) <b>Unclassified</b>		21. No. of Pages <b>83</b>	
				22. Price* <b>\$4.75</b>	

\*For sale by the National Technical Information Service, Springfield, Virginia 22161

NASA-Langley, 1980

National Aeronautics and  
Space Administration

Washington, D.C.  
20546

Official Business

Penalty for Private Use, \$300

THIRD-CLASS BULK RATE

Postage and Fees Paid  
National Aeronautics and  
Space Administration  
NASA-451



1 1 1U,D, 051080 S00903DS  
DEPT OF THE AIR FORCE  
AF WEAPONS LABORATORY  
ATTN: TECHNICAL LIBRARY (SUL)  
KIRTLAND AFB NM 87117

**NASA**

POSTMASTER: If Undeliverable (Section 158  
Postal Manual) Do Not Return

---